

Development of Dual Crosslinked Polymeric Materials for Self-healing

Soyoung An

A Thesis
In the Department
of
Chemistry and Biochemistry

Presented in Partial Fulfillment of the Requirements
For the Degree of Masters of Science (Chemistry) at
Concordia University
Montréal, Quebec, Canada

Dec 2016

© Soyoung An, 2016

CONCORDIA UNIVERSITY
SCHOOL OF GRADUATE STUDIES

This is to certify that the thesis prepared

By: Soyoung An

Entitled: **Development of dual crosslinked polymeric materials for self-healing**

and submitted in partial fulfillment of the requirements for the degree of

Master of Science (Chemistry)

complies with the regulations of the University and meets the accepted standards with respect to originality and quality.

Signed by the final examining committee:

Chair

Dr. Guillaume Lamoureux

Examiner

Dr. Christopher J. Wilds

Examiner

Dr. Louis Cuccia

Thesis Supervisor

Dr. John Oh

Approved by

Chair of Department or Graduate Program Director

Nov.30.2016

Dean of Faculty

Abstract

Development of Dual Crosslinked Polymeric Materials for Self-healing

Soyoung An

Daily damage such as scratches or fractures on most polymeric materials are inevitable, which shorten the lifespan, change/weaken the original integrity, and sometimes lead to the catastrophic failure of the materials. Self-healing or self-repairing is a desired property in the design and development of high-performance materials with their built-in ability to repair physical damage for various applications such as surface coatings, tissue engineering, and sensors.

Intrinsic self-healing utilizing dynamic chemistry is a promising method that allows for the development of effective self-repairing polymeric materials. This method involves the incorporation of non-covalent bonds through physical interactions such as π - π stacking, ionic interaction, metal binding, and hydrogen bonding. However, the use of physical bonding has a major drawback—small mechanical properties of prepared compounds due to the nature of the weak physical interaction. Another method utilizes reversible covalent bonds such as the Diels-Alder/retro-Diels-Alder reaction, alkoxyamine recombination, urea chemistry, and disulfides. Although these dynamic covalent bonds can provide higher mechanical properties compared to the physical interactions, the self-healing behavior often can be limited and require severe external stimuli to achieve a complete self-repairing procedure.

My Masters' research aims to explore the advantages and disadvantages of covalent and supramolecular (physical) networks. Two novel self-healable networks were developed; one network designed with dynamic disulfide linkages and the other with both disulfide and supramolecular metal-ligand associations. Dynamic disulfide linkages are excellent candidates to explore in developing self-healable polymeric materials since they can be readily cleaved/disturbed to thiols or thiyl radicals in response to external stimuli, and then subsequently rebounded to induce self-repair of the damaged parts. In a similar way, the metallo-

complex/ionic links are widely incorporated in forming self-healable polymeric networks because of the dynamic linkages between the ionic crosslinkers and their counter-ions.

For the first network, we explored having poly(methacrylate)-based crosslinked materials for which self-healing is based only on dynamic disulfide-thiol chemistry. Such materials were prepared by the extent oxidation of excess thiols in the lightly crosslinked networks through sulfide linkages. The second system consists of a multiblock copolymer with self-healable blocks and a middle block. The self-healable blocks are poly(methacrylate)-based units with pendant disulfides linkages and/or another pendant carboxylic acids groups. The presence of two different pendant dynamic linkages enables the formation of polymeric crosslinked materials—with dual self-repairing units—through disulfide-thiol exchange and metallo-complexation with metal ions. It is believed that these unique designs along with their tunable self-healing kinetics demonstrate well the versatility of our methods to prepare self-healable polymeric crosslinked networks that have a promising potential for the development of multifunctional industrial applications.

Acknowledgements

I would like to thank my supervisor, Dr. John Oh, for his tremendous help and fruitful guidance throughout my Masters program. He continuously helped and supported me in conducting scientific research, preparing/publishing manuscripts, and writing this thesis. I would like to emphasize that how grateful I am to have him as my Masters thesis supervisor. He has been a true mentor to me, and this thesis would never have been possible without his continuous care for my research, enthusiasm, and expertise in the polymer science field.

Also, I would like to thank my committee members Dr. Louis Cuccia and Dr. Christopher Wilds for their support, helpful comments, and suggestions that guided my research in its forward progress. Their doors always were open whenever I encountered difficulties regarding my research.

Moreover, I would like to thank all of my colleagues from OH group for their continuous support and great friendship. It was a great pleasure to work with all of them. I would like to especially thank Dr. Nicky Chan and Dr. Nare Ko who trained me with all the necessary skills and shared their knowledge with me. They have set a good example as senior researchers, which I always will appreciate.

I would like to thank my family and friends for their love and encouragement. They have been incredibly supportive throughout this entire process and have provided me the requisite breaks from science and the motivation to continuously conduct scientific research.

Last, this work is dedicated to my parents who have supported me in all aspects, and most importantly with the moral support of their endless love.

List of Publications

(Equal contribution is denoted with *.)

1. F. Ren, B. D. Rosal, S. Y. An, F. Yang, E. Carrasco, A. Benayas, J. K. Oh, D. Jaque, A. J. Fuente, F. Ventrone, D. Ma, Development and investigation of ultrastable PbS/CdS/ZnS quantum dots for near-infrared tumor imaging, *Particle & Particle Systems Characterizations*, **2016** (Accepted).
2. D. G. Lee*, S. Y. An*, H. W. Jung, J. K. Oh, Photo-induced thiol-ene crosslinked polymethacrylate networks reinforced with Al₂O₃ nanoparticles, *Polymer*, **2016**, 101, 119-126.
3. S. Y. An, S. W. Hong, J. K. Oh, Biorenewable rosin-based block copolymer intracellular delivery nanocarriers with reduction-responsive sheddable coronas for cancer therapy, *Polymer Chemistry*, **2016**, 7, 4751-4760.
4. S. Y. An, S. Sun, J. K. Oh, Reduction-responsive sheddable carbon nanotubes dispersed in aqueous solution, *Macromolecular Rapid Communications*, **2016**, 37, 705-710
5. S. Y. An, D. Arunbabu, S. M. Noh, Y. K. Song, J. K. Oh, Recent strategies to develop self-healable crosslinked networks, *Chemical Communications*, **2015**, 51, 13058-13070 (Back inside cover)
6. S. Y. An, S. M. Noh, J. H. Nam, J. K. Oh, Dual sulfide-disulfide crosslinked networks with rapid and room temperature self-healability, *Macromolecular Rapid Communications*, **2015**, 36, 1255-1260 (Back cover)
7. N. Chan, N. R. Ko, S. Y. An, J. K. Oh, Dual location reduction-responsive degradable nanocarriers: a versatile strategy for intracellular anticancer drug delivery with accelerated release, *ACS Symposium Series* **2015** (Book chapter)
8. S. Y. An*, D.G. Lee*, J. W. Hwang, K. N. Kim, J. H. Nam, H. W. Jung, S. M. Noh, J. K. Oh, Photo-induced thiol-ene polysulfide-crosslinked materials with tunable thermal and mechanical properties, *Journal of Polymer Science, Part A*, **2014**, 52, 3060-3068
9. S. Y. An, J. K. Oh, Self-healable copolymers and method for the preparation thereof, Invention disclosure/61991832 (2014)

10. N. Chan, N. Yee, S. Y. An, J. K. Oh, Tuning amphiphilic and thermoresponsive self-assembly and in situ disulfide crosslinking of reduction-responsive block copolymers *Journal of Polymer Science. Part A: Polymer Chemistry*, **2014**, 52, 2057-2067
11. N. Chan, S. Y. An, N. Yee, J. K. Oh, Dual redox and thermo-responsive double hydrophilic block copolymers with tunable thermoresponsive properties and self-assembly behavior, *Macromolecular Rapid Communications*, **2014**, 34, 752-757
12. S. Y. An, J. W. Hwang, K. N. Kim, H. W. Jung, S.M. Noh, J. K. Oh, Multifunctional linear methacrylate copolymer polyenes having pendant vinyl groups: synthesis and photo-induced thiol-ene crosslinking polyaddition, *Journal of Polymer Science. Part A: Polymer Chemistry*, **2014**, 52, 572-581.
13. N. Chan, S. Y. An, J. K. Oh, Dual location disulfide degradable interlayer-crosslinked micelles with extended sheddable coronas exhibiting enhanced colloidal stability and rapid release, *Polymer Chemistry*, **2014**, 5, 1637-1649

Contribution of Authors

The majority of the research presented in this thesis was conducted independently by the author of this thesis under the supervision of Dr. John Oh at Concordia University. The chapters 2 and 3 are reproduced in part, with approval from the publisher, from the original article from which they are drawn. Here are the specific contributions.

In Chapter 2, the extrinsic self-healing method was reviewed and written by Dr. Arunbabu Dhamodran who is listed as a co-author of the review paper.

Table of Contents

| | |
|---|-------|
| List of Figures | xii |
| List of Schemes | xvi |
| List of Tables | xvii |
| List of Abbreviations | xviii |
| Chapter 1 Introduction | 1 |
| 1.1 Brief overview of my research and goals..... | 1 |
| 1.2 Self-healing in crosslinked networks | 1 |
| 1.3 Scope of my thesis | 3 |
| Chapter 2 Review of recent strategies to develop self-healable crosslinked networks..... | 4 |
| 2.1 Introduction..... | 4 |
| 2.2 Intrinsic self-healing methods utilizing reversible chemical crosslinking methods | 5 |
| 2.2.1 Redox disulfide chemistry | 6 |
| 2.2.2 Diels-Alder (DA)/retro-DA chemistry | 9 |
| 2.2.3 Hindered urea chemistry | 12 |
| 2.2.4 Other reversible chemistry | 12 |
| 2.3 Intrinsic self-healing methods utilizing reversible physical crosslinking | 13 |
| 2.3.1 Hydrogen bonding interactions..... | 13 |
| 2.3.2 π - π interactions..... | 15 |
| 2.3.3 Metallo-supramolecular interactions..... | 16 |
| 2.3.4 Ionic interactions..... | 17 |
| 2.3.5 Host-guest interactions..... | 19 |
| 2.4 Extrinsic self-healing methods..... | 20 |
| 2.4.1 Ring opening metathesis polymerization (ROMP)..... | 21 |
| 2.4.2 Controlled radical polymerization (CRP) | 23 |
| 2.4.3 Azide-alkyne click chemistry..... | 24 |

| | |
|--|----|
| 2.4.4 Polyaddition | 25 |
| 2.5 Conclusion | 26 |
| Chapter 3 Dual sulfide-disulfide crosslinked networks with rapid and room temperature self-healability..... | 28 |
| 3.1 Introduction..... | 28 |
| 3.2 Experimental section..... | 30 |
| 3.2.1 Instrumentation and analyses | 30 |
| 3.2.2 Differential scanning calorimetry (DSC)..... | 30 |
| 3.2.3 Thermogravimetric analysis (TGA)..... | 31 |
| 3.2.4 Materials | 31 |
| 3.2.5 Synthesis of high molecular weight P2-ene | 31 |
| 3.2.6 Photo-induced thiol-ene radical addition reaction | 32 |
| 3.2.7 Oxidation of sPxNs | 32 |
| 3.2.8 Gel content measurement..... | 32 |
| 3.2.9 FT-IR measurements..... | 32 |
| 3.2.10 Optical microscopy | 33 |
| 3.2.11 Rheological measurements | 33 |
| 3.3 Results and Discussion | 33 |
| 3.3.1 Synthesis of P2-ene having vinyl groups..... | 33 |
| 3.3.2 Preparation of dual sulfide-disulfide crosslinked networks (s-ssPxNs)..... | 35 |
| 3.3.3 Self-healing ability of different s-ssPxNs | 40 |
| 3.3.4 Viscoelastic properties of s-ssPxN..... | 43 |
| 3.4 Conclusion | 45 |
| Chapter 4 Multiblock copolymer-based dual disulfide- and supramolecular crosslinked networks exhibiting dual self-healing..... | 46 |
| 4.1 Introduction..... | 46 |

| | |
|---|----|
| 4.2 Experimental section..... | 48 |
| 4.2.1 Instrumentation and analysis..... | 48 |
| 4.2.2 Materials | 49 |
| 4.2.3 Synthesis of P1 PEG-based difunctional ATRP initiator..... | 49 |
| 4.2.4 Synthesis of P3 triblock copolymers..... | 50 |
| 4.2.5 Synthesis of P5 pentablock copolymers..... | 50 |
| 4.2.6 Hydrolytic cleavage to yield P5-COOH | 51 |
| 4.2.7 Preparation of disulfide-crosslinked gels of P3 triblock copolymers | 51 |
| 4.2.8 Preparation of dual crosslinked gels | 51 |
| 4.2.9 Optical microscopy. | 51 |
| 4.2.10 Rheological measurements. | 52 |
| 4.3 Results and discussion | 54 |
| 4.3.1 Synthesis of triblock and pentablock copolymers..... | 54 |
| 4.3.2 Investigation of disulfide exchange gelation of P3 triblock copolymer..... | 56 |
| 4.3.3 Preparation and characterization of dual crosslinked gels of P5-COOH | 58 |
| 4.3.4 Self-healing studies | 59 |
| 4.3.5 Further investigation of self-healing in P3 disulfide-crosslinked gels..... | 61 |
| 4.4 Conclusion | 62 |
| Chapter 5 Conclusion and future work | 63 |
| References..... | 65 |
| Appendix A..... | 74 |

List of Figures

| | |
|--|----|
| Figure 1.1 Schematic illustration of extrinsic and intrinsic self-healing methods. | 2 |
| Figure 2.1 Reversible dynamic linkages and chemistries that have been explored for the development of novel reversible self-healable materials. | 6 |
| Figure 2.2 Chemical structure of disulfide-crosslinked star-shaped copolymer (left) and time dependent change of height mode AFM image for cut on the surface of reversibly disulfide-crosslinked star-polymer network (right): 3D images (a), 2D height mode images (b), and evolution of damage depth for 12 min at two positions (c). ² Copyright 2012 American Chemical Society..... | 7 |
| Figure 2.3 Illustration of a novel method utilizing click-type photo-induced thiol-ene radical addition and oxidation to synthesize dual sulfide-disulfide crosslinked networks (s-ssPxNs) (a), evolution of microscope images (b) and kinetics of self-healing (c) over time at room temperature for dual s-ssPxN with different cut sizes of 43 μm wide (upper) and 73 μm wide (middle), compared with a control of sPxN with no disulfide (bottom). Copyright 2015 Wiley Interfaces. | 8 |
| Figure 2.4 Illustration of Polycondensation through DA reaction of a four-arm furan-labeled monomer (4F) and a three-arm maleimide-labeled monomer (3M) to form DA-crosslinked materials. ⁶⁰ | 10 |
| Figure 2.5 Schematic illustration of DA and retro-DA reaction occurred in reactive mixtures consisting of a ABA triblock copolymer having pendant furfuryl groups with 1,1'-(methylenedi-4,1-phenylene)bismaleimide for thermally-driven self-healing. ⁶⁹ Copyright 2010 American Chemical Society..... | 11 |
| Figure 2.6 Schematic illustration of self-healing process (a), chemical structures and ratios of components used for the synthesis (b), and selected snapshots during the course of self-healing experiments of HUB-based crosslinked poly(urethane-urea) materials (c). TMPCA: 2,2,6,6,-tetramethylpiperidinylcarboxamide, TBEU: 1-(t-butyl)-1-ethylurea, and DEU: 1,1-diethylurea. ⁵ Copyright 2014 Nature Publishing Group..... | 12 |
| Figure 2.7 Schematic illustration of hydrogen-bonding brush polymer consisting of polystyrene backbone (high T_g) as a hard phase and polyacrylate amide brushes (low T_g) as a soft phase and its supramolecular assembly to form two-phase microstructures, consisting of hard polystyrene domains microphase-separated in soft matrix containing secondary amide | |

| | |
|---|----|
| groups that are capable of forming dynamic supramolecular networks. ⁹⁰ Copyright 2014 Nature Publishing Group. | 15 |
| Figure 2.8 Illustration of π - π interaction between a polydiimide and a pyrenyl end-capped polymer. ⁹⁶ Copyright 2013 Royal Society of Chemistry..... | 16 |
| Figure 2.9 Schematic illustration of metal-ligand interaction between Mebip units and Zn ions ⁹⁸ . Copyright 2011 Nature Publishing Group. | 17 |
| Figure 2.10 Schematic illustration of ionically-crosslinked hydrogels of poly(acrylic acids) with ferric ions (a) and digital images showing the occurrence of autonomous self-healing through dynamic bonding of physical crosslinking (b-f). ¹¹⁰ Copyright 2013 Royal Society of Chemistry..... | 19 |
| Figure 2.11 Schematic illustration of host-guest interactions between PAA-CD and PAA-Fc to form self-healable supramolecular hydrogels (a) and their digital images showing gel-sol transition . ¹²¹ Copyright 2011 Nature Publishing Group. | 20 |
| Figure 2.12 Pictorial depiction of healing mechanism of urea-formaldehyde microcapsule (a), healing chemistry utilizing ROMP of DCPD in the presence of Grubb's catalyst (b), and healing efficiency is obtained by fracture toughness testing of tapered double-cantilever beam (TDCB) specimens (c). ¹²⁹ Copyright 2001 Nature Publishing Group..... | 23 |
| Figure 2.13 Illustration of ATRP of GMA from PMMA-Br macroinitiator for microcapsule-based extrinsic self-healing. | 24 |
| Figure 2.14 Design and extrinsic self-healing of polyisobutylene matrix embedded with microcapsules of small molecular weight alkynes and three-arm star polyisobutylene azides separately via azide-alkyne click reaction in the presence of Cu(I) species. ¹⁴¹ Copyright 2011 Wiley Interfaces. | 24 |
| Figure 2.15 Illustration of various polyaddition mechanisms for the development of novel extrinsic self-healing materials. | 26 |
| Figure 3.1 Schematic illustration to synthesize P1-OH and P2-ene | 34 |
| Figure 3.2 GPC trace (a), DSC trace (b), and ¹ H-NMR spectrum in CDCl ₃ (c) of purified, dried P2-ene. | 35 |
| Figure 3.3 FT-IR spectra of a reactive blend of P2-ene with TriSH at [SH] ₀ /[vinyl] ₀ = 15/1 before and after UV irradiation to monitor the change of peak area at 2570 cm ⁻¹ | 36 |

| | |
|---|----|
| Figure 3.4 Overlaid elastic modulus (G') over angular frequency (ω) for reactive blends consisting of P2-ene and TriSH at various ratio of $[\text{SH}]_0/[\text{vinyl}]_0$ upon UV irradiation. | 37 |
| Figure 3.5 Gel content (%) and SH consumption (%) upon oxidation in the presence of different amount of iodine for sGel-15 prepared with the $[\text{SH}]_0/[\text{vinyl}]_0 = 15/1$. The digital images show s-ssPxN-15/y gels (y denote wt % of iodine) in THF. | 39 |
| Figure 3.6 FT-IR spectra of sPxN-15 before and after treatment with various amounts of iodine. | 39 |
| Figure 3.7 Evolution of microscope images (a-c) and kinetics of self-healing (d) over time at room temperature for dual s-ssPxN-15/6 with different cut sizes of 43 μm wide (a) and 73 μm wide (b), compared with a control of sPxN-1 with no disulfide prepared with $[\text{SH}]_0/[\text{vinyl}]_0 = 1/1$ (c). | 41 |
| Figure 3.8 Evolution of optical microscope image of 80 μm wide and 500 μm long cut over time at room temperature for dual s-ssPxN-15/3, prepared by oxidation of sPxN-15 in the presence of 3% iodine. | 42 |
| Figure 3.9 Evolution of optical microscope image of a 67 μm wide and 340 μm long cut for dual s-ssPxN-10/6, and a 57 μm wide and 1000 μm long cut for dual s-ssPxN-5/6 over time. | 43 |
| Figure 3.10 Viscoelastic properties using a rheometer upon a cyclic change of oscillation force: 5% strain for 1500 s to 100 % for 500 s for dual s-ssPxN-15/6 exhibiting self-healability and s-ssPxN-5/6 with no self-healability. | 44 |
| Figure 4.1 Synthetic scheme of P5-COOH pentablock copolymer. For the P1-xK: x denotes the molecular weight of P1 precursor, OH-PEG-OH. DP of EO was calculated using the molecular weight of OH-PEG-OH. | 53 |
| Figure 4.2 ^1H -NMR spectra P1-10K (a), P3-3 (b) as examples and P5 (c) in CDCl_3 . ^1H -NMR spectrum of P5-COOH (d) in $\text{DMSO}-d_6$. | 56 |
| Figure 4.3 For P3-1 triblock copolymer, sol-gel transition in the presence of a catalytic amount of EDSH in DMF at 42 wt % (a), digital image (inset of b) and viscoelastic properties by frequency sweep mode (b) of disulfide-crosslinked gels prepared by thermal activation method. | 58 |

| | |
|---|----|
| Figure 4.4 Dual crosslinked gels with 1 and 2 equivalent of FeCl_3 (a) and the viscoelastic properties by frequency sweep mode of dual crosslinked gels prepared with 1 equivalent of FeCl_3 (b)..... | 59 |
| Figure 4.5 Digital images of dual crosslinked gels with a cut (a) after two parts were brought into contact (b), after healing 24 hrs (c) stretching the healed crosslinked networks (d) after stretching process (e); as well as without cut before (f) and after stretching (g). | 60 |
| Figure 4.6 Viscoelastic properties using a rheometer upon a cyclic change of oscillation force: 5% strain for 1500 s to 100 % for 500 s for dual crosslinked gels..... | 61 |
| Figure 4.7 Digital images of penetrating cut on disulfide-crosslinked gels in the presence of DMF (42 wt%) at 80 °C (a) and optical microscopy images of the cut (260 μm wide) at room temperature with the aid of chloroform over time (b). | 62 |
| Figure A.1 ^1H -NMR spectra of P1-3K (a), P1-6K (b) and P1-22K (c) in CDCl_3 | 74 |
| Figure A.2 ^1H -NMR spectra of P3-1 (a), P3-2 (b) and P3-4 (c) in CDCl_3 | 75 |
| Figure A.3 GPC traces of P3 triblock copolymers..... | 76 |
| Figure A.4 GPC traces of P5 pentablock copolymer | 77 |

List of Schemes

| | |
|--|----|
| Scheme 3.1 Illustration of our method utilizing click-type photo-induced thiol-ene radical addition and oxidation to synthesize dual sulfide-disulfide crosslinked networks (s-ssPxNs)..... | 30 |
| Scheme 4.1 Illustration of our approach to prepare dual crosslinked networks based on a novel pentablock copolymer exhibiting dual self-healing through covalent disulfide exchange reaction and supramolecular metal-ligand interactions..... | 48 |

List of Tables

| | |
|--|----|
| Table 3.1 Characteristics and properties of thiol-ene reactive blends of P2-ene with various amounts of TriSH at various ratios of $[SH]_0/[vinyl]_0$ upon UV irradiation..... | 37 |
| Table 3.2 Characteristics and properties of dual s-ssPxNs prepared by oxidation of sPxN precursors in the presence of iodine. ^{a)} | 40 |
| Table 4.1 Characteristics of triblock copolymer (P3) | 56 |

List of Abbreviations

| | |
|----------------------|--|
| ¹ H-NMR | Proton nuclear magnetic resonance |
| AFM | Atomic force microscopy |
| AMBN | 2,2'-azobis(2-methybutyronitrile) |
| ATRP | Atom transfer radical polymerization |
| AuNP | Gold nanoparticle |
| BCP | Block copolymer |
| BM | 1,1'-(methylenedi-4,1-phenylene)bismaleimide |
| Br-iBuBr | α -Bromoisobutyryl bromide |
| BTP | 2,6-bis(1,2,3-triazole-4-yl)pyridine |
| CD | Cyclodextrin |
| CDCl ₃ | Deuterated chloroform |
| CF ₃ COOH | Trifluoroacetic acid |
| CMC | Critical micellar concentration |
| CNC | Cellulose nanocrystal |
| COOH | Carboxylic acid |
| CRP | Controlled radical polymerization |
| CuBr | Copper(I) bromide |
| DA | Diels-Alder |
| DCC | <i>N,N'</i> -Dicyclohexyl carbodiimide |
| DCM | Dichloromethane |
| DCPD | Dicyclopentadiene |
| DEU | 1,1-diethylurea |

| | |
|------------------|---|
| DMF | Dimethylformamide |
| DMPAc | 2,2-dimethoxy-2-phenylacetophenone |
| DP | Degree of polymerization |
| DSC | Differential scanning calorimetry |
| DTT | DL-Dithiothreitol |
| E ₃ N | Triethylamine |
| EHMA | 2-ethylhexyl methacrylate |
| Fc | Ferrocene |
| Fe ³⁺ | Iron ion |
| FRP | Free radical polymerization |
| FRP | Free radical polymerization |
| FT-IR | Fourier transform infrared spectroscopy |
| GC | Gas chromatography |
| GMA | gGlycidyl methacrylate |
| GPC | Gel permeation chromatography |
| HEMA | 2-hydroxyethyl methacrylate |
| HMssEt | Pendant disulfide-labeled methacrylate monomer |
| HO-ss-iBuBr | 2-Hydroxyethyl-2-(bromoisobutyl)ethyl disulfide |
| HUB | Hindered urea bond |
| KBr | Potassium bromide |
| LA | 3,6-Dimethyl-1,4-dioxane-2,5-dione (lactide) |
| LiBr | Lithium bromide |
| Mebip | 2,6-Bis(1'-methylbenzimidazolyl)pyridine |
| MeOH | Methanol |
| M _n | Number average molecular weight |

| | |
|----------------|--|
| M _w | Weight average molecular weight |
| PAA | Poly(acrylic acid) |
| PA-Cl | 4-pentenoyl chloride |
| PBA | Poly(n-butyl acrylate) |
| PDI | Polydispersity |
| PEG | Poly(ethylene glycol) |
| PMDETA | N,N,N,N,N-pentamethyldiethylenetriamine |
| PMMA | Poly(methyl metacrylate) |
| PPMS | Polydimethylsiloxane |
| PS | Poly(styrene) |
| RAFT | Reversible addition fragmentation chain transfer |
| ROMP | Ring opening metathesis polymerization |
| SEM | Scanning electron microscope |
| SH | Thiol |
| SS | Disulfides |
| TBEU | 1-(t-butyl)-1-ethylurea |
| tBMA | Tert-butyl methacrylate |
| TDCB | Tapered double-cantilever beam |
| TDS | Thiuram disulfide |
| T _g | Glass transition temperature |
| TGA | Thermal gravimetry analysis |
| THF | Tetrahydrofuran |
| TriSH | Tris(3-mercaptopropionate) |
| Upy | 2-ureido-4-pyrimidinone |
| UV-vis | Ultraviolet-visible |

Chapter 1

Introduction

1.1 Brief overview of my research and goals

My Masters' research focuses on the exploration of reversible (dynamic) disulfide chemistry for the development of efficient methods to synthesize advanced crosslinked polymeric materials exhibiting self-healability at ambient temperature with no external aids. Well-known synthetic techniques in organic and polymer chemistry - including free radical polymerization (FRP), controlled radical polymerization through atom transfer radical polymerization (ATRP), and post-modification methods - were combined to synthesize two new disulfide-crosslinked self-healable networks: 1) dual disulfide-sulfide covalently crosslinked networks by FRP and photo-induced thiol-ene addition and oxidation reactions, and 2) dual covalent disulfide- and physical metallo-complex-crosslinked networks based on a novel pentablock copolymer by ATRP and hydrolytic cleavage reaction. Utilizing the unique reversible/dynamic nature of covalent disulfide and physical metal-ligand interactions, the developed materials exhibit low-temperature self-healing behavior and preferable viscoelastic properties.

1.2 Self-healing in crosslinked networks

Numerous strategies have been proposed for developing self-repairing polymeric materials which can be categorized into extrinsic self-healing and intrinsic self-healing materials (Figure 1.1). Extrinsic self-healing approach requires the encapsulation of additional healing agents such as catalysts and crosslinkers in capsule-like containers (microcapsules) to form porous composites. Upon physical damages, the cracks break microcapsules. Additional healing agents are released from the microcapsules to fill damaged cracks. Then, the desired polymerization takes place inside the crack to initiate self-repairing. This approach can heal relatively large areas of damaged parts; however, self-healing is limited to a single event, since healing agents in microcapsules are depleted in the matrix. In contrast, intrinsic self-healing is the advanced method because it utilizes dynamic (reversible) linkages that are embedded to form dynamic crosslinked networks, allowing repeatable self-repairing. A variety of covalent dynamic

linkages has been incorporated in self-healable materials, including disulfide,^{1, 2, 3} hindered urea,^{4, 5, 6} alkoxyamine,⁷⁻⁸ diarylbibenzofuranone (a dimer of arylbenzofuranone),⁹ boronic ester,¹⁰⁻¹² and etc. Not only dynamic covalent linkages, but also various physical interactions such as hydrogen bonding,¹³⁻¹⁶ host-guest interaction,¹⁷ π - π interaction,¹⁸⁻¹⁹ and metallo-complex interaction²⁰⁻²⁵ have been explored for the development of self-healable materials. Details in recent strategies that allow for the development of a variety of intrinsic and extrinsic self-healable materials (or systems) are summarized in Chapter 2.

Most self-healing materials based on covalent linkages often suffer from stiffness which limits the dynamic behavior of the system. Self-healing of such systems may require external stimuli such as heating, the aid of solvent or catalyst. Meanwhile, many self-healing materials based on physical interactions tend to have low mechanical strength but have a tendency to self-repair at ambient conditions. To overcome this dilemma, a multiphase design for self-healing materials has been proposed in which consists of hard phase for mechanical strength and soft phase for autonomous self-healing.²⁶ Also, a dual crosslinked self-healing system using both supramolecular and covalent networks have been studied.²⁷

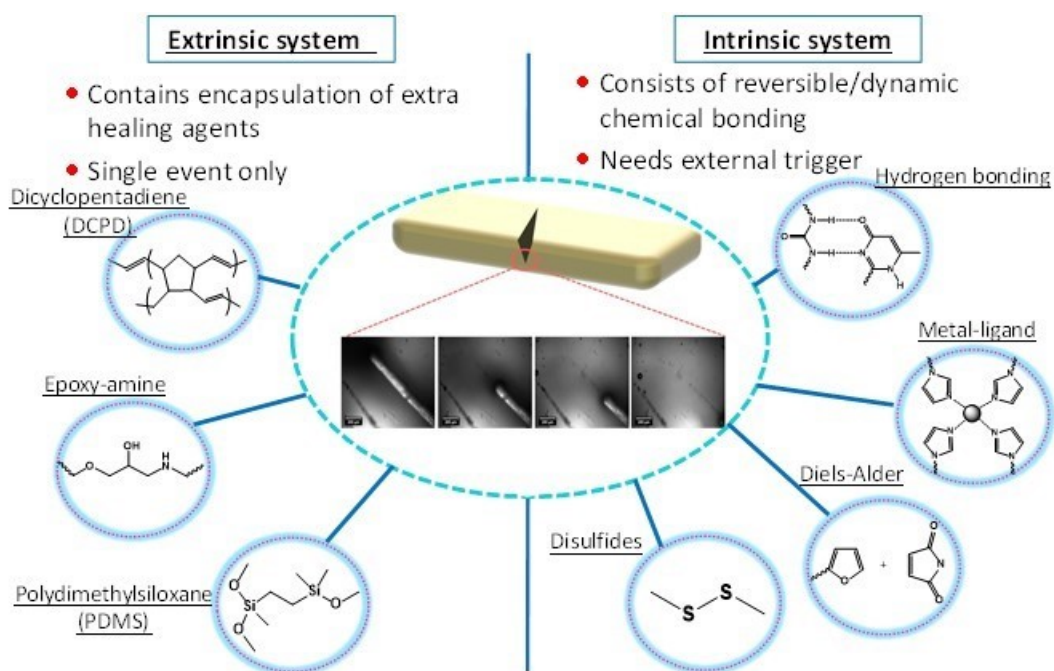


Figure 1.1 Schematic illustration of extrinsic and intrinsic self-healing methods.

1.3 Scope of my thesis

The purpose of my thesis is to provide detailed studies on the synthesis and characterization of dynamically-crosslinked polymeric materials exhibiting self-healability through mainly disulfide chemistry and dual metal-ligand interactions. Chapter 2 presents a literature review focusing on recent strategies and chemistries that have explored for the development of a variety of novel self-healable materials.

Chapter 3 presents the dually crosslinked self-healable composites with sulfide and disulfide linkages. The sulfide linkage as permanent crosslink provides mechanical strength, whereas the disulfide linkage as a reversible crosslink induces self-healing in the networks. These crosslinked materials can rapidly self-heal micro-scale cracks (40 – 70 μm) within 0.5 s to 30 min at room temperature with no aid of external stimuli. They had reversible viscoelastic properties that show a unique self-healing elasticity.

Chapter 4 describes the synthesis of a multiblock copolymer composed of a central poly(ethylene glycol) block and various functional symmetric blocks labeled with two distinct self-healable units: pendant disulfide linkages and carboxylic acid groups. The copolymer was crosslinked with dual disulfide linkages through disulfide-thiol exchange reaction and metallo-complexation through physical metal-ligand interactions. The resulting dually-dynamic networks exhibit rapid self-healing at ambient condition.

Lastly, the concluding remarks and future perspectives are discussed in Chapter 5.

Chapter 2

Review of recent strategies to develop self-healable crosslinked networks

(This chapter is reproduced the article published in *Chemical Communications*, **2015**, 51, 13058-13070 with permission from the publisher)

2.1 Introduction

Three-dimensionally crosslinked polymers are effective building blocks to develop a variety of novel multifunctional materials for various applications in nanoscience, biotechnology, and industrial fields.²⁸⁻³⁶ The effectiveness of high-performance crosslinked materials is due to their dimensional stability, mechanical strength, thermal stability, and solvent resistance. Introducing the built-in ability to repair physical damage and cracks can effectively prevent catastrophic failure, thus extending the lifetime of materials. Consequently, the development of self-healing materials defined as "materials where damage automates a healing response" has currently attracted significant attention.³⁷⁻³⁸

A number of strategies have been reported to develop self-healing polymers. Based on the nature of self-healing and external triggers applied, they can be classified into non-autonomous and autonomous systems. Non-autonomous self-healing polymers require external triggers such as light, temperature, and pH, whereas autonomous self-healing materials do not need any triggers to initiate the self-healing process. Alternatively, numerous strategies can be classified as intrinsic and extrinsic.³⁹⁻⁴⁰ Extrinsic self-healing involves the encapsulation of external healing agents, in the form of microcapsules or fibers, impregnated deliberately in the polymer matrix.⁴¹⁻⁴² When cracks or damages occur, the contents encapsulated in these containers are released to fill the disrupted parts, which then begin self-repairing either by polymerization or chemical reactions. In contrast to extrinsic self-healing occurring in a single event, intrinsic self-healing is repeatable and occurs in multiple events. Intrinsic self-healing materials are designed with

reversible crosslinks, and self-healing is accomplished by bonding upon mechanical damage to the system.⁴³⁻⁴⁴ When the damage is below the critical limit, the damaged portion can be rejoined with the aid of either chemical crosslinking through dynamic covalent bond formation⁴⁵ or physical crosslinking through supramolecular (non-covalent) interactions.¹⁹ This article reviews the recent advances in the design and development of crosslinked materials exhibiting self-healability, with a focus on the synthesis and methodology of intrinsic and extrinsic self-healing polymers reported in recent years.

2.2 Intrinsic self-healing methods utilizing reversible chemical crosslinking methods

The design of these materials involves the incorporation of dynamic covalent bonds as crosslinkages in self-healable networks. These reversible linkages are later utilized through the reformation of covalent bonds to reattach the fractured materials caused by mechanical forces (i.e. cracks or cuts). Unlike physical crosslinking methods based on supramolecular interactions, the chemical crosslinking methods utilizing reversible covalent bond formation provide higher mechanical strength and dimensional stability. These features can be advantageous in the development of tough self-healable materials. Figure 2.1 illustrates several reversible dynamic linkages and chemistries that have been explored for the development of novel reversible self-healable materials.

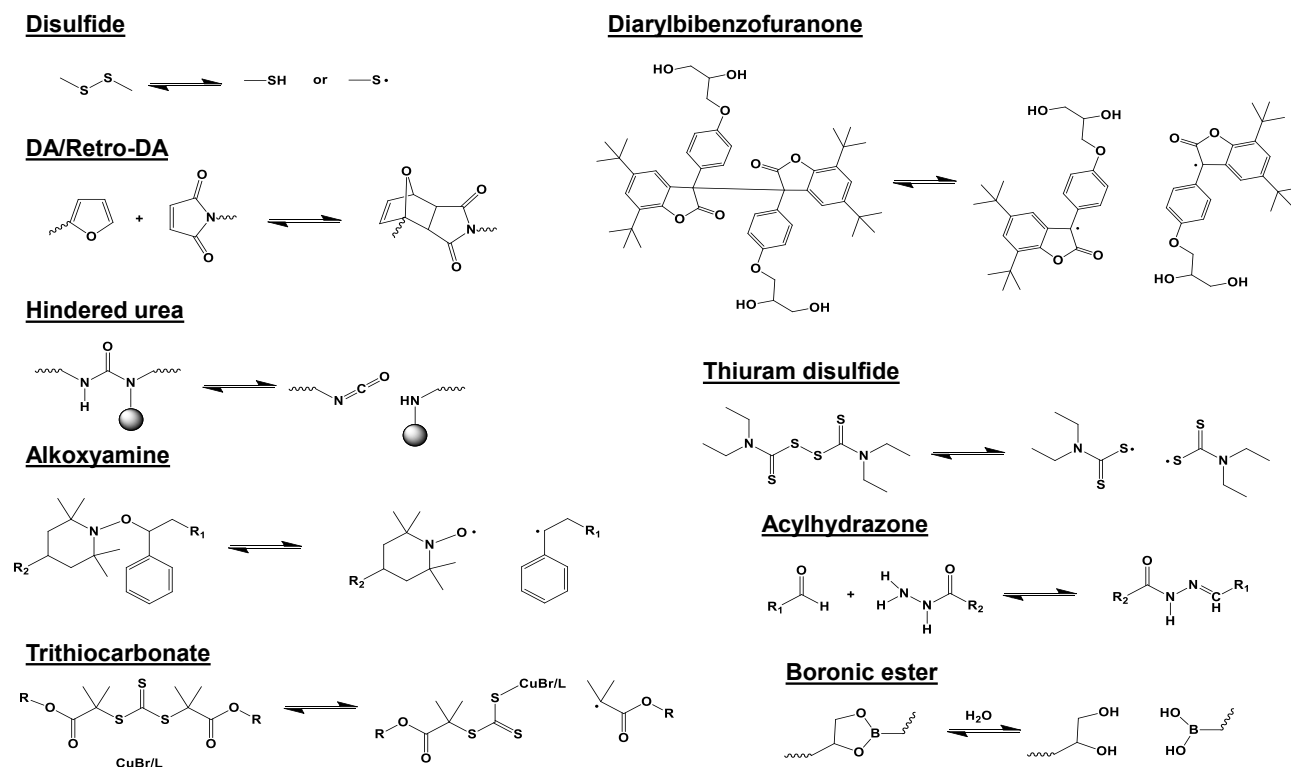


Figure 2.1 Reversible dynamic linkages and chemistries that have been explored for the development of novel reversible self-healable materials.

2.2.1 Redox disulfide chemistry

Disulfide linkages (SS) are cleaved to the corresponding thiols either under a reducing condition in the presence of reducing agents such as phosphines or through thiol-disulfide exchange reactions in the presence of thiols.⁴⁶⁻⁴⁷ They can also be cleaved to the corresponding thiyl radicals under conditions such as thermal scission,⁴⁸ mechanical stress,⁴⁹ or photoirradiation.⁵⁰ Reversibly, the formed thiols or thiyl radicals are utilized to reform disulfide bonds by several reactions: oxidation of thiols, thiol-disulfide exchange reaction, and recombination of thiyl radicals. Further, disulfide linkages can be exchanged through disulfide metathesis (or disulfide rearrangement) catalyzed by phosphine,⁵¹ tertiary amine,⁵²⁻⁵³ or photoirradiation.⁵⁴ These unique redox chemistries enabling the reformation of dynamic disulfide bonds have been utilized in the design and construction of disulfide-containing self-healable materials.^{1-3, 55-58}

Polysulfide-crosslinked epoxy-based thermoset materials with a glass transition temperature (T_g) of $-35\text{ }^{\circ}\text{C}$ were synthesized by polycondensation via a click-type epoxy-thiol reaction of an epoxy resin bearing disulfide linkages and a polythiol. These materials are designed to have multiple disulfide linkages positioned in long side chains tethered from crosslinked networks; this enables the enhanced mobility of disulfide linkages in damaged areas (i.e. cracks or scratches). Initial cuts disappeared and mechanical strength was fully restored within 1 hr at $60\text{ }^{\circ}\text{C}$.^{1,55} In addition, not only the number (or density) but also the mobility of disulfide linkages available within polymeric network are important parameters that significantly influence self-healability through disulfide redox chemistry.⁵⁶

Methacrylate-based disulfide-crosslinked materials were synthesized by atom transfer radical polymerization (ATRP) for the chain extension of a disulfide-functionalized dimethacrylate from star-shaped core-crosslinked copolymers as macroinitiators. The materials are composed of core-crosslinked stars bearing poly(butyl acrylate) arms, with the average number of arms per star-shaped core = 23, which are crosslinked with dynamic disulfide linkages at their branched peripheries. Sol-gel transition through a reduction-oxidation process allows for the preparation of reversibly disulfide-crosslinked star-polymer networks. As seen in Figure 2.2, atomic force microscopy (AFM) analysis shows a decrease in the depth of cuts over the time, suggesting the occurrence of self-healing at room temperature.²

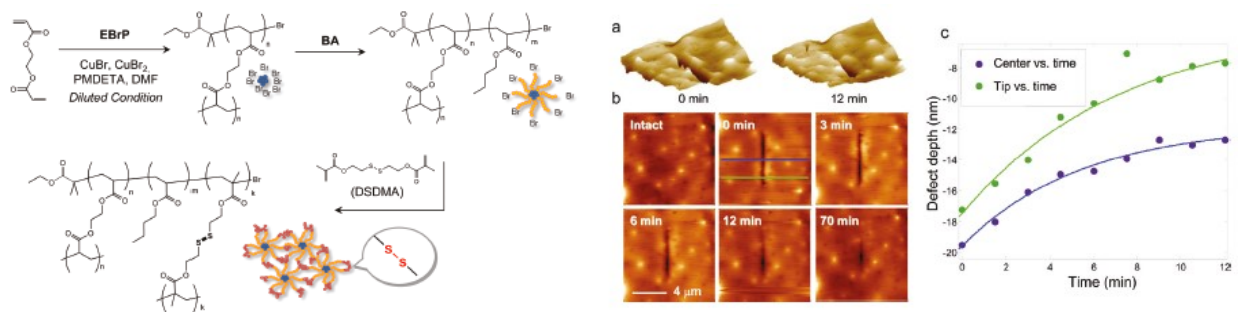


Figure 2.2 Chemical structure of disulfide-crosslinked star-shaped copolymer (left) and time dependent change of height mode AFM image for cut on the surface of reversibly disulfide-crosslinked star-polymer network (right): 3D images (a), 2D height mode images (b), and evolution of damage depth for 12 min at two positions (c).² Copyright 2012 American Chemical Society.

More recently, novel dual-sulfide-disulfide crosslinked materials (s-ssPxNs) based on linear methacrylate copolymers were developed by utilizing a combination of photo-induced

thiol-ene radical addition and oxidation. As illustrated in Figure 2.3, permanent sulfide-crosslinkages retain the integrity of self-healable s-ssPxN materials with high mechanical strength upon physical damage, while dynamic disulfide crosslinkages ensure rapid and room temperature self-healing in cracks. Methacrylate copolymers having pendant vinyl groups were synthesized by free radical polymerization (FRP) followed by post-modification. They were then mixed with a polythiol in a non-stoichiometric balance to form lightly crosslinked networks having excess thiols (sPxNs) upon UV irradiation. Subsequent oxidation on sPxNs yielded dual s-ssPxNs with self-healable disulfide linkages. The resulting s-ssPxN networks exhibit the occurrence of rapid self-healing within 30 seconds to 30 minutes, as well as self-healing elasticity with reversible viscoelastic properties.⁵⁹

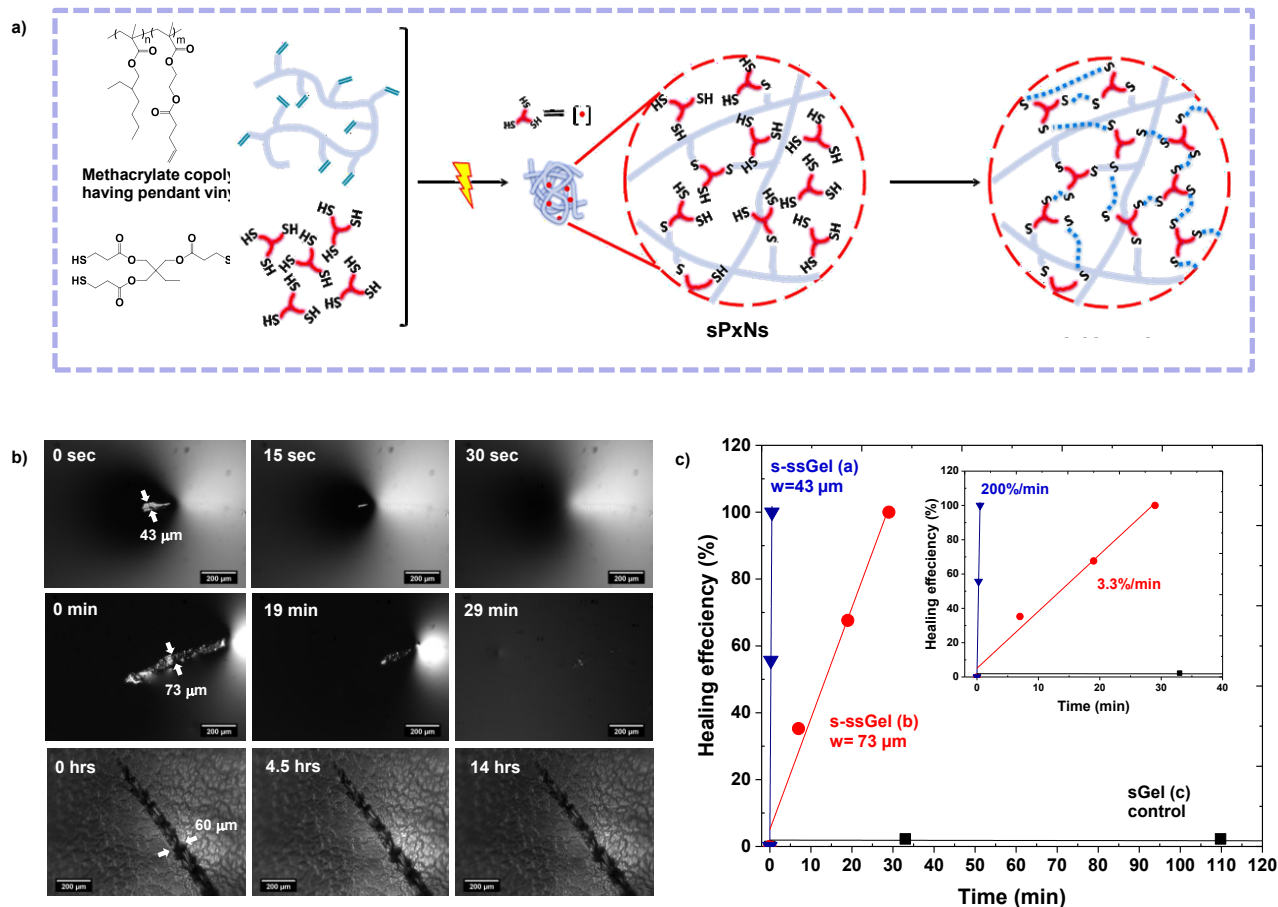


Figure 2.3 Illustration of a novel method utilizing click-type photo-induced thiol-ene radical addition and oxidation to synthesize dual sulfide-disulfide crosslinked networks (s-ssPxNs) (a), evolution of microscope images (b) and kinetics of self-healing (c) over time at room temperature for dual s-ssPxN

with different cut sizes of 43 μm wide (upper) and 73 μm wide (middle), compared with a control of sPxN with no disulfide (bottom). Copyright 2015 Wiley Interfaces.

2.2.2 Diels-Alder (DA)/retro-DA chemistry

DA reaction is a thermally-induced [4+2] cycloaddition of a diene and a dienophile. Furan group and maleimide groups are generally used as typical diene and dienophile, respectively. The resulting DA adduct undergoes a cleavage reaction (called retro-DA reaction) at high temperatures, re-generating the corresponding diene and dienophile. They then reform DA linkages. This reversible DA/retro-DA reaction has been utilized for the development of thermally-induced, self-healable materials. Various approaches that have been explored can be classified based on the chemical structures of polydienes and polydienophiles for step-growth polymerization through polyaddition.

Approach I utilizes the direct polyaddition of small molecules of polydienes and polydienophiles at a moderate temperature ($\approx 60\text{-}80\text{ }^{\circ}\text{C}$).⁶⁰⁻⁶¹ As illustrated in Figure 2.4, thermally remendable crosslinked materials were synthesized by polyaddition of a four-arm furan-labeled monomer (4F) and a three-arm maleimide-labeled monomer (3M). The rate of polymerization increased with an increasing DA reaction temperature. For the resulting DA-crosslinked materials, the healing efficiency of cracks through retro-DA reactions was 50% at 150 $^{\circ}\text{C}$ and 41% at 120 $^{\circ}\text{C}$.⁶⁰ Single-component DA-crosslinked polymeric materials were synthesized by polyaddition of a bifunctional monomer functionalized with cyclopentadiene acting as both diene and dienophile. The monomer was generated by the retro-DA reaction of the corresponding dicyclopentadiene-based monomer. The mending efficiency of the network was 40-60%.⁶² These materials were further used to enhance interlaminar properties in epoxy-based composites. An introduction of a plasticizer into DA-crosslinked materials can enhance the reformation efficiency of DA-adducts followed by retro-DA reaction. For example, the use of benzyl alcohol as a plasticizer allows for the improvement of self-healing recovery in DA-crosslinked materials composed of a polyfunctional furan and 1,1'-(methylenedi-4,1-phenylene)bismaleimide (BM). Such enhancement is attributed to an increase in free volume and molecular mobility of the polymeric network.⁶³ Details on the synthesis and self-healing of DA-based crosslinked materials have been summarized in a review.⁶⁴

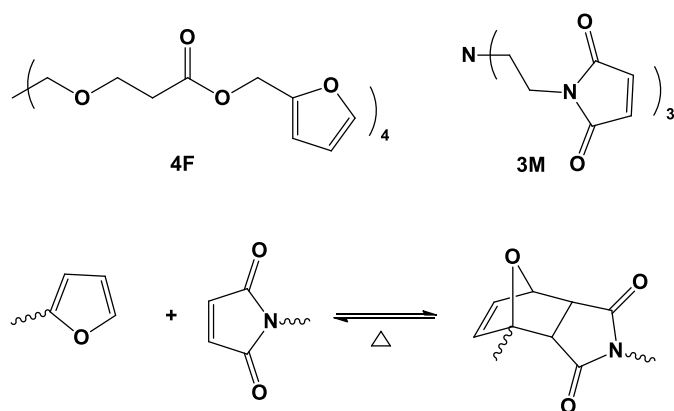


Figure 2.4 Illustration of Polycondensation through DA reaction of a four-arm furan-labeled monomer (4F) and a three-arm maleimide-labeled monomer (3M) to form DA-crosslinked materials.⁶⁰

Approach II involves the synthesis of polymethacrylates bearing pendant furan groups by chain-growth polymerization of a methacrylate functionalized with a furan group. Random copolymers having pendant furan groups were synthesized by controlled radical polymerization methods including ATRP⁶⁵⁻⁶⁷ or reversible addition fragmentation chain transfer (RAFT) polymerization.⁶⁸ The resulting copolymers were crosslinked with BM through DA reactions. FT-IR technique was used to investigate thermal reversibility of the resulting DA-crosslinked networks by monitoring a decrease in a peak for furan rings (1010 cm^{-1}) for DA reaction and a disappearance of a peak for C=C vibration (1630 cm^{-1}) for retro-DA reaction. The DA linkages were disrupted to the corresponding diene and dienophile at $100\text{ }^{\circ}\text{C}$, and then restored upon cooling down to room temperature. Scanning electron microscopy (SEM) images show that the distinctive cracks made on the surface of networks were completely healed upon heating at $120\text{ }^{\circ}\text{C}$ for 4 hrs.⁶⁷ Further, ABA-type triblock copolymers consisting of a soft poly(2-ethylhexyl acrylate) in the middle (B block) and a glassy and hard poly(furfuryl methacrylate) at the ends (A blocks) were synthesized by ATRP. The resulting polymers formed DA-crosslinked networks in the presence of BM crosslinker. Similar results of thermally-driven self-healing behavior on damaged films were observed (Figure 2.5).⁶⁹

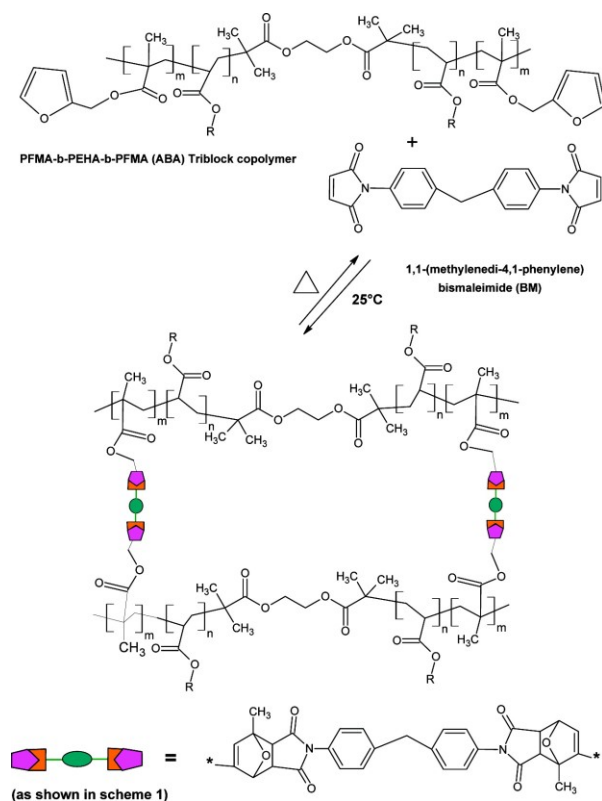


Figure 2.5 Schematic illustration of DA and retro-DA reaction occurred in reactive mixtures consisting of a ABA triblock copolymer having pendant furfuryl groups with 1,1'-(methylenedi-4,1-phenylene)bismaleimide for thermally-driven self-healing.⁶⁹ Copyright 2010 American Chemical Society.

Approach III involves the synthesis of linear polymers having pendant furan groups by post-modification of polybutadiene,⁷⁰⁻⁷¹ polyamides,⁷² or polyketones⁷³ with furfuryl amine. For example, furan-functionalized polyketones were synthesized by Paal-Knorr reaction of the polyketones with furfuryl amine. The resulting polyketones were then mixed with BM to form DA-crosslinked materials at 50 °C. Repeatabile self-healing of the materials through retro-DA reaction was observed at 110 °C within <30 min.⁷³

Other approaches have also been reported to synthesize self-healable materials; including DA-crosslinked networks based on epoxy resin by polycondensation⁷⁴⁻⁷⁵ and DA-labeled block copolymer at the block junction by ATRP.⁴⁰

2.2.3 Hindered urea chemistry

Urea bonds bearing a bulky group on the nitrogen atom can dissociate into the corresponding isocyanate and amine; they then reversibly form the urea bonds.⁴ This dynamic hindered urea chemistry has been explored in the development of catalyst-free, low-temperature crosslinked self-healing of poly(urethane-urea) containing hindered urea bonds (HUBs). As illustrated in Figure 2.6, the HUBs in cuts were involved in the reverse process of typical urea bond formation, leading to the occurrence of autonomous repairing for 12 hrs at 37 °C.⁵ This chemistry has been further explored to synthesize hydrolyzable polyureas bearing HUBs.⁶

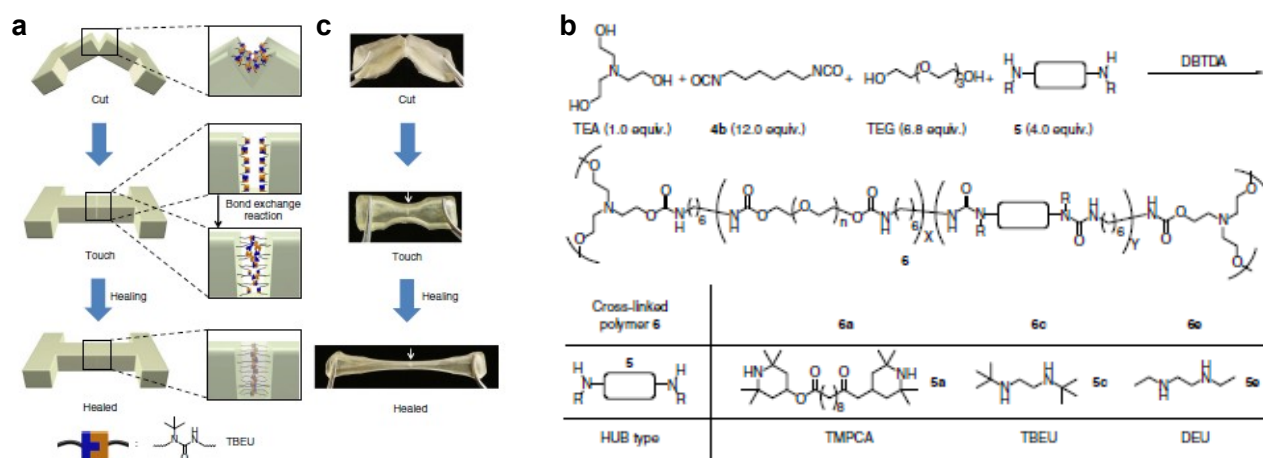


Figure 2.6 Schematic illustration of self-healing process (a), chemical structures and ratios of components used for the synthesis (b), and selected snapshots during the course of self-healing experiments of HUB-based crosslinked poly(urethane-urea) materials (c). TMPCA: 2,2,6,6-tetramethylpiperidinylcarboxamide, TBEU: 1-(t-butyl)-1-ethylurea, and DEU: 1,1-diethylurea.⁵ Copyright 2014 Nature Publishing Group.

2.2.4 Other reversible chemistry

Thiuram disulfide (TDS) moieties were introduced into polyurethane-based crosslinked materials. When exposed to visible light, TDS units underwent radical reshuffling with neighboring TDS units to reform disulfide bonds through radical transfer reaction or radical crossover reaction. This disulfide reshuffling induced self-healing on damaged areas. Their self-healing behavior was followed by cutting a cylindrical sample into two pieces, which were contacted under visible light at room temperature. After 24 hrs, the ruptured pieces were re-

annealed together, exhibiting similar mechanical properties as before the physical damage.⁷⁶ In addition, alkoxyamine,⁷⁻⁸ diarylbibenzofuranone (a dimer of arylbenzofuranone),⁹ trithiocarbonate,⁷⁷ acylhydrazone,⁷⁸⁻⁸⁰ and imine,⁸¹ as well as olefin metathesis,⁸² boronic ester,¹⁰⁻¹² and coumarin dimer⁸³ have also been explored for the development of intrinsic self-healing materials.

2.3 Intrinsic self-healing methods utilizing reversible physical crosslinking

The methods utilize non-covalent interactions, typically hydrogen bonding, π - π , metal complexation, ionic, and host-guest interactions. The formed physical crosslinks are easily disrupted in response to external stimuli such as pH, temperature, heat, and mechanical stress. Such physical disruptions are restored to their original interactions due to the unique reversibility of the physical crosslinks.

2.3.1 Hydrogen bonding interactions

Hydrogen bonding strategy for the development of self-healable supramolecular materials requires the introduction of hydrogen bonding motifs as donors and acceptors into polymers as in pendant chains, in arms, or at chain ends. Widely-explored hydrogen bonding motifs include 2-ureido-4-pyrimidinone (Upy)⁸⁴ and secondary amide groups. Thymine/2,6-diaminotriazine,⁸⁵ urea moieties,⁸⁶ and carboxylic acids⁸⁷⁻⁸⁸ have also been used. These groups enable the formation of reversible supramolecular crosslinking networks through their intermolecular hydrogen bonding. Upon physical damages, the supramolecular crosslinks are disrupted; however, they can be reformed because of their unique reversibility. Monofunctional and difunctional Upy-conjugated poly(ethylene glycol) (UPy-PEG) was synthesized by a facile conjugation of UPy and PEG. The mixture of these conjugates self-assembled in water to form fibril-embedded hydrogels. Their structural and mechanical properties, as well as self-healability, were regulated by varying the ratios of monofunctional to crosslinking difunctional UPy-PEG.⁸⁹

A concern for most self-healable materials utilizing hydrogen bonding interactions is their weak mechanical strength due to the use of soft polymers as self-healable matrix. A promising strategy that has been proposed to overcome this challenge is the incorporation of hard domains into soft supramolecular polymeric matrix containing hydrogen bonding motifs. The presence of hard domains provides toughness and mechanical strength, while soft matrix

promotes the mobility of hydrogen bonding groups for self-healing. For example, well-controlled bottle brush polymers were synthesized by a combination of FRP and ATRP. They consist of polystyrene (PS) backbone (high T_g) as a hard phase and polyacrylate amide (PA-amide) brushes (low T_g) as a soft phase. The brush polymers collapsed into core-shell nanostructures, which further assembled to two-phase nanostructures. They consist of hard polystyrene domains microphase-separated in a soft matrix, which contains secondary amide groups that are capable of forming dynamic supramolecular networks, having both hydrogen bond donor and acceptor functionalities. The resulting supramolecular assembly was reversibly broken and reformed, affording spontaneous self-healing behavior (Figure 2.7).⁹⁰ Diblock copolymers synthesized by RAFT polymerization consist of a hard PS block and a soft poly(n-butyl acrylate) (PBA) block, functionalized with an UPy motif at one end, thus forming PS-PBA-UPy. Dimerization of two UPy units allowed for the synthesis of well-controlled ABA triblock copolymers, thus forming PS-b-PBA-(UPy-UPy)-PBA-b-PS. These copolymers formed a microphase-separated thermoplastic elastomers of hard PSt domains in PBA soft matrix with reversible hydrogen bonding interactions to afford dynamic self-healing properties.⁹¹ Similar approaches have also been reported, including ABA triblock copolymers with pendant amide groups in the A blocks,²⁶ core-shell particles having amide groups in arms,¹³ and polyurethanes having UPy groups.¹⁵

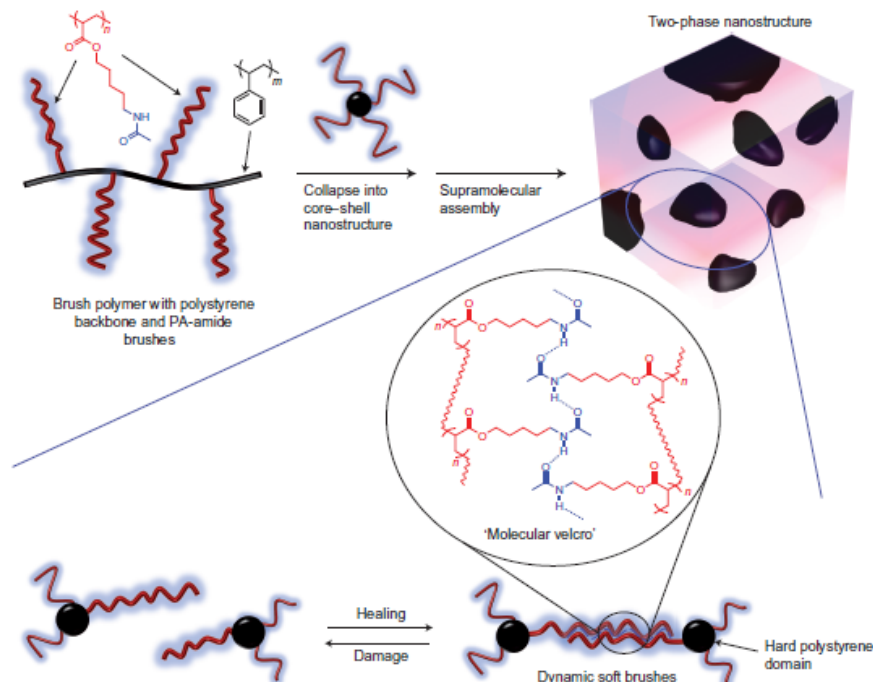


Figure 2.7 Schematic illustration of hydrogen-bonding brush polymer consisting of polystyrene backbone (high T_g) as a hard phase and polyacrylate amide brushes (low T_g) as a soft phase and its supramolecular assembly to form two-phase microstructures, consisting of hard polystyrene domains microphase-separated in soft matrix containing secondary amide groups that are capable of forming dynamic supramolecular networks.⁹⁰ Copyright 2014 Nature Publishing Group.

2.3.2 π - π interactions

Self-healing through dynamic π - π stacking utilizes aromatic units, mostly pyrene moieties as π -electron-rich residues and diimide units, as π -electron-deficient residues. The two residues form complexes adopting chain-folded conformation through π - π stacking interactions. These supramolecular interactions can be disrupted and reoriented upon thermal response. As a consequence, physical damages are subsequently healed. As a typical example, Figure 2.8 illustrates a polymer blend consisting of a chain-folding polydiimide (1) and a telechelic polyurethane with pyrenyl end groups (2). The reactive blend yielded supramolecular crosslinked material induced by π - π stacking with thermal reversibility. Self-healing behavior was observed at temperatures >50 °C.⁹²⁻⁹³ Further, the design of new monomers with multiple aromatic units⁹⁴ or the introduction of cellulose nanocrystals (CNCs)⁹⁵ and gold nanoparticles (AuNPs)⁹⁶ enhanced mechanical strength of the self-healable networks.

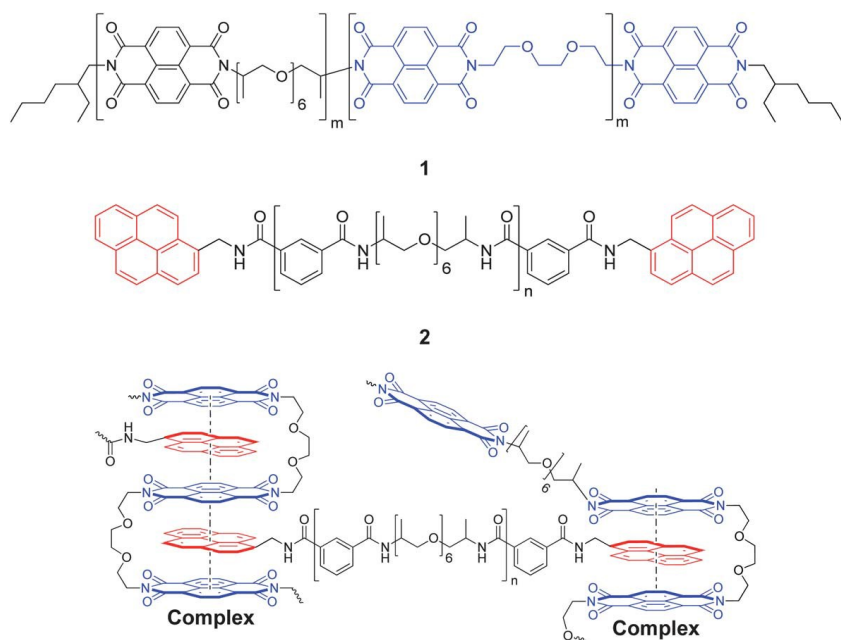


Figure 2.8 Illustration of π - π interaction between a polydiimide and a pyrenyl end-capped polymer.⁹⁶ Copyright 2013 Royal Society of Chemistry.

2.3.3 Metallo-supramolecular interactions

This method utilizes metal-ligand interactions where polymeric ligands are designed to have ligand motifs that bind to metal ions at the chain ends or in the side chains. Upon the incorporation of metal ions, such as Zn, Fe, Co, and Ni, linear supramolecular polymer or supramolecular crosslinked network can be formed through specific metal-ligand interaction. These interactions can be disrupted physically, thermally, or upon UV irradiation. Subsequent restoration of such interaction can induce self-healing behavior of the material.

2,6-Bis(1'-methylbenzimidazolyl)pyridine (Mebip) and its oxy-derivatives⁹⁷ have been used as a ligand motifs that bind to zinc ions. For example, poly(ethylene-co-butylene) copolymers having Mebip ligands at their termini were synthesized and interacted with Zn ions through metal-ligand interactions to form metallo-supramolecular polymers (Figure 2.9). The resulting network had relatively high mechanical strength with storage modulus (G') $\approx 10^7$ Pa. After exposure to UV, the Mebip-Zn interactions were electronically excited. The absorbed energies were converted into heat to induce the dissociation of network. When UV-light was off, the metal-ligand interactions were reassembled, leading to the occurrence of self-healing.⁹⁸ An

introduction of CNCs into the supramolecular mixture reinforced mechanical properties ($G' \approx 10^8$ Pa at higher concentration of Zn^{2+}).⁹⁹ In addition, poly(butyl acrylate-co-methyl methacrylate) bearing pendant Mebip units were synthesized. An addition of Zn metal ions resulted in the formation of metallo-supramolecular crosslinked network containing hard metal-ligand rich-domains phase-separated in soft polyacrylate phases. The healing process was observed both optically and thermally. Further unique triple shape memory transitions were studied at different temperatures.¹⁰⁰

Other ligand motifs have also been explored for the development of metallo-supramolecular self-healable materials, including 2,6-bis(1,2,3-triazole-4-yl)pyridine (BTP),¹⁰¹⁻¹⁰³ imidazole,¹⁰⁴ tyrosine,¹⁰⁵ polyethyleneimine,¹⁰⁶ triazole,¹⁰⁷ and terpyridine.¹⁰⁸⁻¹⁰⁹

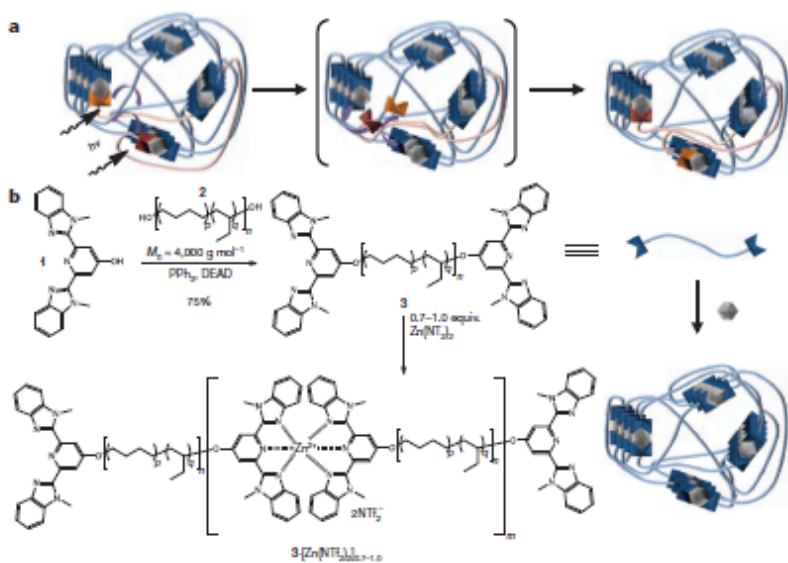


Figure 2.9 Schematic illustration of metal-ligand interaction between Mebip units and Zn ions⁹⁸. Copyright 2011 Nature Publishing Group.

2.3.4 Ionic interactions

This method toward reversible physical self-healing utilizes ionic crosslinking between anionic polymers and cationic species as metal ions, small molecules, or macromolecules. The

formed ionic crosslinking networks can be broken when physically disrupted and subsequently restored in response to change in stimuli at an ambient condition.

Multivalent ferric ions were used to form ionically-crosslinked self-healable materials with chemically-crosslinked hydrogels based on poly(acrylic acid) having pendant COOH groups¹¹⁰⁻¹¹¹ and catechol-functionalized polyallylamine.²¹ As seen in Figure 2.10, the ionically-crosslinked hydrogels with relatively low storage modulus ($G' \approx 10^4$ Pa) exhibit autonomous self-healing through dynamic bonding of physical crosslinking and migration of ferric ions.¹¹⁰ Cationic macromolecules (oligomers or polymers) have been used.¹¹²⁻¹¹³ One example is high-water-content moldable hydrogels consisting of sodium poly(acrylic acid), with a multivalent G3-dendrimer functionalized with terminal guanidinium ion groups in the presence of clay nanosheets.¹¹² Other ionically crosslinked hydrogels were prepared by ionic interactions of poly(allylamine) mixed with multivalent anions such as tripolyphosphate,¹¹⁴ or poly(N,N-dimethylacrylamide) with clay particles.¹¹⁵

Layer-by-layer approaches of anionic and cationic species through ionic interactions have also been explored. The resulting multi-layered hydrogels exhibit self-healing; further, healability was promoted by swelling and hydration in the presence of moistures.¹¹⁶⁻¹²⁰

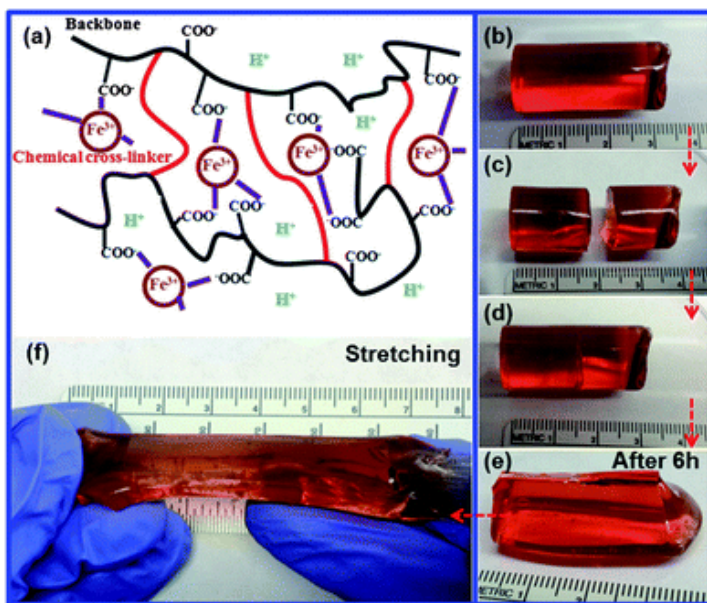


Figure 2.10 Schematic illustration of ionically-crosslinked hydrogels of poly(acrylic acids) with ferric ions (a) and digital images showing the occurrence of autonomous self-healing through dynamic bonding of physical crosslinking (b-f).¹¹⁰ Copyright 2013 Royal Society of Chemistry.

2.3.5 Host-guest interactions

Specific interlocking host-guest interactions are reversibly disassembled in response to stimuli such as redox potential, pH, and temperature. Such reversibility has been explored in the design of self-healing polymeric materials in the form of supramolecular hydrogels, nanofibers, and organo-gels. Details on synthesis and self-healing through host-guest interactions have been described in a review.¹⁷

Cyclodextrin (CD) moieties as host molecules and ferrocene (Fc) moieties as guest molecules have been used. Uncharged Fc moieties formed strong complexes with CD moieties in host-guest manner. On the other hand, charged Fc moieties upon oxidation induced the dissociation of host-guest complexes which can be restored under a reductive condition.¹²¹⁻¹²³ Poly(acrylic acid) (PAA) was modified with CD, forming PAA-CD, and with Fc, yielding PAA-Fc. As illustrated in Figure 2.11, the mixture of PAA-CD and PAA-Fc formed supramolecular hydrogels through host-guest interactions. Upon oxidation and reduction of Fc moieties, these two pieces were rejoined and the crack was sufficiently healed to form one gel after standing for 24 hrs.¹²¹ Two types of oligo(ethylene glycol) terminated with CD and Fc were synthesized and

mixed at a 1/1 mole ratio of host/guest units to form supramolecular fibrous nanostructures in aqueous solution due to interlocking host-guest interactions. Transmission electron microscopy images show self-degradation of nanofibrous structure upon oxidation and reassembly of degraded fibers upon reduction within 2 hrs.¹²³

Crown ether-based molecular recognition has been explored for the synthesis of self-healable materials.¹²⁴⁻¹²⁵ For example, copolymers based on poly(methyl methacrylate) having pendant crown ether units as host moieties was synthesized. These host moieties were crosslinked with alkyl dialkylammonium guest moieties, forming crosslinked organogels. A few minutes after their macroscopic damages, the occurrence of self-healing on cuts was visible to the naked eye. Further, the self-healable gels show repeatable restoration of G' and G'' .¹²⁴

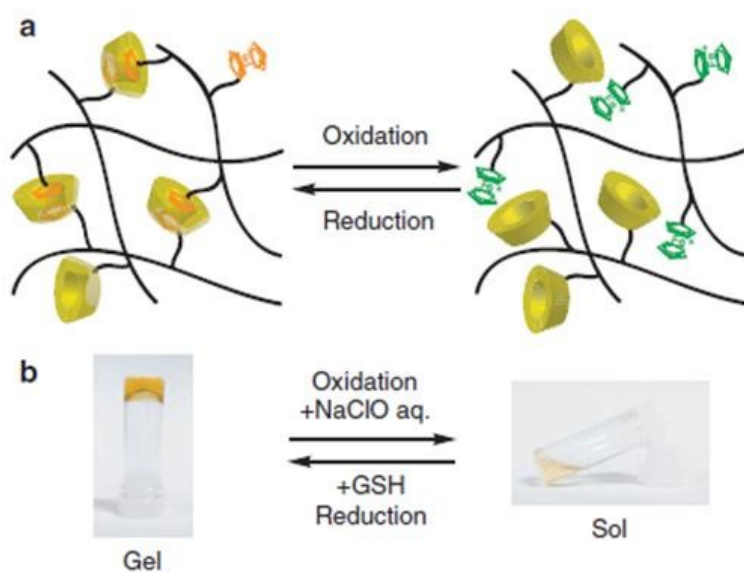


Figure 2.11 Schematic illustration of host-guest interactions between PAA-CD and PAA-Fc to form self-healable supramolecular hydrogels (a) and their digital images showing gel-sol transition .¹²¹ Copyright 2011 Nature Publishing Group.

2.4 Extrinsic self-healing methods

In contrast to intrinsic self-healing systems, where materials themselves are self-healable through reversible chemical reactions or physical interactions, extrinsic self-healing systems contain external healing agents such as monomers, catalysts, or crosslinkers in the forms of

capsules, fibers, or vasculatures. These reactive containers are impregnated in polymeric matrix. When crack or damage occurs, the healing agents are released into cracks from ruptured containers to heal the materials by a designed polymerization or a chemical reaction. Extrinsic self-healing materials can be categorized into two self-healing systems: capsule-based and microvascular. This section focuses on only capsule-based extrinsic self-healing materials. Details for microvascular systems are summarized in review and recent publications.¹²⁶⁻¹²⁷

Capsule-based extrinsic self-healing systems require the design of micron-sized capsules that sequester either healing agents or catalysts. Microcapsules, in most cases, are embedded in polymeric matrix (or coatings) that contain healing agents that are needed for self-healing. Upon the rupture of the microcapsules via puncture or crack in the matrix, the sequestered healing agents flow into crack planes via capillary action and mix with other healing agents for polymerization or crosslinking to plug crack planes. A number of parameters have to be considered in the design and synthesis of microcapsules for effective microcapsule-based self-healing. These parameters include not only size (micron to nano) and uniform distribution of capsules but also mechanical strength and miscibility of shells with matrix. The shells should be designed to be strong enough to retain the integrity of capsules embedded in the dried coatings. Typical shell-forming polymers include urea-formaldehyde, melamine-formaldehyde, and polyurethane resins. They are generally prepared by *in situ* and interfacial encapsulation techniques utilizing the occurrence of polymerization at interfaces of droplets in an oil-in-water (o/w) emulsion. Several strategies using well-known polymerization methods and chemical reactions have been explored to develop capsule-based extrinsic self-healing materials.

2.4.1 Ring opening metathesis polymerization (ROMP)

The first generation of microcapsule-based self-healing materials has utilized living ROMP.¹²⁸ Microcapsules of dicyclopentadiene (DCPD) in urea-formaldehyde shells (50 - 200 μm) were prepared by a general protocol for interfacial encapsulation method. Hydrophobic DCPD monomers were emulsified in the presence of ethylene maleic anhydride copolymers in aqueous solution containing urea. Under agitation, an addition of formaldehyde yielded microcapsules, which were isolated and air-dried. As illustrated in Figure 2.12a, the formed DCPD-containing microcapsules were embedded in epoxy-based matrix formulated with a first-generation Grubb's catalyst. When mechanical damage occurred, self-healing was triggered by

the rupture of microcapsules, releasing DCPD into the cracks and driven by capillary force. The released DCPD was mixed with ruthenium-based Grubb's catalyst to be polymerized via ROMP at room temperature within minutes (Figure 2.12b). The crack-healing efficiency of these epoxy composites was assessed by fracture test using a tapered double cantilever beam specimen. As seen in Figure 2.12c, the self-healable composites required greater load for the fracture, compared with control composite with no self-healable microcapsules.¹²⁹ The effect of ruthenium catalysts¹³⁰ and stereoisomers of DCPD¹³¹ on self-healing kinetics have been further explored.

Several approaches to maximize self-healing efficiency for the epoxy materials have been explored. Wax-protected catalysts in microspheres enabled the improvement of poor dispersibility of catalysts in epoxy matrix.¹³²⁻¹³³ The size of microcapsules is critical in that the amount of DCPD delivered to the cracks linearly increased with their size. Self-healing reached maximum levels when sufficient DCPD is available to entirely fill the cracks.¹³⁴ In contrast to micron-sized capsules, nanometer-sized capsules can be beneficial in thin films or microelectronic coatings, which usually have cracks on smaller length scales. Emulsion (or miniemulsion)-solvent evaporation methods allow for the synthesis of submicron-sized capsules containing Grubb's catalyst¹³⁵ and nanocapsules containing self-healing agents.¹³⁶

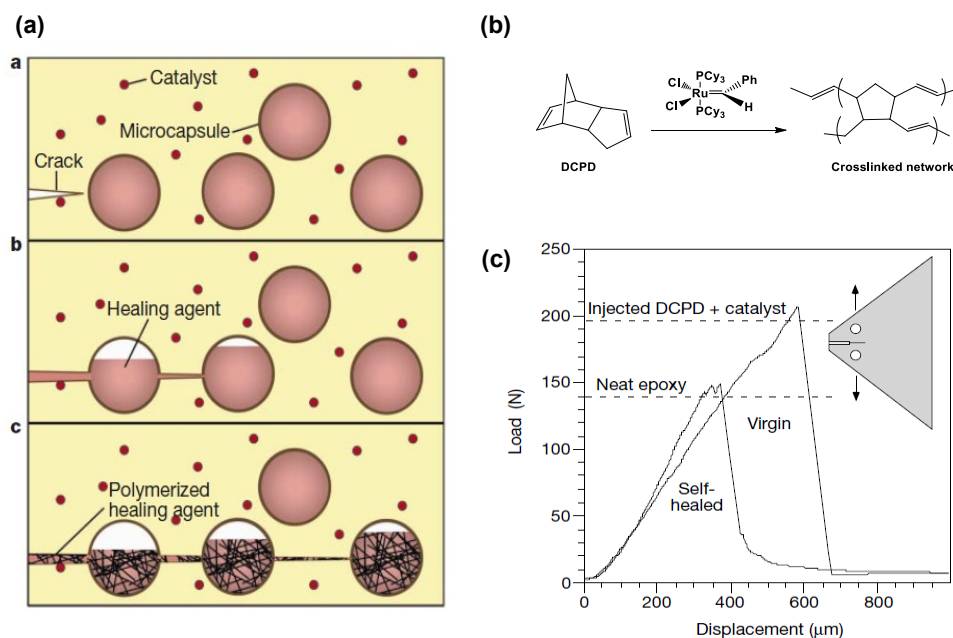


Figure 2.12 Pictorial depiction of healing mechanism of urea-formaldehyde microcapsule (a), healing chemistry utilizing ROMP of DCPD in the presence of Grubb's catalyst (b), and healing efficiency is obtained by fracture toughness testing of tapered double-cantilever beam (TDCB) specimens (c).¹²⁹ Copyright 2001 Nature Publishing Group.

2.4.2 Controlled radical polymerization (CRP)

ATRP is a versatile and powerful CRP technique that allows for the synthesis of well-controlled (co)polymers with narrow molecular weight distribution.¹³⁷⁻¹³⁸ As illustrated in Figure 2.13, ATRP has been explored to heal damage. Microcapsules of glycidyl methacrylate in melamine-formaldehyde shells were dispersed in matrix consisting of poly(methyl methacrylate) terminated with Br groups (PMMA-Br) prepared via ATRP. When the microcapsules were ruptured, the released glycidyl methacrylate (GMA) was chain-extended through ATRP from PMMA-Br ATRP macroinitiators mediated with Cu species at ambient temperatures to form PMMA-*b*-PGMA diblock copolymers. Such chain extension via ATRP enabled self-healing.¹³⁹ RAFT polymerization has also been utilized in self-healing. Similarly, polystyrene prepared via RAFT polymerization was mixed with melamine-formaldehyde microcapsules containing GMA. Upon the rupture, GMA was polymerized from polystyrene macroinitiator under a RAFT polymerization condition on damage, offering the recovery of impact strength.¹⁴⁰

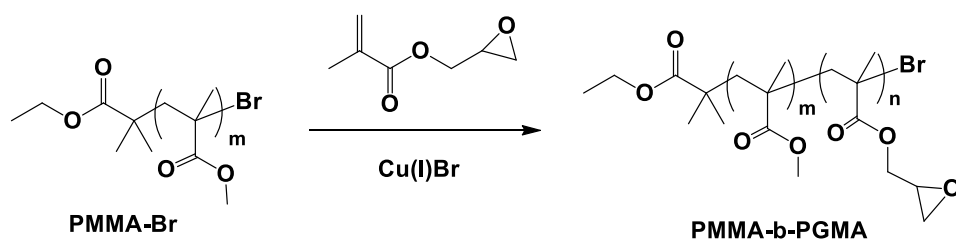


Figure 2.13 Illustration of ATRP of GMA from PMMA-Br macroinitiator for microcapsule-based extrinsic self-healing.

2.4.3 Azide-alkyne click chemistry

Small molecular weight alkynes and three-arm star polyisobutylene azides were encapsulated separately in phenol-formaldehyde microcapsules; they were impregnated in high molecular weight polyisobutylene matrix containing Cu(I) species. As illustrated in Figure 2.14, azide-alkyne click reaction in the presence of Cu(I) species was triggered to heal cracks when microcapsules were ruptured upon impact releasing sequestered alkyne and azide.¹⁴¹

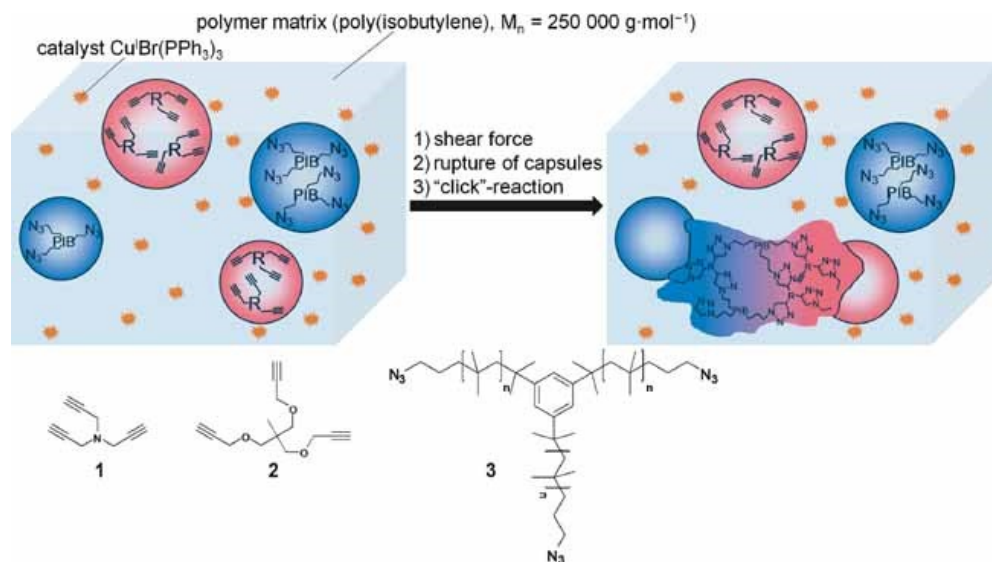


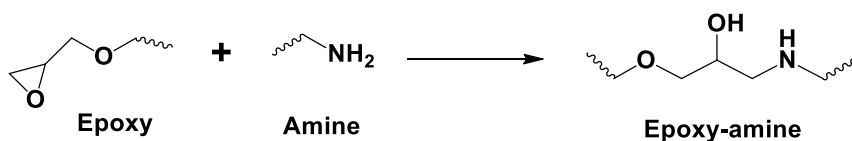
Figure 2.14 Design and extrinsic self-healing of polyisobutylene matrix embedded with microcapsules of small molecular weight alkynes and three-arm star polyisobutylene azides separately via azide-alkyne click reaction in the presence of Cu(I) species.¹⁴¹ Copyright 2011 Wiley Interfaces.

2.4.4 Polyaddition

A number of unique chemistries have been explored; Figure 2.15 illustrates typical examples. In addition to the use of ROMP described above, epoxy-amine reaction has been utilized for the development of self-healable epoxy-based materials. Reports describe the design and use of microcapsules containing solvent/reactive epoxy in urea-formaldehyde shell,¹⁴² epoxy/mercaptan in melamine-formaldehyde shell,¹⁴³ and reactive amine in polyurethane shell.¹⁴⁴ These reactive microcapsules were embedded in self-healable epoxy composites and ruptured to be able to cure epoxy. Transition metal-catalyzed hydrosilylation has been explored to develop polydimethylsiloxane (PDMS)-based self-healing materials.¹⁴⁵⁻¹⁴⁶ Particular materials contained siloxane-based healing agents phase-separated in vinyl ether matrix and polyurethane microcapsules containing di-n-butyl tin dilaurate catalyst. Upon the damage, capsules were broken to release tin catalysts. Tin-catalyzed polycondensation of hydroxyl-terminated PDMS with polydiethoxysiloxane in the contact with tin catalysts resulted in self-healing.

One of the drawbacks of most extrinsic self-healing systems via ROMP, controlled radical polymerization, and tin-catalyzed polycondensation is associated with the presence of catalysts. These drawbacks include catalyst availability, cost, and environmental toxicity, as well as stability, materials processing, and residual catalysts remaining in materials. Recently, catalyst-free extrinsic self-healing systems have been reported. A system utilizes polyaddition through the formation of urea linkages in the presence of moisture. Polyurethane-based microcapsules containing reactive isocyanates such as isophorone diisocyanate¹⁴⁷ or an isocyanate-rich polyurethane prepolymer¹⁴⁸ were prepared by an interfacial encapsulation technique in O/W emulsion. Another system utilizes a photo-induced chain-growth polymerization.¹⁴⁹⁻¹⁵⁰ A vinyl-functionalized PDMS and a photo-initiator were encapsulated in urea-formaldehyde microcapsules. Upon the crack, photo-crosslinking of the released reagents from the microcapsules occurred to attain photo-induced self-healing. These materials could be useful for self-healing anticorrosion and protection coatings.

Epoxy-amine reaction



Pt Catalyzed Hydrosilylation

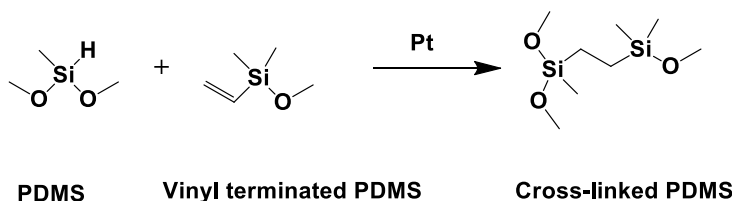


Photo-induced [2+2] cycloaddition

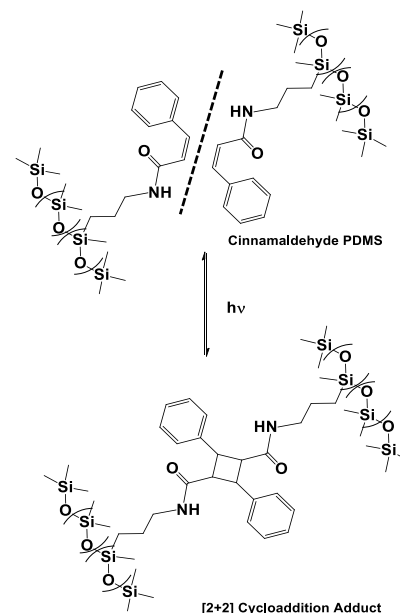


Figure 2.15 Illustration of various polyaddition mechanisms for the development of novel extrinsic self-healing materials.

2.5 Conclusion

Recent advances in the development of intrinsic and extrinsic methods to synthesize novel self-healable polymeric materials are summarized. Extrinsic self-healing methods utilize the encapsulation of extra healing agents such as monomers, crosslinkers, and catalysts in capsules-like structures. Upon damage, the encapsulated healing agents are released to fill the fractured parts where polymerization takes place to heal the cracks. Even though most methods can heal large damaged areas, they exhibit a single event of self-healing due to the depletion of the encapsulated healing agents. In contrast, intrinsic self-healing methods utilize reversible (or dynamic) chemical crosslinking through the formation of dynamic covalent bonds and non-covalent crosslinking through supramolecular interactions. Numerous approaches to synthesize reversible, repeatable self-healing networks have been proposed; however, most intrinsic self-healing systems require initiation by external stimuli such as temperature, pH, light, or chemicals.

Future design and development of effective self-healing materials that can be used in a wide range of biomedical and industrial applications require a high degree of control over properties. They include i) the occurrence of multiple self-healing events, ii) the minimal or no use of

external stimuli, iii) the unchanged integrity of original materials upon multiple healing cycles, and iv) the high mechanical strength while also maintaining dynamic physical or chemical interactions. Numerous crosslinked systems are built on soft polymeric materials such as hydrogels and organogels. Most of them exhibit great self-healability; however, they still suffer from various applications requiring high mechanical strength. In an attempt to enhance toughness while retaining self-healability for supramolecular materials, an innovative design featuring the incorporation of hard domains or nanoparticles into soft matrix has been explored. Nevertheless, more studies should be focused on the development of tough self-healing polymeric materials. Further, most self-healing materials that have been reported utilize single dynamic interactions: future designs could explore the occurrence of self-healing through dual or multiple interactions.

Chapter 3

Dual sulfide-disulfide crosslinked networks with rapid and room temperature self-healability

This chapter is reproduced the article published in *Macromolecular Rapid Communications*, **2015**, 36, 1255-1260 with permission from the publisher.

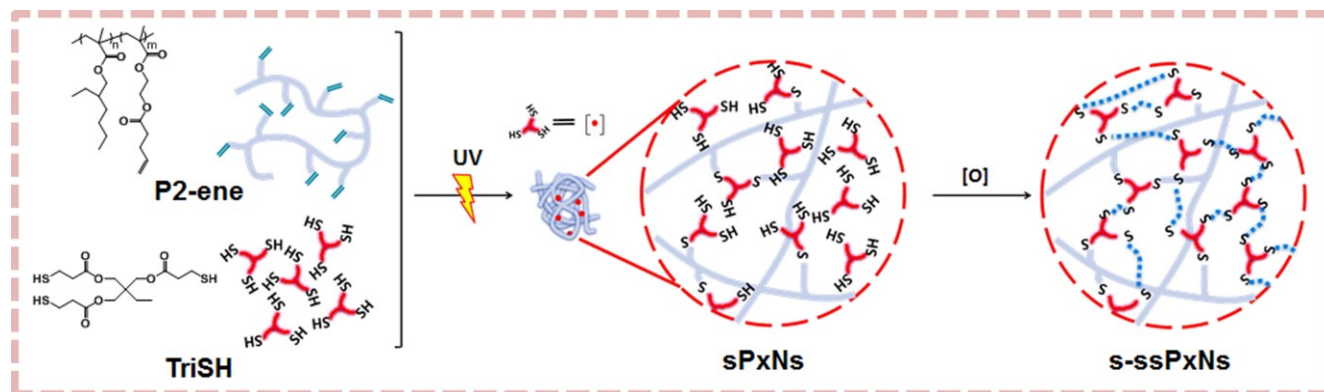
3.1 Introduction

Inspired by nature, self-healing or self-repairing is a desired property in the design and development of high-performance polymeric materials in a broad range of applications, such as surface coatings, tissue engineering, and sensors. Such increasing attention to the development of novel self-healable materials is attributed to their built-in ability to repair physical damages, effectively preventing catastrophic failure and extending the lifetime of materials. The physical damages at micro- and meso-scale to be healed include fractures due to mechanical deformation, chemical corrosion, and degradation by irradiation.

Several strategies have been proposed to develop self-healing polymeric materials.^{38, 42, 126, 151} Extrinsic self-healing method involves the encapsulation of extra healing agents such as crosslinkers and catalysts in nanocontainers such as microcapsules and porous composites.^{41, 150} These extra agents are then released after a crack reached mostly microcapsules and can be subsequently polymerized within the crack after contact with catalyst/initiator embedded in the matrix.¹⁵² Although this method could heal large damaged volumes, it is not reversible upon the release of extra healing agents.¹⁵³ More promisingly, intrinsic self-healing method involves the incorporation of functionalities that are utilized to reattach the fractured parts of self-healable materials with no aids of extra agents.⁴⁵ An approach involves the use of non-covalent bonds through physical crosslinking mechanisms¹⁹ such as π - π stacking,¹⁸⁻¹⁹ ionic interaction,¹¹⁰ metal-

ion binding,²⁰⁻²⁵ hydrogen bonding,¹³⁻¹⁶ host-guest interactions,¹⁷ and redox.¹²³ In contrast, the use of reversible covalent bond formation can provide higher mechanical strength and higher stability for self-healing materials. The dynamic covalent bonds are able to reform after having sustained damages. Typical examples for reversible bond formation include mainly Diels-Alder/retro-Diels-Alder reactions,^{64, 67, 74, 154-155} alkoxyamine recombination,⁷⁻⁸ urea chemistry,^{5, 156} and living polymerization.^{40, 157} However, these reactions require the external stimuli such as heat, light, chemicals, or oxygen that trigger the bond reformation or the use of specific urea molecules having large groups. In this context, the development of methods that enable rapid self-healing with no aids of external stimuli at room or even lower temperature is highly desired.⁹ Disulfide chemistry is unique in that the exchange of disulfides and the corresponding thiols and thiyl radicals is reversible.^{76, 158} Examples include self-healing at higher temperature (65 °C) in epoxy-based disulfide-containing resins prepared by polycondensation¹ or even under ambient conditions in disulfide-crosslinked films based on star-shaped copolymers.² A report also describes room-temperature self-healing through disulfide metathesis in the presence of a phosphine as an external reducing agent.³ Despite these advances, however, the exploration of disulfide chemistry to synthesize polymeric materials based on chain-growth polymers exhibiting self-healability at ambient temperature is in infancy.

Herein, we report dual sulfide-disulfide crosslinked materials (s-ssPxNs) based on methacrylate copolymers exhibiting the rapid occurrence of room temperature self-healing within tenth seconds to minutes, with no extra healing agents and no change in any environmental conditions. As illustrated in Scheme 3.1, our method combines photo-induced thiol-ene click-type radical addition of methacrylate copolymers having pendant vinyl groups (P2-ene) with a polythiol in a non-stoichiometric balance, generating lightly sulfide-crosslinked polysulfide-based networks with excess thiols, and their oxidation, creating dynamic disulfide crosslinkages to yield dual s-ssPxNs. An advantage of the approach is to easily tune disulfide-crosslinking densities (i.e. tunable kinetics of self-healing) with the extent of oxidation (i.e. the amount of oxidizing agent). Another is to retain integrity of crosslinked materials when damaged by external force, which is attributed to both sulfide (permanent) and disulfide (reversible) crosslinkages in dual sulfide-disulfide crosslinked network.



Scheme 3.1 Illustration of our method utilizing click-type photo-induced thiol-ene radical addition and oxidation to synthesize dual sulfide-disulfide crosslinked networks (s-ssPxNs).

3.2 Experimental section

3.2.1 Instrumentation and analyses

^1H -NMR spectra were recorded using a 500 MHz Varian spectrometer. The CDCl_3 singlet at 7.26 ppm was selected as the reference standard. Monomer conversion was determined by gravimetry (120 °C/4 hr). Molecular weight and molecular weight distribution were determined by gel permeation chromatography (GPC). An Agilent GPC was equipped with a 1260 Infinity Isocratic Pump and a RI detector. Two Agilent columns (PLgel mixed-D and mixed-C) were used with DMF containing 0.1 mol% LiBr at 50 °C at a flow rate of 1.0 mL/min. Linear poly(methyl methacrylate) standards from Fluka were used for calibration. Aliquots of polymer samples were dissolved in DMF/LiBr. The clear solutions were filtered using a 0.25 μm PTFE filter to remove any solvent-insoluble species. A drop of anisole was added as a flow rate marker.

3.2.2 Differential scanning calorimetry (DSC)

Thermal properties including glass transition temperature (T_g) of polymers and gels were measured with a TA Instruments DSC Q20 differential scanning calorimeter. Polymer samples were dried under vacuum for 24 hrs at room temperature to remove residual solvents. Temperature range was from -70 to 200 °C with heating and cooling cycles conducted at a rate

of 10 °C/min (cycles: cool to -70 °C, heat up to 200 °C (1st run), cool to -70 °C, heat up to 200 °C (2nd run), and cool to 25 °C). The T_g values were determined from the 2nd heating run.

3.2.3 Thermogravimetric analysis (TGA)

TGA measurements were carried out using a TA instruments Q50 analyzer. Typically, polymer samples (5-10 mg) were placed into a platinum pan and heated from 25 °C to 800°C at a heating rate of 20 °C per minute under nitrogen flow.

3.2.4 Materials

Triethylamine (Et_3N , > 99.9%), 2,2-dimethoxy-2-phenylacetophenone (DMPAc, 99%) as a photoinitiator, 2,2'-azobis(2-methylbutyronitrile) (AMBN, > 98%), tris(3-mercaptopropionate) (TriSH > 95%), iodine (> 99.8%), KBr (> 99%), and 4-pentenoyl chloride (PA-Cl, 98%) were purchased from Aldrich and used as received. EHMA and HEMA from Aldrich were purified by passing them through a column filled with basic alumina to remove inhibitors.

3.2.5 Synthesis of high molecular weight P2-ene

To synthesize P1-OH precursor by FRP, EHMA (3.0 g, 15 mmol), HEMA (0.84 g, 6.5 mmol), and anisole (4.2 mL) were mixed in a 50 mL Schlenk flask. The mixture was deoxygenated by purging under nitrogen for 40 min and placed in an oil bath pre-set at 75 °C. A nitrogen-prepurged solution of AMBN (39 mg, 0.19 mmol) in anisole (0.5 g) was injected into the Schlenk flask to initiate polymerization. Polymerization was stopped after 3 hrs by cooling the reaction vessel in an ice bath. For purification, as-synthesized polymer solutions were precipitated from cold MeOH. The precipitates were then dried in vacuum oven at room temperature for 18 hrs. To synthesize P2-ene, a clear solution of PA-Cl (1.4 mL, 13 mmol) in anhydrous tetrahydrofuran (THF, 10 mL) was added drop wise into a mixture containing of the purified dried P1-OH (3.8 g, 6.5 mmol of OH groups), Et_3N (2.7 mL, 19 mmol), and THF (190 mL) in an ice bath under stirring. The resulting mixture was stirred at room temperature for 18 hrs. The formed solids as by-products ($\text{Et}_3\text{N-HCl}$ adducts) were removed by vacuum filtration. The resulting mixture was then washed 5 times with water (200 mL). As-synthesized polymer solutions were precipitated from cold MeOH. The precipitates were then dried in vacuum oven at room temperature for 18 hrs.

3.2.6 Photo-induced thiol-ene radical addition reaction

To synthesize sulfide-crosslinked gels (sGels), a series of thiol-ene reactive blends at different mole ratios of $[\text{SH}]_0/[\text{vinyl}]_0 = 1/1\text{-}20/1$ were prepared. As a typical example to prepare sGel-15, the purified, dried P2-ene (0.38 g, 0.65 mmol of vinyl groups), TriSH (1.3 g, 9.8 mmol of SH groups), and DMPAc (51 μL , 0.1 g/mL stock solution in THF) were dissolved in THF (11 g) to prepare a reactive blend at $[\text{SH}]_0/[\text{vinyl}]_0 = 15/1$ in THF. Aliquots of the resulting blend were exposed to UV light at $\lambda = 350\text{ nm}$ for 10 min to synthesize sGel-15. Similar procedure was used to synthesize other sGels from the reactive blends containing different amounts of TriSH.

3.2.7 Oxidation of sPxNs

To synthesize dual sulfide-disulfide crosslinked gels (s-ssGels), the same amount of sGels (0.33 g) was mixed with different amounts of a stock solution of iodine in THF (1 g) for 12 hrs. The resulting mixtures were then dried under vacuum for 48 hrs to completely remove THF.

3.2.8 Gel content measurement

Aliquots of sGels and s-ssGels (approximately 0.1 g) were mixed with THF (9.5 mL) under magnetic stirring for 48 hrs. The mixtures were subjected to centrifugation (5000 rpm x 15 min x 4 $^{\circ}\text{C}$). After the supernatants were decanted, the precipitates were dried in vacuum oven for 48 hrs to remove the trace of THF. Gel content was calculated as the weight ratio of dried precipitates to (P2-ene+TriSh) in the reactive mixtures.

3.2.9 FT-IR measurements

FT-IR spectra of all the samples were recorded on a Nicolet 6700 FT-IR spectrometer using KBr pellets. All spectra were recorded with 64 scans in resolution of 4 cm^{-1} at room temperature in the range of 400-4000 cm^{-1} . The dried sGels and ssGels were mixed with KBr powders to prepare pellets for FT-IR measurements. Background noises were corrected with pure KBr. For data processing, the baselines of all spectra were corrected.

3.2.10 Optical microscopy

Self-healing behavior of s-ssGels was observed by a microscope (Olympus BX51) with fluorescence filters (BP 460-490 excitation and BA520IF emission) coupled with a digital camera. For non-oxidized gels such as sGel-1, no filters were needed. Fresh cuts were made using a sharp blade on surfaces of s-ssGels and sGel-1 to monitor their healing behavior at room temperature.

3.2.11 Rheological measurements

Viscoelastic properties (G' and G'' moduli) of sGels were measured on a DHT-2 rheometer (TA Instruments, USA) in amplitude oscillatory shear mode with parallel plate geometry (8 mm diameter). The gap was set to obtain an axial force around 1 N at room temperature, and oscillation frequency was varied from 0.1 to 100 rad/s at 5% strain. In addition, the elasticity of ssGels were tested by applying cyclic changes of amplitude oscillatory from 5% strain for 1500 s to 100% strain for 500 s. The gap was set to obtain an axial force of 1N at room temperature and this cycle is repeated three times.

3.3 Results and Discussion

3.3.1 Synthesis of P2-ene having vinyl groups

As a proof-of-concept of our strategy to fabricate self-healing dual s-ssPxN networks, a high molecular weight P2-ene having pendant vinyl groups was synthesized by an industrially-friendly polymerization method (called free radical polymerization, FRP), followed by post-modification through a facile coupling reaction. As illustrated in Figure 3.1, a FRP of 2-ethylhexyl methacrylate (EHMA) and 2-hydroxyethyl methacrylate (HEMA) in anisole at 75 °C yielded a P(EHMA-co-HEMA) random copolymer (P1-OH) consisting of both pendant ethylhexyl and functional OH groups randomly-distributed along main polymethacrylate chains.¹⁵⁹ After purification, the pendant OH groups in P1-OH precursor reacted with 4-pentenoyl chloride in the presence of triethylamine (a base). The resulting product was characterized with molecular weight as weight average molecular weight (M_w) = 138 kg/mol by gel permeation chromatography; glass transition temperature (T_g) = -10.4 °C by differential scanning calorimetry (DSC); and 30 mol % vinyl group by ¹H-NMR (Figure 3.2). These results

indicate the successful synthesis of a high molecular weight P2-ene having pendant 30 mol% vinyl groups.

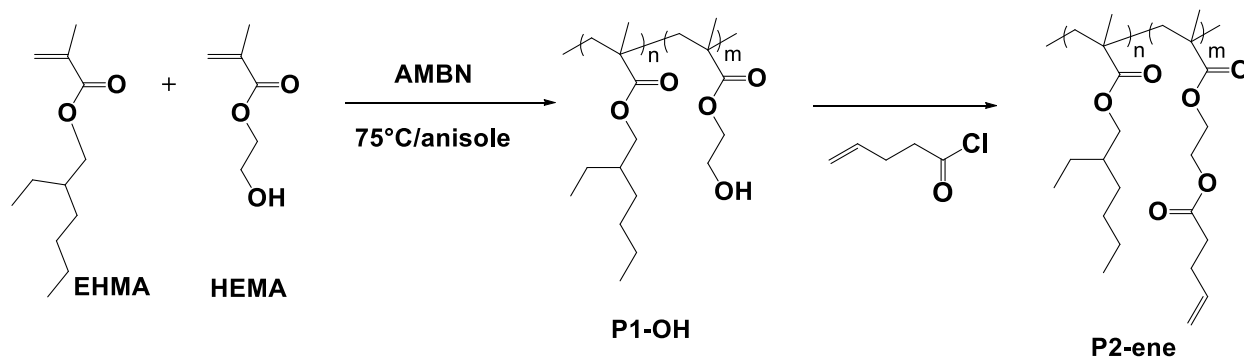


Figure 3.1 Schematic illustration to synthesize P1-OH and P2-ene

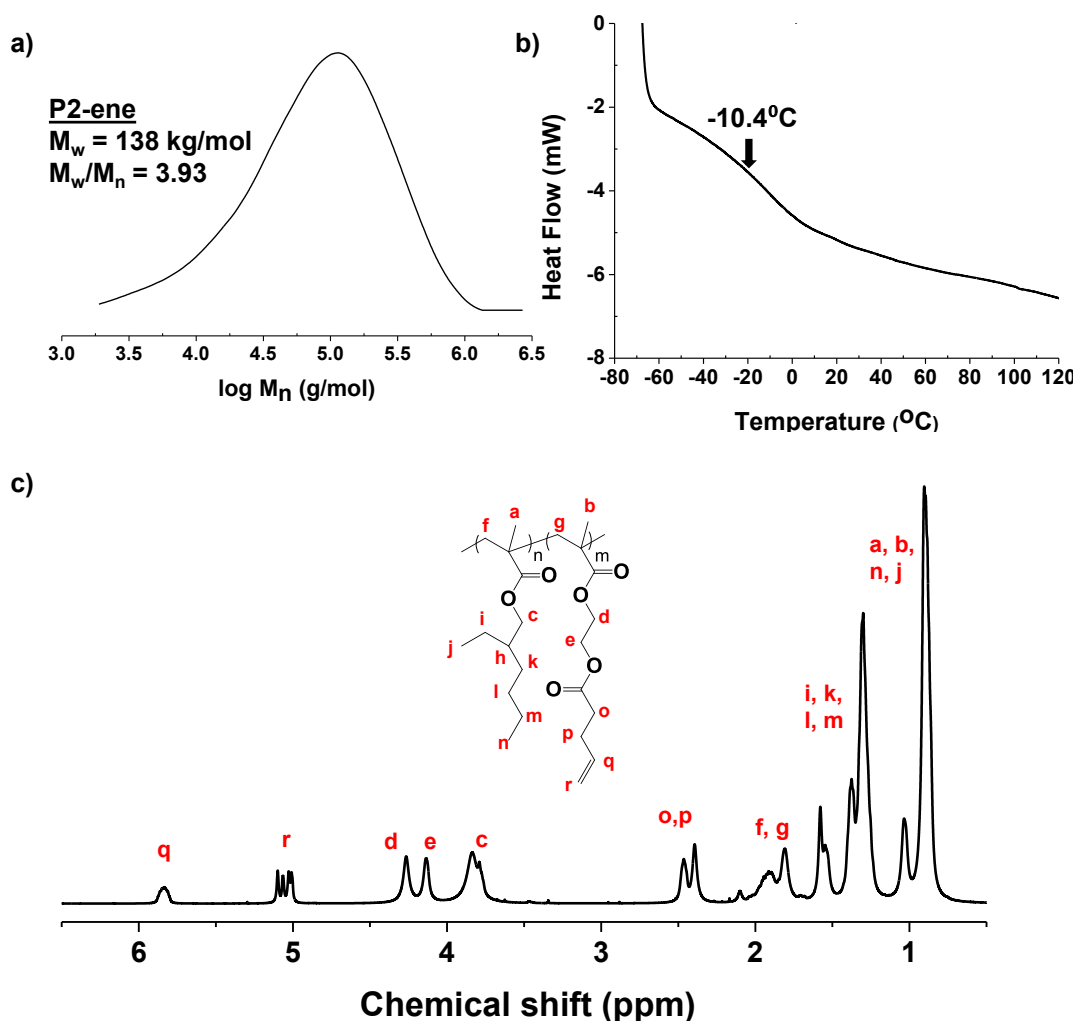


Figure 3.2 GPC trace (a), DSC trace (b), and ^1H -NMR spectrum in CDCl_3 (c) of purified, dried P2-ene.

3.3.2 Preparation of dual sulfide-disulfide crosslinked networks (s-ssPxNs)

The P2-ene contains pendant vinyl groups, which enable the reaction with SH groups of a polythiol through thiol-ene radical addition upon UV irradiation.¹⁶⁰⁻¹⁶¹ This click-type photo-induced thiol-ene reaction yields crosslinked network through the formation of sulfide crosslinkages (denoted as sPxN) as a result from the consumption of SH groups in the reactive blends of P2-ene and polythiol. The use of excess polythiol (i.e. SH groups) could result in the formation of a lightly-crosslinked polysulfide materials with free SH groups.

Trimethyloxypropane tris(3-mercaptopropionate) (TriSH) was examined as a model polythiol. A

series of reactive blends at varying mole equivalent ratios of $[\text{SH}]_0/[\text{vinyl}]_0 = 1/1$ to $20/1$ was prepared by mixing the same amount of P2-ene with different amounts of TriSH in tetrahydrofuran (THF). Note that the larger ratio represents more excess SH groups in the reactive blends. Aliquots of the series of reactive mixtures were exposed to UV for 10 min. The occurrence of photo-induced thiol-ene radical addition between P2-ene and TriSH was followed by FT-IR measurements.¹⁶² The decrease in the peak area at 2570 cm^{-1} corresponding SH stretching vibration before and after UV irradiation allowed for the determination of the SH consumption as a consequence of thiol-ene addition with vinyl groups of P2-ene (see the FT-IR spectrum in Figure 3.3 for a reactive blend at $[\text{SH}]_0/[\text{vinyl}]_0 = 15/1$ as an example). As presented in Table 3.1, the SH concentration ($[\text{SH}]/\text{P2-ene}$) increased in the sPxN network when the amount of TriSH increased in the reactive blends. Further, the resulting dried sPxNs were then characterized with gel content using gravimetry as well as mechanical properties using rheometer. With an increasing $[\text{SH}]_0/[\text{vinyl}]_0$ ratio, gel content and maximum elastic modulus (G') decreased and reached plateau at the $[\text{SH}]_0/[\text{vinyl}]_0 > 15/1$ (Figure 3.4). Such decrease in both gel content and maximum G' modulus is presumably attributed to the formation of lightly crosslinked network with less sulfide crosslinking density as well as co-existence of residual TriSH.

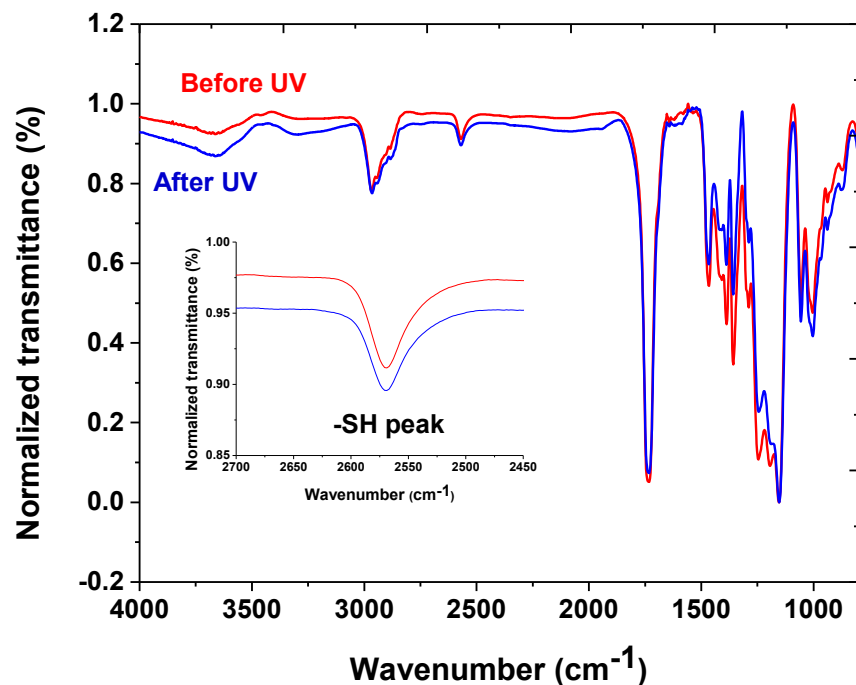


Figure 3.3 FT-IR spectra of a reactive blend of P2-ene with TriSH at $[\text{SH}]_0/[\text{vinyl}]_0 = 15/1$ before and after UV irradiation to monitor the change of peak area at 2570 cm^{-1} .

Table 3.1 Characteristics and properties of thiol-ene reactive blends of P2-ene with various amounts of TriSH at various ratios of $[\text{SH}]_0/[\text{vinyl}]_0$ upon UV irradiation.

| sPxN ^{a)} | $[\text{SH}]_0/[\text{vinyl}]_0$ | SH ^{b)} Consumption (%) | Thiol-ene ^{c)} Conversion (%) | $[\text{SH}]/\text{P2-ene}$ (mmol/g) ^{d)} | Gel content (%) ^{e)} | Max G' (kPa) |
|--------------------|----------------------------------|-------------------------------------|---|---|----------------------------------|-----------------|
| sPxN-1 | 1/1 | 62.2 | 62.2 | 0.6 | 98.8 | 459.4 |
| sPxN-5 | 5/1 | 12.1 | 60.5 | 7.5 | 75.6 | 27.5 |
| sPxN-10 | 10/1 | 11.8 | ≈ 100 | 15.0 | 57.8 | 6.4 |
| sPxN-15 | 15/1 | 9.9 | ≈ 100 | 23.0 | 38.7 | 1.8 |
| sPxN-20 | 20/1 | 5.6 | ≈ 100 | 32.2 | 39.7 | 2 |

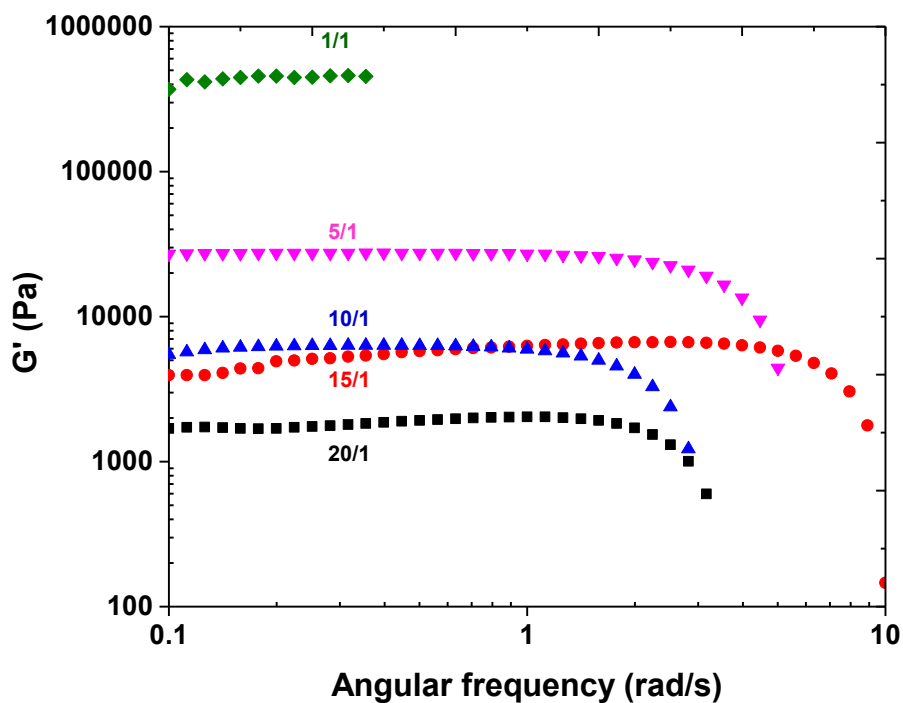


Figure 3.4 Overlaid elastic modulus (G') over angular frequency (ω) for reactive blends consisting of P2-ene and TriSH at various ratio of $[\text{SH}]_0/[\text{vinyl}]_0$ upon UV irradiation.

The availability of sufficient concentration of free SH groups in sPxN materials (containing TriSH) could create a dual s-ssPxNs upon oxidation through the formation of new disulfide linkages. The oxidation was investigated for the sPxN-15 precursor having relatively

high concentration of SH groups (23 mmol/g P2-ene), prepared with $[\text{SH}]_0/[\text{vinyl}]_0 = 15/1$. The aliquot was treated with different amounts of iodine as an oxidizing agent up to 9 wt% in THF in 20 mL vials at room temperature for 18 hrs. The use of iodine for oxidation of thiols is described elsewhere.^{2, 163} As seen in the digital images in Figure 3.5, the occurrence of oxidation was first evidenced with a change of flow-type gel solutions (13 wt% solid content) to free-standing gels after the treatment of sPxNs with iodine. Further, the conversion of free SH groups to the corresponding disulfide linkages upon oxidation was quantitatively analyzed by FT-IR measurements before and after the treatment with iodine (Figure 3.6). The decrease in the peak area at 2570 cm^{-1} allowed for the estimation of SH consumption and thus newly-formed disulfide concentration in s-ssPxNs. As summarized in Figure 3.5, the SH consumption increased when the amount of iodine increased in the mixtures, and it reached to completion when the amount of iodine is greater than 6%. In addition, the gel content based on solubility in THF increased with an increasing amount of iodine. These results from both FT-IR and gel content measurements indicate the formation of dual s-ssPxNs with self-healable disulfide linkages. Further, sulfide-crosslinked sPxN network and unreacted TriSH consist of free SH groups which upon its oxidation form s-ssPxNs. This network could contain heterogeneous domains rich in disulfide linkages formed from residual TriSH (see Scheme 3.1).

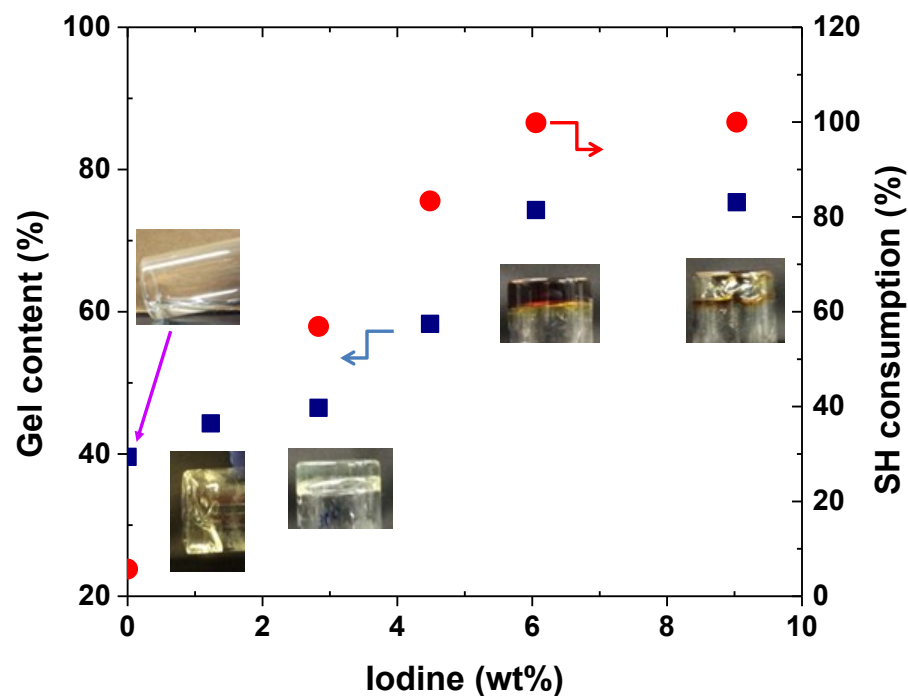


Figure 3.5 Gel content (%) and SH consumption (%) upon oxidation in the presence of different amount of iodine for sGel-15 prepared with the $[\text{SH}]_0/[\text{vinyl}]_0 = 15/1$. The digital images show s-ssPxN-15/y gels (y denote wt % of iodine) in THF.

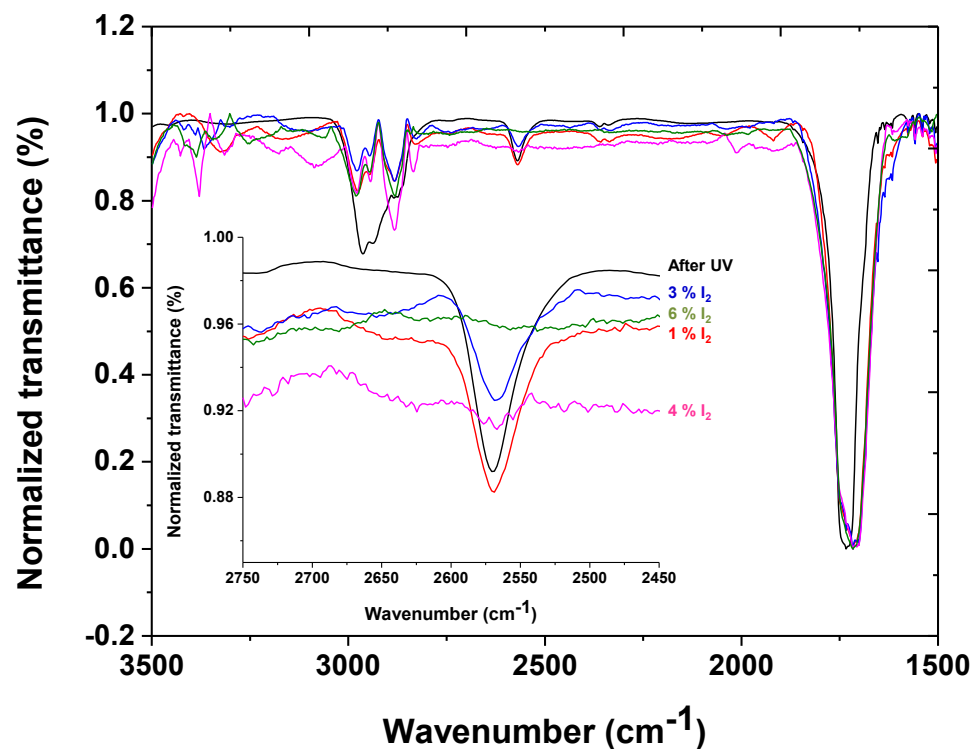


Figure 3.6 FT-IR spectra of sPxN-15 before and after treatment with various amounts of iodine.

3.3.3 Self-healing ability of different s-ssPxNs

The self-healability of the resulting dual s-ssPxNs upon cuts (or microcracks) through the reformation of disulfide linkages at room temperature was investigated. The dried s-ssPxN-15/6 oxidized with 6% iodine (with $\approx 100\%$ SH consumption) was initially examined for self-healability because of the relatively higher concentration of newly-formed disulfide linkages (see Table 3.2). Two cuts with different widths of 43 and 73 μm were made on their surfaces using a knife and the occurrence of their self-healing properties at room temperature was followed by microscopy. As seen in Figure 3.7a, the self-healing was completed within 30 sec on the 43 μm wide cut. Further, the complete self-healing occurred within 30 min on the relatively larger 73 μm wide cut (Figure 3.7b). These promising results are compared with no occurrence of self-healing on sPxN-1 having no disulfide linkages as a control (Figure 3.7c). These results indicate rapid self-healing at room temperature with no aids of external stimuli. Further to investigate the kinetics of self-healing for dual s-ssPxNs compared with the control (sPxN-1), the healing efficiency was estimated based on the decrease in the length of the cuts over time (Figure 3.7d). From the linear regression, the healing rate was calculated to be 200%/min for the 43 μm wide cut and 3.3%/min for 73 μm wide cut, suggesting the dependence of self-healing kinetics on the sizes and lengths of cuts.

Table 3.2 Characteristics and properties of dual s-ssPxNs prepared by oxidation of sPxN precursors in the presence of iodine.^{a)}

| s-ssPxNs | Cuts ^{b)} | | Iodine (%) ^{c)} | [SS]/P2-ene (mmol/g) ^{d)} | Healing efficiency (%/min) |
|--------------|-------------------------|--------------------------|--------------------------|------------------------------------|----------------------------|
| | Width (μm) | length (μm) | | | |
| s-ssPxN-15/6 | 43 | 170 | 6 | 10.9 | 200 |
| s-ssPxN-15/6 | 73 | 700 | 6 | 10.9 | 3.3 |
| s-ssPxN-15/3 | 80 | 500 | 4 | 7.9 | No healing |
| s-ssPxN-10/6 | 67 | 350 | 6 | 7.5 | No healing |
| s-ssPxN-5/6 | 57 | 1000 | 6 | 3.7 | No healing |

s-ssPxN-x/y: x denotes the ratio of $[\text{SH}]_0$ in thiol-ene reactive blends and y denotes the wt% of iodine; ^{b)} Optical microscopy; ^{c)} wt% based on sPxN precursors; ^{d)} estimated by FT-IR before and after oxidation.

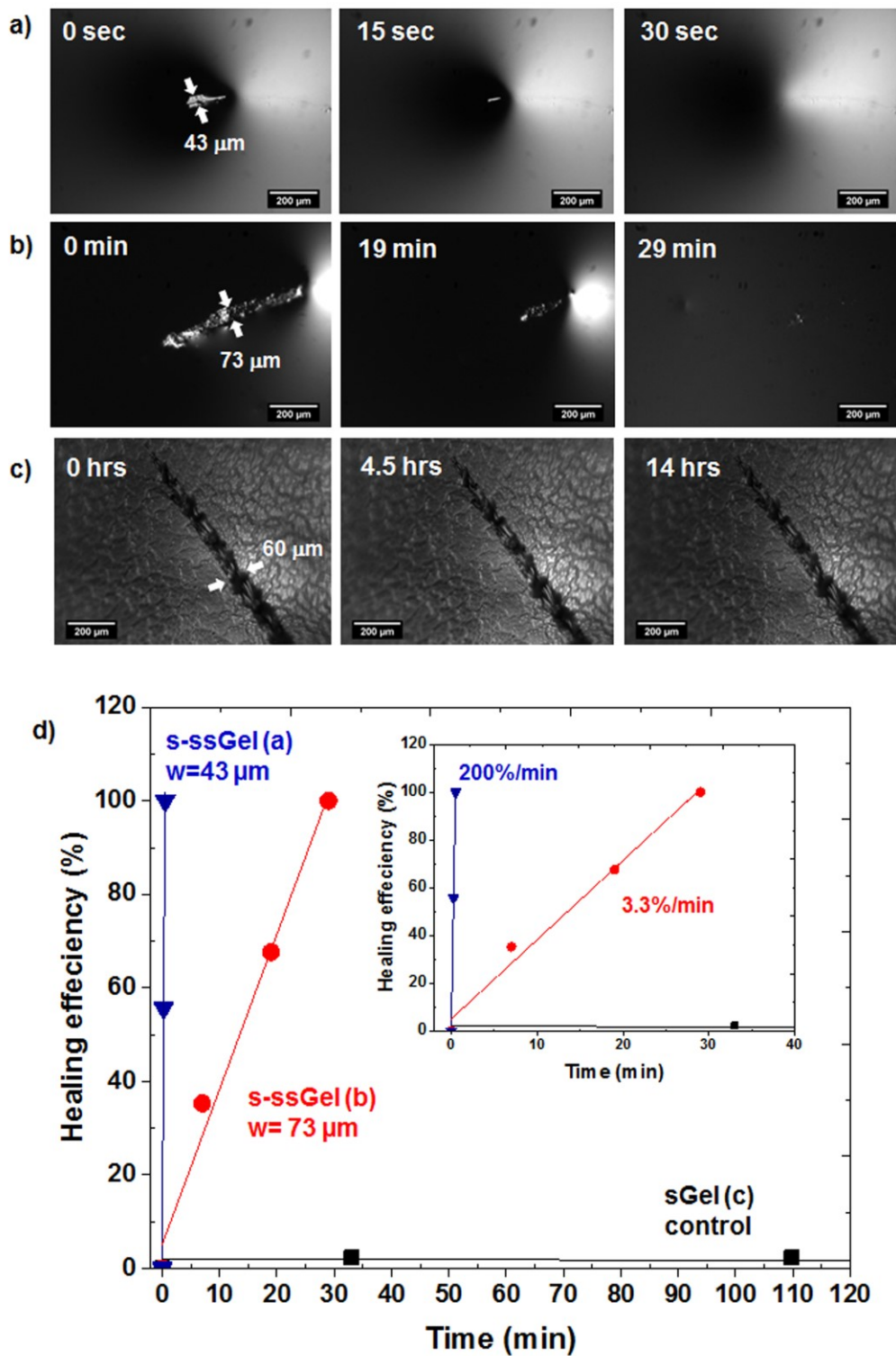


Figure 3.7 Evolution of microscope images (a-c) and kinetics of self-healing (d) over time at room temperature for dual s-ssPxN-15/6 with different cut sizes of 43 μm wide (a) and 73 μm wide (b), compared with a control of sPxN-1 with no disulfide prepared with $[\text{SH}]_0/[\text{vinyl}]_0 = 1/1$ (c)

Given the promising self-healing results with s-ssPxN-15/6 network, the self-healing behavior of other s-ssPxNs having different concentrations of newly-formed disulfide crosslinkages was further examined. Because of the occurrence of self-healing through the reformation of disulfides, the results could allow for the correlation between disulfide concentration and self-healing behavior of s-ssPxNs, as well as effective construction of self-healing windows for the preparation of s-ssPxN materials with suitable disulfide concentration, oxidation, and TriSH concentration. Under similar conditions (no external agents and at room temperature), no self-healing was observed on s-ssPxN-15/3 (prepared in the presence of 3 % iodine) (Figure 3.8) as well as s-ssPxN-10/6 and s-ssPxN-5/6 prepared by treatment of the corresponding sPxN-10 and sPxN-5 with 6 % iodine (Figure 3.9). One plausible reason for no self-healing behaviors is due to the less densities of disulfides in those three s-ss-PxN networks (<8 mmol/g of P2-ene, compared to 11 mmol/g for s-ssPxN-15/6, Table 3.2). These results suggest the requirement of the sufficient concentration of self-healable disulfides in dual s-ssPxN networks for self-healability.



Figure 3.8 Evolution of optical microscope image of 80 μm wide and 500 μm long cut over time at room temperature for dual s-ssPxN-15/3, prepared by oxidation of sPxN-15 in the presence of 3% iodine.

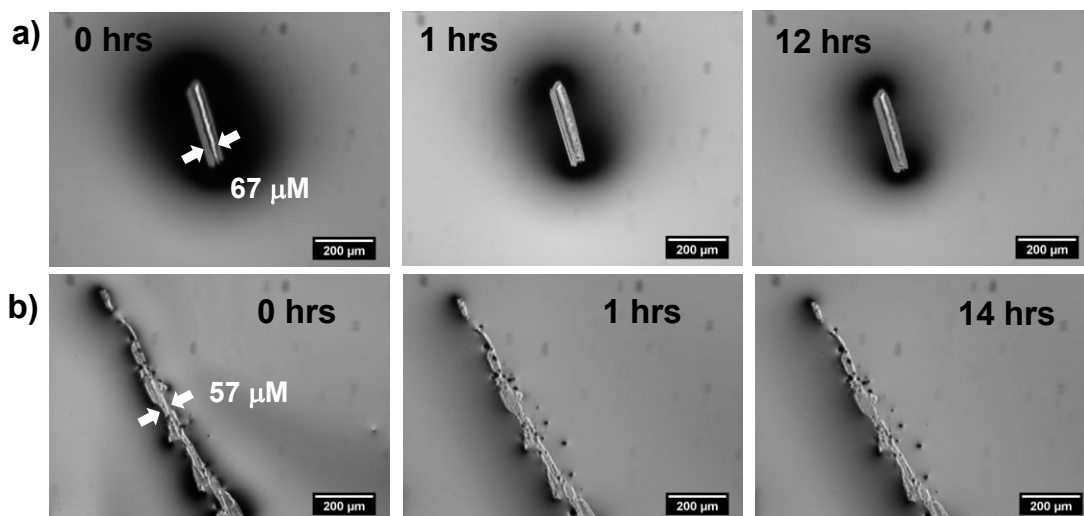


Figure 3.9 Evolution of optical microscope image of a 67 μm wide and 340 μm long cut for dual s-ssPxN-10/6, and a 57 μm wide and 1000 μm long cut for dual s-ssPxN-5/6 over time.

3.3.4 Viscoelastic properties of s-ssPxN

Further to get an insight into self-healability of dual s-ssPxNs, the self-healing elasticity was examined as to measure their viscoelastic properties using a rheometer upon a cyclic change of oscillation force: 5% strain for 1500 sec to 100% strain for 500 sec. As seen in Figure 3.10a, the elastic modulus (G') of s-ssPxN-15/6 gradually increased when a 5% strain was applied for 1500 sec. Upon the change of oscillation force to 100% strain, the G' modulus suddenly dropped for 500 sec. Then, the G' modulus was restored when the oscillation force was recovered back to 5% strain. Such a reversible restoration of G' modulus was able to be repeated several times, exhibiting self-healing elasticity of s-ssPxN-15/6 networks. In contrast, sPxN-5/6 exhibiting no occurrence of self-healing did not show the reversibility of G' modulus upon the cyclic change of oscillation force (Figure 3.10b).

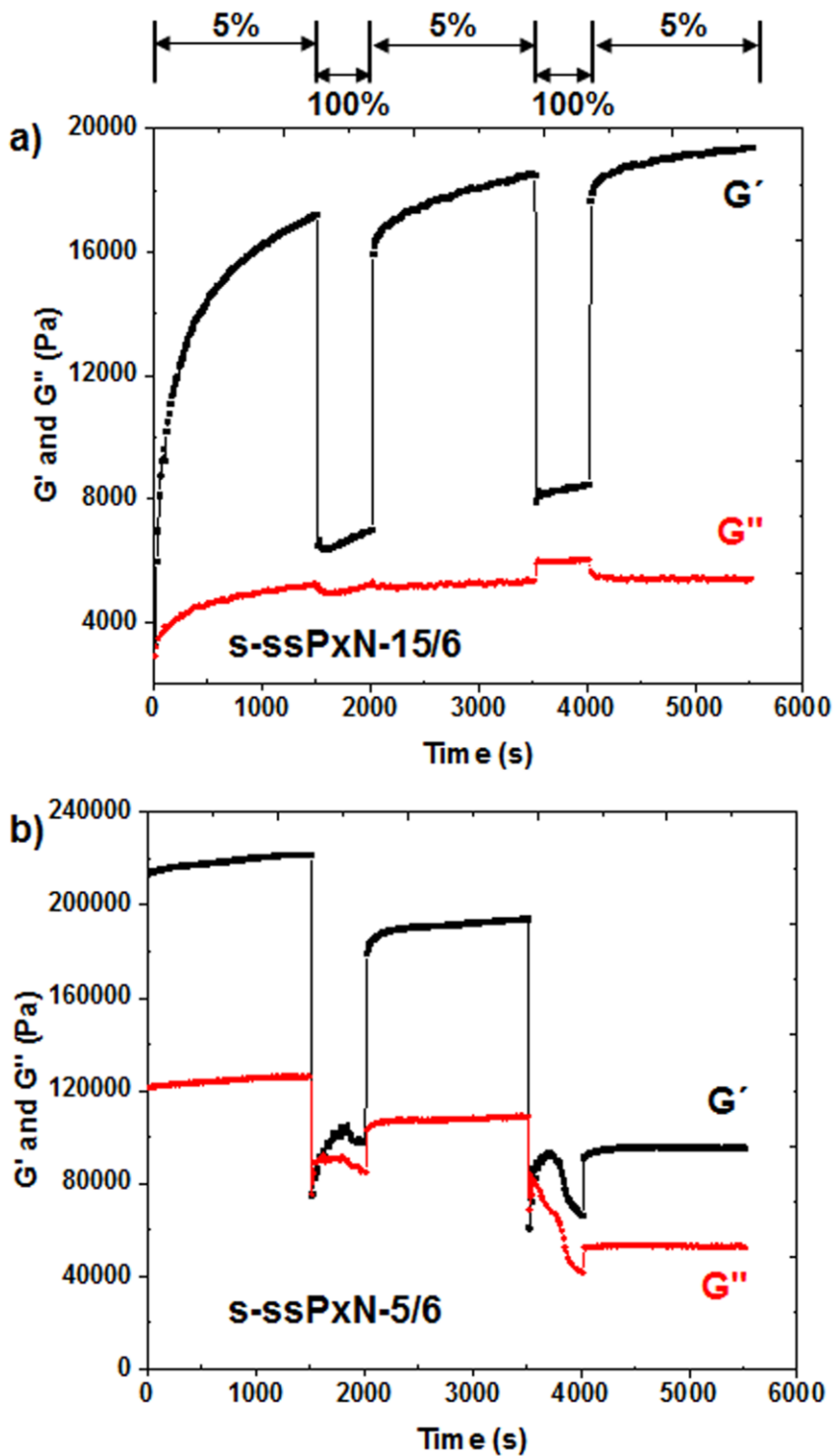


Figure 3.10 Viscoelastic properties using a rheometer upon a cyclic change of oscillation force: 5% strain for 1500 s to 100 % for 500 s for dual s-ssPxN-15/6 exhibiting self-healability and s-ssPxN-5/6 with no self-healability.

3.4 Conclusion

The effective method utilizing photo-induced thiol-ene radical addition and oxidation enabled the synthesis of dual sulfide-disulfide crosslinked s-ssPxN networks exhibiting rapid self-healing properties at room temperature with no aids of external stimuli. The sufficient density of disulfide crosslinkages was required for rapid self-healing to occur within 0.5 – 30 min at room temperature. In addition, self-healable s-ssPxN enabled to maintain its integrity when damaged by external force as well as exhibited the self-healing elasticity with reversible restoration of viscoelastic properties. Further, self-healing kinetics was tuned with disulfide-crosslinking densities (i.e. concentration of disulfide linkages and extent of oxidation). Given the versatility of the method to synthesize rapid and room temperature self-healing networks, further studies on important parameters that can influence self-healing kinetics and properties such as densities of pendant vinyl groups and molecular weights of copolymers as well as comonomers and polythiols will be required toward the development of smart industrial applications.

Chapter 4

Multiblock copolymer-based dual disulfide- and supramolecular crosslinked networks exhibiting dual self-healing

4.1 Introduction

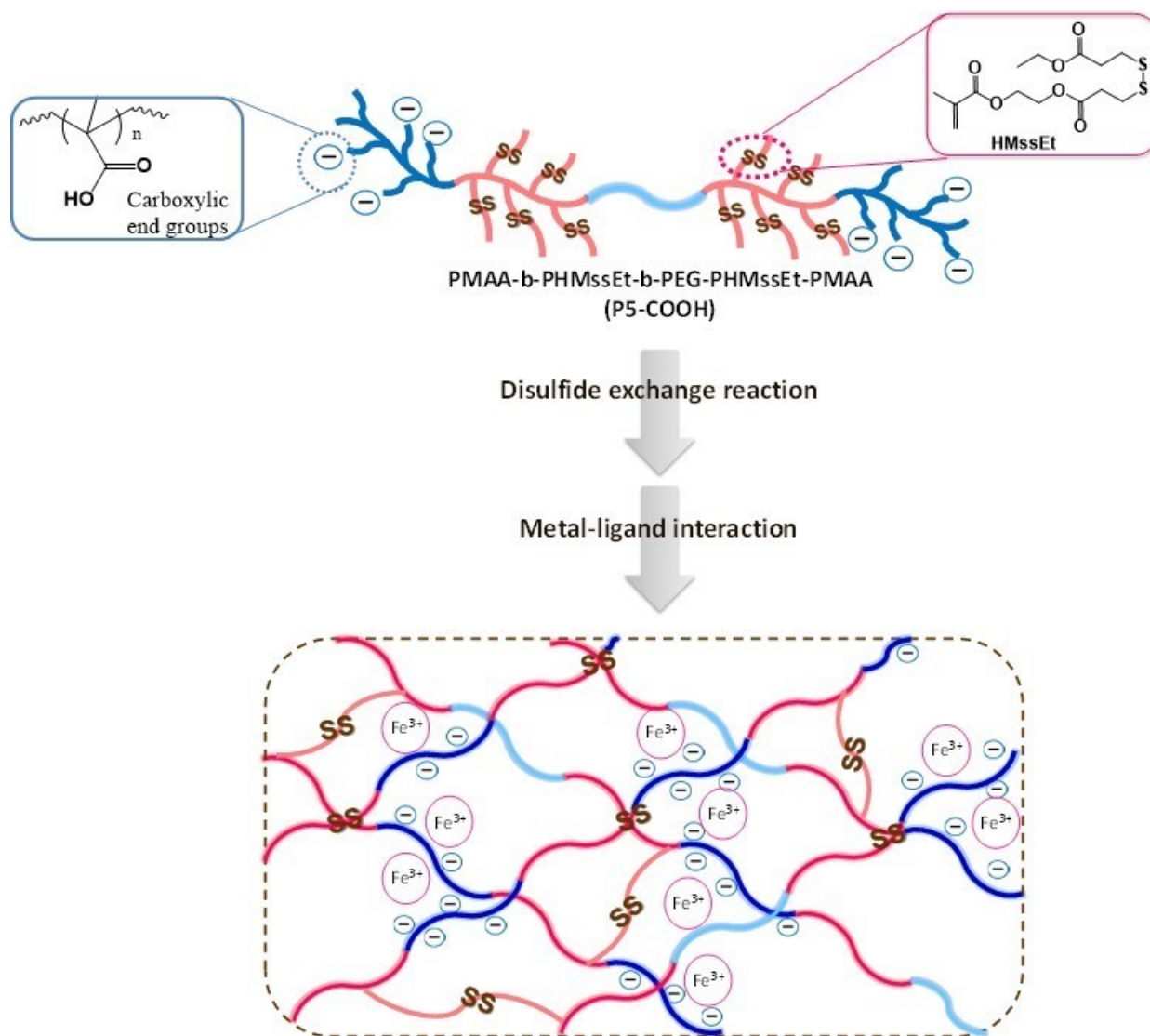
In recent years, crosslinked polymeric networks exhibiting self-healability have been extensively explored as effective building blocks in the development of high-performance multifunctional materials for various applications in nanoscience and industrial fields. Further to the features of conventionally-crosslinked networks including enhanced mechanical properties as well as improved thermal and chemical stabilities, self-healable networks have their built-in ability to autonomously self-repair initial damages. This feature prevents catastrophic failure of the materials and thus extends their lifetimes.^{37-38, 164}

Most initial development of self-healable materials utilizes the extrinsic self-healing method. The method requires the embedment of additional healing agents such as crosslinkers or catalysts inside capsule-like materials in the polymer matrix.^{41, 150} Upon physical damages, these embedded capsules are ruptured to release the healing agents and to repair the damaged parts. Although enabling the repair of large-sized damages, the main drawback of this method involves the occurrence of self-healing in a single event upon the depletion of healing agents. In contrast, the intrinsic method utilizes reversible crosslinking chemistries with dynamic covalent or physical crosslinkages in the networks. Typical examples include disulfide chemistry,^{1, 3, 55, 57, 165} Diels-Alder/retro-Diels-Alder reactions,^{64, 67, 74, 154-155} and hindered urea chemistry⁵⁻⁶ for reversible covalent bond formation, and π - π stacking,¹⁸⁻¹⁹ ionic interaction,^{110, 166} metal-ion binding,^{20-22, 24-25, 167-168} hydrogen bonding,¹³⁻¹⁶ and host-guest interactions¹⁷ for physical crosslinking mechanisms. Because of the dynamic ability of intrinsic method and thus the occurrence of repeatable self-healing, a number of intrinsic self-healing systems have been constructed with the use of single dynamic crosslinkages (either covalent or supramolecular linkages) that induce self-healing in the dynamic networks.^{39, 43}

A recent advance is the development of dual crosslinked self-healing systems,¹⁶⁹ designed with a combination of permanent covalent crosslinkages with dynamic supramolecular crosslinkages through hydrogen bonding¹⁷⁰⁻¹⁷¹ and metal-ligand interaction.¹⁷² The permanent crosslinkages retain the integrity of networks with mechanical strength, while supramolecular crosslinkages induce rapid self-healing upon physical damages. Although dual crosslinked network with both covalent sulfide (permanent) and disulfide (dynamic) crosslinkages has also been reported,¹⁷³ most dual crosslinked networks have designed with the occurrence of self-healing by a single mechanism, mostly supramolecular interactions. Further, advanced dual crosslinked networks with two dynamic covalent crosslinkages through disulfide exchange and acylhydrazone exchange reactions¹⁷⁴ as well as a combination of aromatic disulfides and supramolecular hydrogen bonds⁵² were reported. Although these systems show the occurrence of dual self-healing, the crosslinkages are randomly co-distributed in the networks.

We have recently focused on the development of effective self-healable materials in dual or multiple self-healable mechanisms based on multiblock copolymer strategy. This strategy centers on the synthesis of novel block copolymers designed with different self-healing motifs incorporated into each of the blocks. These self-healing motif (dynamic linkages) can be concentrated in localized areas as domains or in the matrix, thus maximizing the efficiency of their self-healabilities. Additionally, mechanical and chemical properties of the materials can be easily tuned with varying middle blocks.

Herein, as the first step towards our long-term research goals, we report our proof-of-concept design of a novel ABCBA-type pentablock copolymer (P5-COOH) consisting of a poly(ethylene glycol) middle “C” block and self-healable symmetric blocks. The self-healable blocks comprise of polymethacrylates with pendant disulfide linkages (PHMssEt) in two “B” blocks, and poly(methacrylic acid) (PMAA blocks) in two “A” blocks. The block copolymers dissolved in organic solvents were crosslinked with covalent disulfide linkages formed through disulfide exchange reactions of PHMssEt blocks and metal-ligand supramolecular crosslinkages through following physical interactions of pendant carboxylic acids with ferric (Fe^{3+}) ions. The formed dual crosslinked networks were characterized and further evaluated for rapid self-healing and excellent self-healing elasticity by dual mechanisms through disulfide exchange reactions and metal-ligand interactions upon macro-scale damages at multiple times at room temperature.



Scheme 4.1 Illustration of our approach to prepare dual crosslinked networks based on a novel pentablock copolymer exhibiting dual self-healing through covalent disulfide exchange reaction and supramolecular metal-ligand interactions.

4.2 Experimental section

4.2.1 Instrumentation and analysis

^1H -NMR spectra were recorded using a 500 MHz Varian spectrometer. The CDCl_3 singlet at 7.26 ppm or DMSO-d_6 quintet at 2.50 ppm was selected as the reference standards. Monomer conversion was determined by ^1H -NMR spectroscopy. Molecular weight and

molecular weight distribution were determined by gel permeation chromatography (GPC). An Agilent GPC was equipped with a 1260 Infinity Isocratic Pump and an RI detector. Two Agilent columns (PLgel mixed-D and mixed-C) were used with DMF containing 0.1 mol% LiBr at 50 °C at a flow rate of 1.0 mL/min. Linear poly(methyl methacrylate) standards from Fluka were used for calibration. Aliquots of polymer samples were dissolved in DMF/LiBr. The clear solutions were filtered using a 0.25 µm PTFE filter to remove any solvent-insoluble species. A drop of anisole was added as a flow rate marker.

4.2.2 Materials

α -bromoisobutyl bromide (iBuBr, 98%), triethylamine (Et₃N, >99.9%), copper(I) bromide (CuBr, >99.99%), N,N,N,N,N-pentamethyldiethylenetriamine (PMDETA, >98%), 2,2'-(ethylenedioxy)diethanethiol (EDSH, >95%), iron(III) chloride (FeCl₃, 98%), trifluoroacetic acid (CF₃COOH), and poly(ethylene glycol) with different molecular weights (OH-PEG-OH, >99%) purchased from Aldrich were used as received. A methacrylate bearing a pendant disulfide linkage (HMssEt), was synthesized as described elsewhere.¹⁷⁵

4.2.3 Synthesis of P1 PEG-based difunctional ATRP initiator

As a typical example to synthesize P1-3K, a clear solution of iBuBr (1.0 g, 4.5 mmol) dissolved in DCM (15 mL) was added dropwise to a solution consisting of OH-PEG-OH with molecular weight = 3350 g/mol (5.0 g, 3.0 mmol of OH), Et₃N (0.45 g, 4.5 mmol) and DCM (300 mL) in an ice-bath for 30 min. The resulting mixture was stirred at room temperature for 18 hrs, washed extensively with water (200 mL x 5 times), and then precipitated from hexane. The precipitate was isolated and further dried in a vacuum oven at room temperature for 13 hrs to yield P1-3K. Similar procedure was utilized for the synthesis of P1-6K with the use of OH-PEG-OH with molecular weight = 6000 g/mol (5.6 g, 1.9 mmol of OH), iBuBr (4.3 g, 18 mmol) and Et₃N (1.4 g, 14 mmol), for P1-10K with OH-PEG-OH with molecular weight 10,000 g/mol (10 g, 2.0 mmol of OH), iBuBr (4.6 g, 20 mmol) and Et₃N (2.5 g, 25 mmol) and for P1-22K with OH-PEG-OH with molecular weight = 22,000 g/mol (5.7 g, 0.52 mmol of OH), iBuBr (0.3 g, 1.3 mmol) and Et₃N (0.18 g, 1.8 mmol).

4.2.4 Synthesis of P3 triblock copolymers

As a typical example to prepare a P3-1 triblock copolymer, P1-3K (0.45 g, 0.13 mmol), HMssEt (1.5 g, 4.3 mmol), PMDETA (27 μ L, 0.13 mmol) and anisole (5.9 mL) were added to a Schlenk flask. The resulting mixture was deoxygenated by using freeze-pump-thaw cycles. The reaction flask was filled with nitrogen and CuBr (15 mg, 0.10 mmol) was added to the frozen solution. The flask was sealed, purged under vacuum and backfilled with nitrogen once. The mixture was thawed and the flask was then immersed in an oil bath preheated to 50 °C to start the polymerization. After 45 min, the polymerization was stopped by cooling and exposing the reaction mixture to air. For purification, the as-prepared polymer solution was diluted with DCM and passed through a basic alumina column to remove residual copper species. The solvent was removed under rotary evaporation at room temperature. The resulting polymer was isolated by precipitation from hexane and then dried under vacuum at room temperature for 15 hrs.

Similar procedure was utilized for the synthesis of P3-2 with P1-6K (0.82 g, 0.13 mmol), HMssEt (1.5 g, 4.3 mmol), PMDETA (27 μ L, 0.13 mmol), CuBr (15 mg, 0.10 mmol) and anisole (9.3 mL); and for P3-3 with P1-10K (1.3 g, 0.13 mmol), HMssEt (1.5 g, 4.3 mmol), PMDETA (27 μ L, 0.13 mmol), CuBr (15 mg, 0.10 mmol) and anisole (11 mL). For the synthesis of P3-4, ATRP was conducted for 3 hrs with the use of P1-22K (1.4 g, 0.069 mmol), HMssEt (0.8 g, 2.3 mmol), PMDETA (14 μ L, 0.068 mmol), CuBr (7.9 mg, 0.055 mmol) and anisole (14 mL).

4.2.5 Synthesis of P5 pentablock copolymers

P3-3 (1.3 g, 0.073 mmol), tBMA (1.0 g, 7.3 mmol), PMDETA (15 μ L, 0.072 mmol) and anisole (9.2 mL) were added to a Schlenk flask. The resulting mixture was deoxygenated by using freeze-pump-thaw cycles. The reaction flask was filled with nitrogen and CuBr (8.4 mg, 0.059 mmol) was added to the frozen solution. The flask was sealed, purged under vacuum and backfilled with nitrogen once. The mixture was thawed and the flask was then immersed in an oil bath preheated to 50 °C to start the polymerization. After 2 hrs, the polymerization was stopped by cooling and exposing the reaction mixture to air. For purification, the as-prepared polymer solution was diluted with DCM and passed through a basic alumina column to remove residual copper species. The solvent was removed under rotary evaporation at room temperature. The

resulting polymer was isolated by precipitation from hexane and then dried under vacuum at room temperature for 15 hrs.

4.2.6 Hydrolytic cleavage to yield P5-COOH

A clear solution of the purified, dried P5 (0.44 g, 0.23 mmol tBMA units) dissolved in DCM (20 mL) was mixed with CF₃COOH (174 μ L; 10 mole equivalence to t-butoxy groups) and stirred for 18 hrs at room temperature. The reaction mixtures were precipitated from hexane and then the precipitates were dried in vacuum oven for 18 hrs.

4.2.7 Preparation of disulfide-crosslinked gels of P3 triblock copolymers

The purified, dried P3-1 (0.1 g, 0.2 mmol of SS) was mixed with EDSH (7.9 mg, 0.2 mole equivalent to disulfides) in DMF. The mixture was placed in an oven preheated at 80 °C for 48 hrs to form a standing gel. In another set, P3-3 (0.25 g, 0.54 mmol of disulfides) was dissolved in chloroform (0.25 g) and the resulting mixture was placed in a vacuum oven pre-set at 80 °C for 18 hrs. The formed crosslinked gels were further dried in a vacuum oven for 18 hrs.

4.2.8 Preparation of dual crosslinked gels

Aliquots of P5-COOH (0.24 g, 0.28 mmol of disulfides and 0.19 mmol of COOH groups) were dissolved in chloroform (0.24 g) and the resulting mixture was placed in a vacuum oven at 80 °C for 18 hrs to induce *in situ* disulfide crosslinking. Then, an aqueous solution of FeCl₃ (33 mg, 0.21 mol for Fe³⁺/COOH = 1/1 ratio; 66mg, 0.41 mol for Fe³⁺/COOH = 2/1 ratio) in water (0.2 mL) was added to the disulfide crosslinked gels, and the resulting mixture was allowed to stay for 18 hrs to induce metal-ligand physical crosslinking. The formed dual crosslinked gels were further dried in a vacuum oven for 18hrs.

4.2.9 Optical microscopy.

Self-healing of crosslinked materials was observed by a microscope (Olympus BX51) coupled with a digital camera. Fresh cuts were made using a sharp blade on surfaces of the crosslinked materials to monitor their healing behavior at room temperature.

4.2.10 Rheological measurements.

Viscoelastic properties (G' and G'' moduli) of disulfide-crosslinked materials and dual-crosslinked materials were measured on a DHT-2 rheometer (TA Instruments, USA) in frequency sweep mode, and amplitude strain shear mode with parallel plate geometry (8 mm diameter). The dried gels prepared as above were customized with the diameter of 8 mm. For the frequency sweep mode, the gap was set to obtain an axial force around 5 N, and frequency was varied in the range of 1 rad/s and 100 rad/s. For the strain mode, the dried crosslinked materials were loaded on the plates and the % strain was varied in the range of 0.1 to 140 % strain at 1 rad/s frequency. Lastly, the elasticity of the crosslinked materials was tested by applying cyclic changes of amplitude oscillatory from 5% strain for 1500 s to 300% strain for 500 s. The gap was set to obtain an axial force of 5N at room temperature, and this cycle is repeated three times.

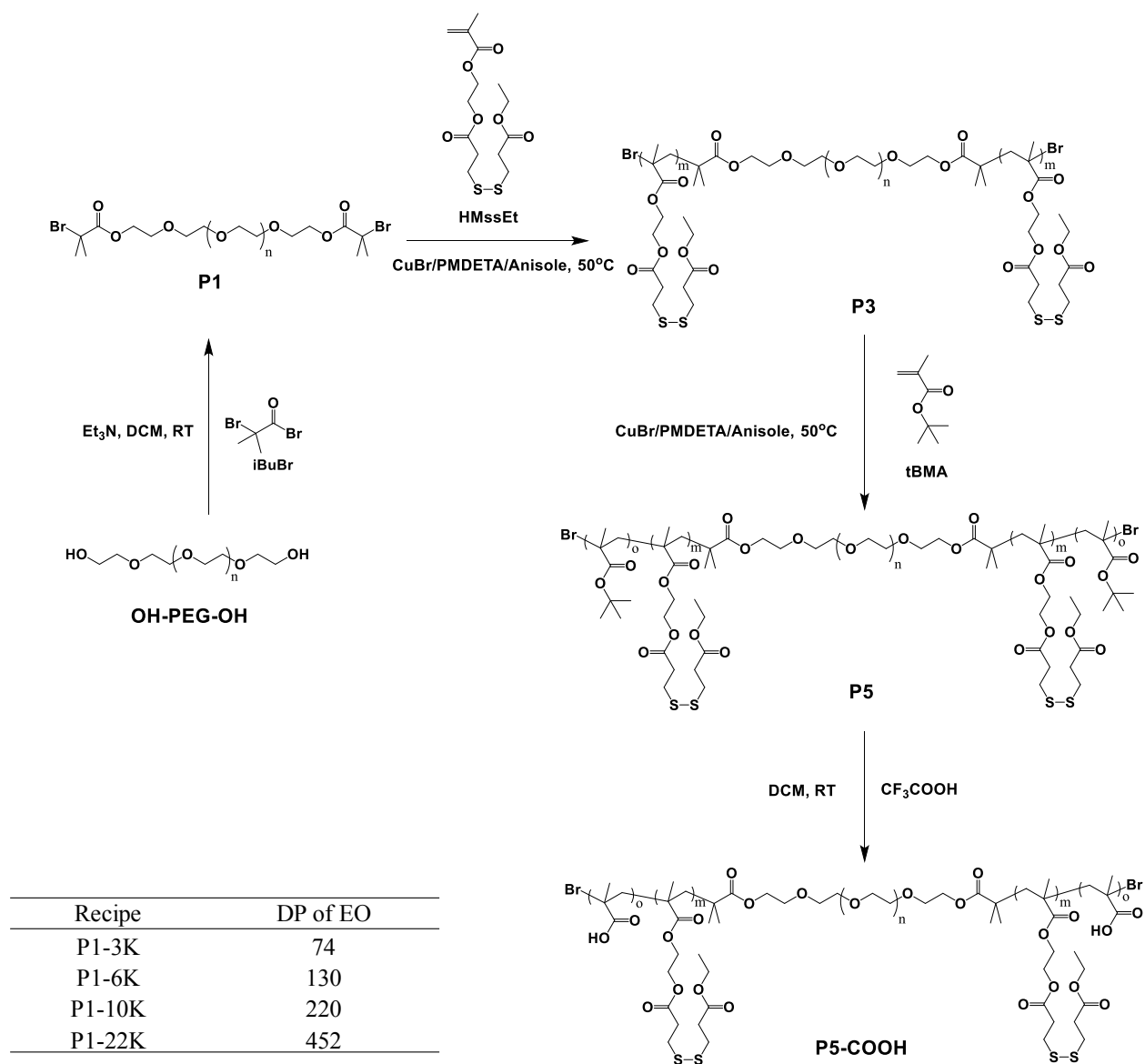


Figure 4.1 Synthetic scheme of P5-COOH pentablock copolymer. For the P1-xK: x denotes the molecular weight of P1 precursor, OH-PEG-OH. DP of EO was calculated using the molecular weight of OH-PEG-OH.

4.3 Results and discussion

4.3.1 Synthesis of triblock and pentablock copolymers

Figure 4.1 illustrates our scheme for multi-step synthesis of a novel pentablock copolymer consisting of 1) a PEG central block, 2) polymethacrylate blocks having pendant disulfide linkages (PHMssEt), and 3) polymethacrylate blocks having pendant carboxylic acids (COOH) groups (PMAA: poly(methacrylic acid)), thus PMAA-b-PHMssEt-b-PEG-b-PHMssEt-PMAA, hereafter, P5-COOH.

The first step is the synthesis of PEG-based difunctional ATRP macroinitiators (P1) labeled with bromine groups at both ends of PEG, by a facile coupling reaction of OH-PEG-OH with *i*BuBr in the presence of Et₃N (a base catalyst). Excess Et₃N and *i*BuBr should be used to ensure the complete esterification of hydroxyl groups in OH-PEG-OH. The resulting product was purified by precipitation from hexane. ¹H-NMR spectrum of P1-10K as an example in Figure 4.2a shows the peak at 4.3 ppm (b) corresponding to methylene protons adjacent to ester groups and the peak at 1.9 ppm (a) corresponding to two methyl protons. The integral ratio of these peaks indicates the quantitative esterification with >99%. Similar procedure was used to synthesize a series of PEG-based difunctional bromine initiators with various molecular weights of OH-PEG-OH, ranging from 3 to 22 kg/mol, presented in a table of Figure 4.1. Figure A.1 shows their ¹H-NMR spectra.

The second step is the chain extension of P1(Br-PEG-Br) with PHMssEt blocks to synthesize well-defined triblock copolymers, PHMssEt-b-PEG-b-PHMssEt (P3). A direct process for ATRP of HMssEt was examined in the presence of P1 macroinitiator in anisole at 50 °C. Conditions include [HMssEt]₀/[P1]₀/[CuBr]₀/[PMDETA]₀ = 17/1/0.4/0.49. The polymerization was stopped after 45 min for most reactions and 3 hrs for P3-4 to allow monomer conversion to reach > 60 %. As-synthesized polymer solutions were purified by passing through a basic aluminum oxide column to remove Cu species and then precipitating from hexane to remove unreacted monomers. ¹H-NMR spectrum of P3-3, as an example, in Figure 4.2b shows the presence of methylene groups adjacent to disulfide groups at 2.2-3.0 ppm (g,h) and poly(ethylene oxide) (EO) moieties at 3.3-3.4 ppm. Using the integral ratio of the peaks (e,d/EO), the degree of polymerization (DP) of each PHMssEt block was calculated to be 10, thus PHMssEt₁₀-b-PEG-b-PHMssEt₁₀. Its molecular weight with the average number molecular

weight, M_n was determined to be 29 kg/mol with $M_w/M_n = 1.1$ by GPC. Similar procedure was utilized to synthesize a series of P3 copolymers with the DP of PHMssEt blocks = 8-15, but with different PEG molecular weights (as PEG wt% in the copolymers). The detailed synthesis and characteristics of the P3 copolymers are summarized in Table 4.1, and their ^1H -NMR spectra and GPC traces are shown in Figure A.2 and A.3, respectively.

The third step is the chain extension of P3 with PtBMA blocks. Typically, the P3-3 triblock copolymer was selected because of its good solubility in both protic and aprotic solvent. A consecutive ATRP of tBMA (t-butyl methacrylate) was conducted in the presence of the purified, dried P3-3 difunctional macroinitiator in anisole at 50°C under the condition of $[\text{tBMA}]_0/[\text{P3-3}]_0/[\text{CuBr}]_0/[\text{PMDETA}]_0 = 50/1/0.4/0.49$, thus forming a pentablock copolymer. The polymerization was stopped after 2 hrs and conversion reached to 25 %. After the purification of P5, the resulted copolymer was characterized by ^1H -NMR spectrum. Figure 4.2c shows the typical peaks at 3.5-3.7 ppm corresponding to EO protons in the PEG block and a peak at 1.5 ppm (n) corresponding to t-butoxy protons in the PtBMA blocks. Using their integrals, the DP of each PtBMA block was determined to be ≈ 18 , thus $\text{PtBMA}_{18}\text{-b-PHMssEt}_{10}\text{-b-PEG-b-PHMssEt}_{10}\text{-b-PtBMA}_{18}$, P5. GPC results indicate its molecular weight, $M_n = 30$ kg/mol with $M_w/M_n = 1.1$ (Figure A.4).

The last step is the hydrolytic cleavage of pendant t-butoxy groups in PtBMA blocks of P5 pentablock copolymer to the corresponding PMAA in the presence of excess CF_3COOH . ^1H -NMR spectrum in Figure 4.2d shows the complete disappearance of the peak (n) corresponding to t-butoxy protons. This result indicates the successful cleavage of pendant t-butoxy groups upon acidic hydrolysis, yielding P5-COOH.

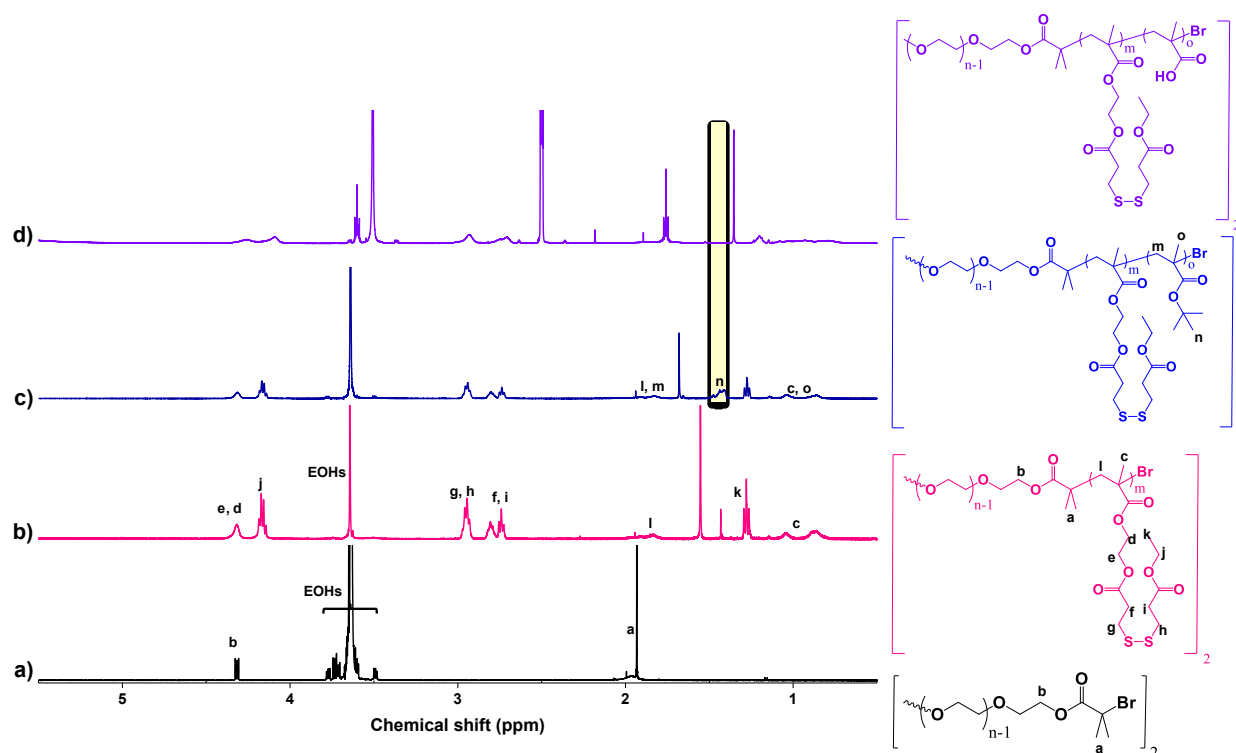


Figure 4.2 ^1H -NMR spectra P1-10K (a), P3-3 (b) as examples and P5 (c) in CDCl_3 . ^1H -NMR spectrum of P5-COOH (d) in $\text{DMSO}-d_6$.

Table 4.1 Characteristics of triblock copolymer (P3)

| Recipe | P1 | Reaction time (hr) | Conversion ^{b)} (%) | M_n^a (kg/mol) | PDI ^{a)} | DP of each PHMssEt block ^{b)} | PEG (wt%) |
|--------|--------|--------------------|------------------------------|------------------|-------------------|--|-----------|
| P3-1 | P1-3K | 0.75 | 64 | 15 | 1.2 | 15 | 24 |
| P3-2 | P1-6K | 0.75 | 60 | 19 | 1.2 | 15 | 36 |
| P3-3 | P1-10K | 0.75 | 60 | 29 | 1.1 | 10 | 58 |
| P3-4 | P1-22K | 3 | 60 | 40 | 1.1 | 8 | 78 |

^{a)} Determined by DMF-GPC; ^{b)} Determined by ^1H -NMR

4.3.2 Investigation of disulfide exchange gelation of P3 triblock copolymer

The resulting P5-COOH is an ABCBA-type pentablock copolymer having pendant disulfide linkages in two “B” blocks and COOH groups in two “A” blocks. The copolymer is designed to form dual crosslinked networks with new disulfide crosslinkages (“B” blocks) and

supramolecular metal-ligand (Fe^{3+} -COOH) association. Before the preparation of dual crosslinked gels of P5-COOH pentablock copolymer, the disulfide-based gelation of PHMssEt blocks having pendant disulfide linkages was investigated with P3 copolymers having central PEG and two PHMssEt blocks, a precursor for P5-COOH pentablock copolymer. Two gelation methods were examined for the formation of new *in situ* disulfide crosslinkages between P3 copolymer chains through disulfide exchange reaction of pendant disulfide linkages.

For the first method, aliquots of P3-1 were treated with a catalytic amount of EDSH (0.2 mole equivalent to disulfide linkages) in DMF at 42 wt % at 80 °C. As seen in Figure 4.3a, the reactive solution became a standing gel in a vial over 48 hrs. The resulting organogel was characterized for gel content based on its solubility in THF, a good solvent to both P3-1 and EDSH. Note that gels are defined as insoluble species in THF. Its gel content was 92 ± 2.3 %, suggesting the formation of highly crosslinked networks. However, this system appeared to require elevated temperatures for disulfide exchange gelation. This is because disulfide-thiol exchange reaction is slower for aliphatic disulfide linkages in PHMssEt units, compared to the corresponding aromatic disulfides.^{52, 176}

For the other method, an aliquot of P3-3 copolymer dissolved in chloroform at 50 wt % was heated at 80 °C for 18 hrs. As seen in Figure 4.3b inset, this thermal activation method allows for the formation of gels through disulfide metathesis or exchange reaction.¹⁷⁷ The formed gel was characterized for gel content to be 98 ± 6.1 % in THF. This method could be advantageous because of no need of dithiol reducing agents for disulfide exchange gelation. Further, the dried gel was characterized for its viscoelastic properties by a frequency sweep mode using a rheometer. As seen in Figure 4.3b, the loss modulus (G'') slightly increased with an increasing frequency up to 100 rad/s. The elastic modulus (G') kept unchanged up to 10 rad/s and then abruptly decreased upon a further increase in frequency, which presumably due to the loss of integrity of the dried gels.

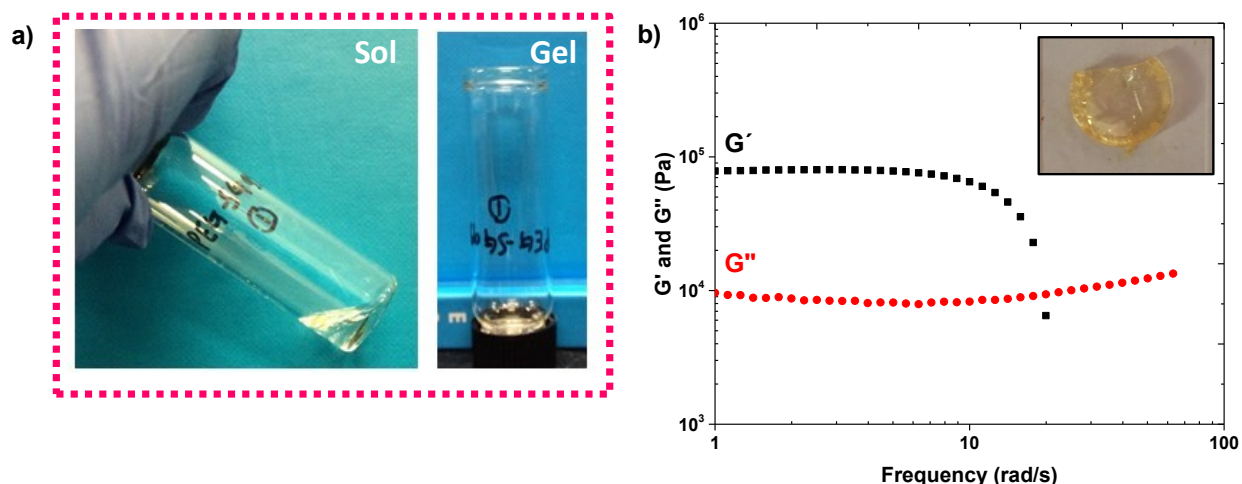


Figure 4.3 For P3-1 triblock copolymer, sol-gel transition in the presence of a catalytic amount of EDSH in DMF at 42 wt % (a), digital image (inset of b) and viscoelastic properties by frequency sweep mode (b) of disulfide-crosslinked gels prepared by thermal activation method.

4.3.3 Preparation and characterization of dual crosslinked gels of P5-COOH

Dual crosslinked gels of P5-COOH copolymer were prepared by sequential crosslinking reactions through disulfide exchange of PHMssEt blocks and metal-ligand association of PMAA blocks. For its disulfide exchange gelation, the similar procedure of thermal activation method of pendant disulfide linkages with no aids of reducing agents was examined for a clear solution of P5-COOH dissolved in chloroform at 50 wt % in a vacuum oven at 80 °C. As seen in Figure 4.4a, the solution turned to a standing gel in a vial over 18 hrs. For the metal-ligand gelation, the formed gels in vials were then treated with an aqueous FeCl_3 solution at room temperature overnight. After the removal of aqueous solutions, the resulting light brown-colored gels were further dried in a vacuum oven. Figure 4.4a shows the digital images of the dual crosslinked gels prepared at two different ratios of Fe^{3+} to COOH groups = 2/1 and 1/1. Note that the formed gels kept its integrity under weak force at the 1/1 ratio, while easily being broken to small pieces at the 2/1 ratio; thus the gel prepared at the 1/1 was further characterized. Its gel content was determined to be >95%, based on its solubility in THF (a good organic solvent). Figure 4.4b shows its viscoelastic properties by a frequency sweep mode. The loss modulus (G'') slightly increased with an increasing frequency up to 100 rad/s. The elastic modulus (G') kept unchanged up to 10 rad/s and then abruptly decreased upon a further increase in frequency. Note that the maximum G' values were smaller for P5-COOH gels ($\approx 10^4$ Pa) than P3 gels ($\approx 10^5$ Pa),

suggesting that the incorporation of the supramolecular network decreases mechanical strength of dual crosslinked network.

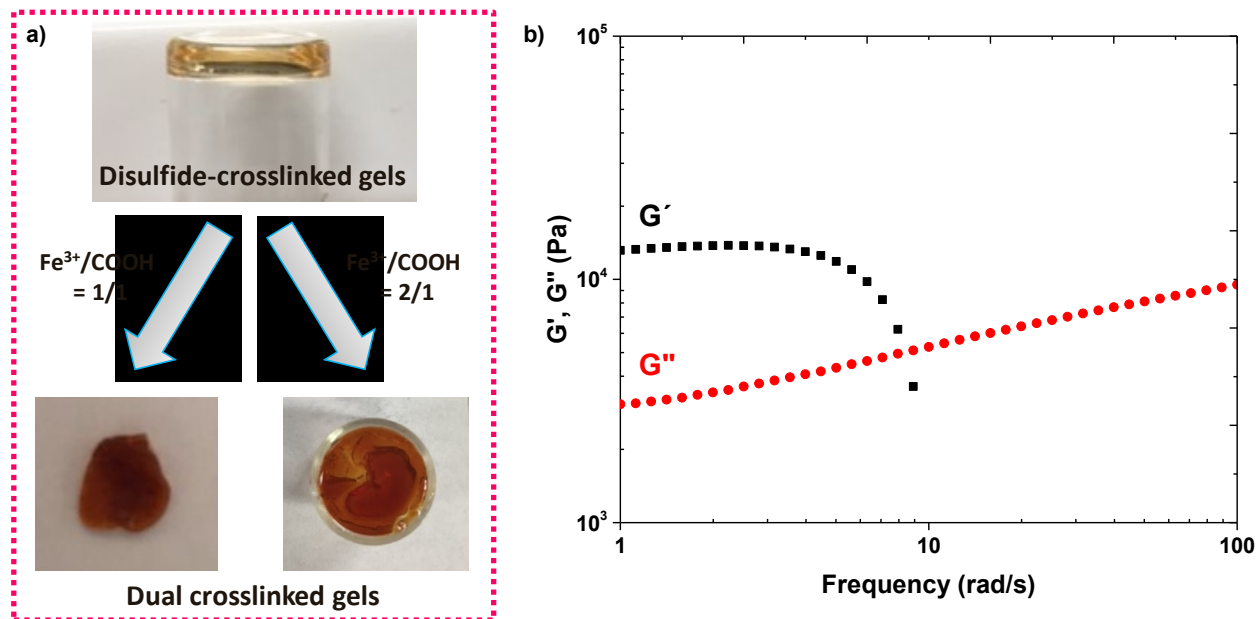


Figure 4.4 Dual crosslinked gels with 1 and 2 equivalent of FeCl_3 (a) and the viscoelastic properties of frequency sweep mode of dual crosslinked gels prepared with 1 equivalent of FeCl_3 (b).

4.3.4 Self-healing studies

Figure 4.5 shows the digital images of dual crosslinked gels prepared at the 1/1 ratio illustrating their self-healing at room temperature with no external aids. The dried gels with 1.3 cm long was cut into two halves (Figure 4.5a). The two halves brought into contact for 24 hrs (Figure 4.5b-c). The occurrence of self-healing is confirmed when the damaged gels with a cut was stretched in opposite directions (Figure 4.5d). The crosslinked networks were still intact with the appearance of no ruptures upon extensive stretching up to $\approx 200\%$ of its original length. For comparison, the corresponding gels with no cuts were also stretched up to $\approx 200\%$ as controls (Figure 4.5f-g). More promisingly, the occurrence of self-healing through stretching process was repeated multiple times at the same sites.

Further to get an insight into self-healability of dual crosslinked gels, their self-healing elasticity was examined as to measure G' and G'' moduli upon a cyclic change of oscillation

force: 5% strain for 1500 sec to 100 % strain for 500 sec. The angular frequency was set to 1 rad/s based on their previous frequency sweep studies. When a 5 % strain was applied for 1500 sec, G' value was constant with its maximum ($\approx 10^4$ Pa). However, G' modulus decreased abruptly upon high shear (100 % strain), suggesting rupture/disturbance of the networks. Then, the G' value was restored when the oscillation force was recovered back to 5% (Figure 4.6). Such reversible restoration in G' modulus was examined at multiple times, showing excellent self-healing elasticity features for the dual crosslinked gels.

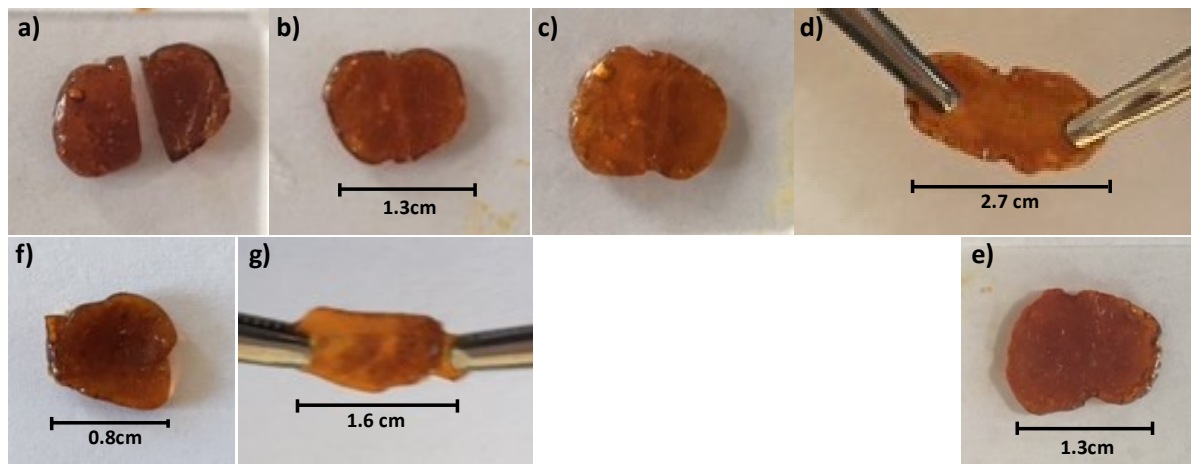


Figure 4.5 Digital images of dual crosslinked gels with a cut (a) after two parts were brought into contact (b), after healing 24 hrs (c) stretching the healed crosslinked networks (d) after stretching process (e); as well as without cut before (f) and after stretching (g).

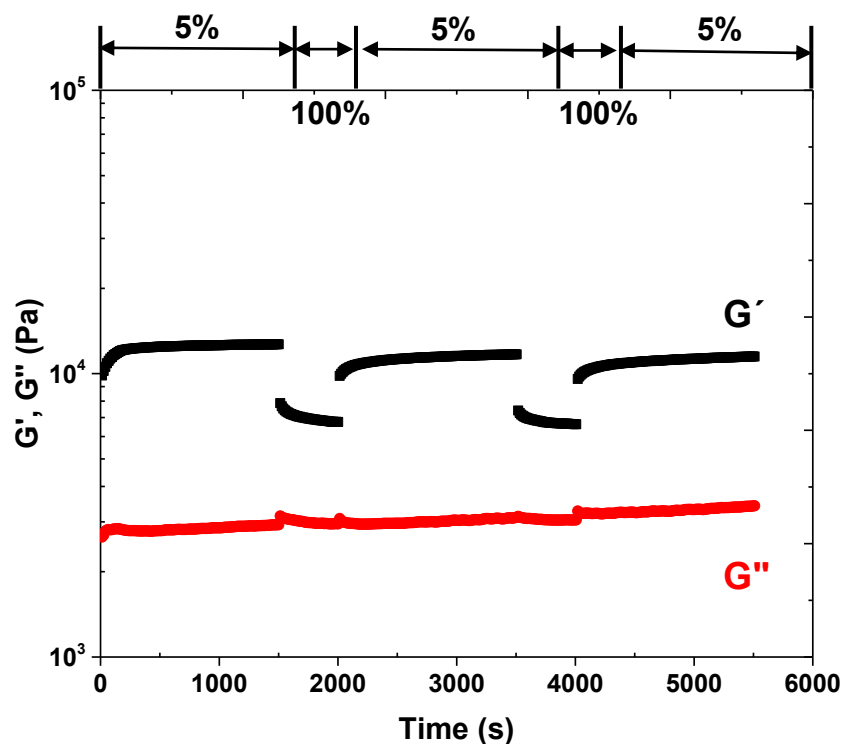


Figure 4.6 Viscoelastic properties using a rheometer upon a cyclic change of oscillation force: 5% strain for 1500 s to 100 % for 500 s for dual crosslinked gels

4.3.5 Further investigation of self-healing in P3 disulfide-crosslinked gels.

Dual covalent and supramolecular crosslinked gels based on P5-COOH pentablock copolymers are designed for self-healing by dual mechanisms through dynamic disulfide chemistry and metal-ligand interaction. Unfortunately, it appeared that it is not easy to investigate the dual self-healing. Alternatively, self-healing of P3 disulfide-crosslinked gels by dynamic disulfide chemistry through disulfide exchange or metathesis was examined.

As illustrated in Figure 4.7, cuts made on P3-1 gels were healed; however, moderate temperature and the presence of solvent are required for rapid self-healing in the system. The plausible reason could be due to slow disulfide exchange of aliphatic disulfides of PHMssEt domains. Therefore, further future designs could utilize aromatic disulfide moieties.

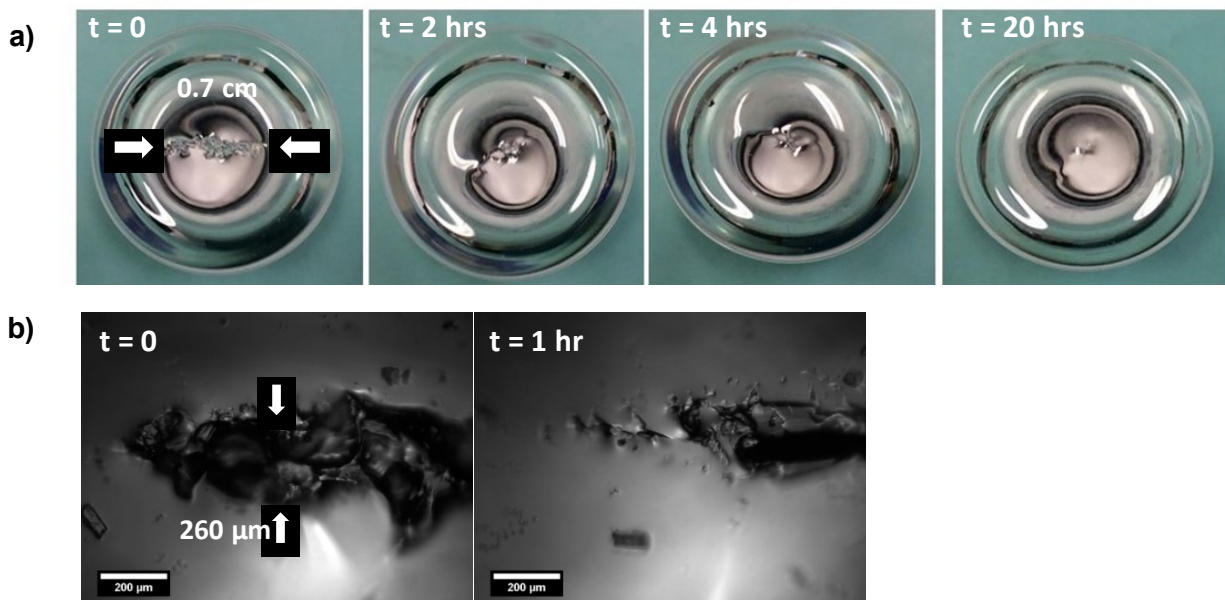


Figure 4.7 Digital images of penetrating cut on disulfide-crosslinked gels in the presence of DMF (42 wt%) at 80 °C (a) and optical microscopy images of the cut (260 μm wide) at room temperature with the aid of chloroform over time (b).

4.4 Conclusion

As a proof-of-concept, a pentablock copolymer having hydrophilic PEG middle block with PHMssEt and PMAA symmetric blocks (P5-COOH) was synthesized by a consecutive ATRP followed by acid hydrolysis. PHMssEt blocks were crosslinked with *in situ* disulfide crosslinkages through disulfide exchange reactions at moderate temperature to form covalent disulfide crosslinked network. Further, PMAA blocks were crosslinked in the presence of ferric ions at room temperature through metal-ligand interactions to form supramolecular networks, thus yielding dual crosslinked networks. The resulting networks exhibit rapid self-healing at macro-scale at room temperature as well as have self-healing elasticity. These promising results demonstrate that our multiblock copolymer strategy offers unique versatility in the development of smart self-healable materials.

Chapter 5

Conclusion and future work

Development of dynamic polymeric networks exhibiting self-healability has been extensively explored for great potential to overcome the negative consequences of physical damages. Recent strategies that allow for the synthesis of extrinsic and intrinsic self-repairing materials are mapped out in Chapter 2. The extrinsic method requires the micro-sized capsules of extra healing agents that are released to fill the fractured parts. When these extra healing agents are depleted, self-healing no longer occurs. On the other hand, the intrinsic self-healing method utilizes the reversible crosslinks created through the breakage and reformation of dynamic chemical/physical bonds. Due to the unique reversible characteristics, the self-repairing on damaged materials occur in a repeatable manner even at the same site.

Chapter 3 focuses on the effective design of dual disulfide-sulfide crosslinked network that exhibits rapid self-healing at room temperature. The network was prepared by a combination of free radical polymerization and post modification by a photo-induced thiol-ene radical addition and oxidation. Disulfide linkages were incorporated for self-healing through reversible disulfide chemistry, while sulfide linkages allowed for retaining the integrity of the network upon damages. Self-healing kinetics could be adjusted with the densities of disulfide crosslinks (formed through oxidation of thiols of the precursors) in the networks. With respect to physical damage/high shear force, the dual crosslinked network enabled to restore its original integrity due to its unique self-healing elasticity.

Chapter 4 describes the proof-of-concept approach to develop advanced dual crosslinked networks for dual self-healing through dynamic covalent disulfide and supramolecular chemistries. A novel P5-COOH, an ABCBA-type pentablock copolymer (P5-COOH) consisting of a PEG middle block with PHMssEt and PMAA symmetric blocks was synthesized by a combination of ATRP and hydrolytic cleavage. Well-known disulfide exchange reaction of PHMssEt blocks and metal-ligand association of PMAA blocks enabled to the formation of dual crosslinked networks with *in situ* disulfide and metal-ligand supramolecular crosslinkages. The

network exhibits the occurrence of self-healing plausibly by dual dynamic mechanisms on the networks evidenced with optical healing, elongation, and self-healing viscoelasticity.

Overall, most of the self-healable materials, including our two systems, have been designed with soft polymers (with low T_g) for rapid void-filling and thus self-repairing ability at ambient temperatures with no aids of external stimuli. The current and future design of effective self-healable networks require the balance of their toughness and their rapid void-filling ability to flow to fill the damaged parts. An incorporation of hard segments (or domains) into the soft self-healable matrices, such as cluster formation, nanoparticles incorporation, and microphase separation, could be a potential approach towards their successful industrial applications.

References

1. Pepels, M.; Pilot, I.; Klumperman, B.; Goossens, H., Self-healing systems based on disulfide-thiol exchange reactions. *Polymer Chemistry* **2013**, *4* (18), 4955-4965.
2. Yoon, J. A.; Kamada, J.; Koynov, K.; Mohin, J.; Nicolay, R.; Zhang, Y.; Balazs, A. C.; Kowalewski, T.; Matyjaszewski, K., Self-Healing Polymer Films Based on Thiol-Disulfide Exchange Reactions and Self-Healing Kinetics Measured Using Atomic Force Microscopy. *Macromolecules* **2012**, *45* (1), 142-149.
3. Lei, Z. Q.; Xiang, H. P.; Yuan, Y. J.; Rong, M. Z.; Zhang, M. Q., Room-Temperature Self-Healable and Remoldable Cross-linked Polymer Based on the Dynamic Exchange of Disulfide Bonds. *Chemistry of Materials* **2014**, *26* (6), 2038-2046.
4. Hutchby, M.; Houlden, C. E.; Ford, J. G.; Tyler, S. N. G.; Gagne, M. R.; Lloyd-Jones, G. C.; Booker-Milburn, K. I., Hindered Ureas as Masked Isocyanates: Facile Carbamoylation of Nucleophiles under Neutral Conditions. *Angewandte Chemie* **2009**, *48* (46), 8721-8724.
5. Ying, H.; Zhang, Y.; Cheng, J., Dynamic urea bond for the design of reversible and self-healing polymers. *Nature Communication* **2014**, *5*, 4218/1-4218/9.
6. Ying, H.; Cheng, J., Hydrolyzable polyureas bearing hindered urea bonds. *Journal of the American Chemical Society* **2014**, *136* (49), 16974-16977.
7. Zhang, Z. P.; Rong, M. Z.; Zhang, M. Q.; Yuan, C.-e., Alkoxyamine with reduced homolysis temperature and its application in repeated autonomous self-healing of stiff polymers. *Polymer Chemistry* **2013**, *4* (17), 4648-4654.
8. Yuan, C. e.; Rong, M. Z.; Zhang, M. Q.; Zhang, Z. P.; Yuan, Y. C., Self-Healing of Polymers via Synchronous Covalent Bond Fission/Radical Recombination. *Chemistry of Materials* **2011**, *23* (22), 5076-5081.
9. Imato, K.; Nishihara, M.; Kanehara, T.; Amamoto, Y.; Takahara, A.; Otsuka, H., Self-Healing of Chemical Gels Cross-Linked by Diarylbibenzofuranone-Based Trigger-Free Dynamic Covalent Bonds at Room Temperature. *Angewandte Chemie* **2012**, *51* (5), 1138-1142.
10. Cash, J. J.; Kubo, T.; Bapat, A. P.; Sumerlin, B. S., Room-Temperature Self-Healing Polymers Based on Dynamic-Covalent Boronic Esters. *Macromolecules* **2015**, *48* (7), 2098-2106.
11. Cromwell, O. R.; Chung, J.; Guan, Z., Malleable and Self-Healing Covalent Polymer Networks through Tunable Dynamic Boronic Ester Bonds. *Journal of the American Chemical Society* **2015**, *137* (20), 6492-6495.
12. Meng, H.; Xiao, P.; Gu, J.; Wen, X.; Xu, J.; Zhao, C.; Zhang, J.; Chen, T., Self-healable macro-/microscopic shape memory hydrogels based on supramolecular interactions. *Chemical Communications* **2014**, *50* (82), 12277-12280.
13. Chen, Y.; Guan, Z., Self-assembly of core-shell nanoparticles for self-healing materials. *Polymer Chemistry* **2013**, *4* (18), 4885-4889.
14. Chen, Y.; Guan, Z., Multivalent hydrogen bonding block copolymers self-assemble into strong and tough self-healing materials. *Chemical Communication* **2014**, *50* (74), 10868-10870.
15. Lin, Y.; Li, G., An intermolecular quadruple hydrogen-bonding strategy to fabricate self-healing and highly deformable polyurethane hydrogels. *Journal of Material Chemistry B* **2014**, *2* (39), 6878-6885.
16. Hentschel, J.; Kushner, A. M.; Ziller, J.; Guan, Z., Self-Healing Supramolecular Block Copolymers. *Angewandte Chemie* **2012**, *51* (42), 10561-10565.
17. Yang, X.; Yu, H.; Wang, L.; Tong, R.; Akram, M.; Chen, Y.; Zhai, X., Self-healing polymer materials constructed by macrocycle-based host-guest interactions. *Soft Matter* **2015**, *11* (7), 1242-1252.
18. Vaiyapuri, R.; Greenland, B. W.; Colquhoun, H. M.; Elliott, J. M.; Hayes, W., Molecular recognition between functionalized gold nanoparticles and healable, supramolecular polymer blends - a route to property enhancement. *Polymer Chemistry* **2013**, *4* (18), 4902-4909.

19. Hart, L. R.; Harries, J. L.; Greenland, B. W.; Colquhoun, H. M.; Hayes, W., Healable supramolecular polymers. *Polymer Chemistry* **2013**, *4* (18), 4860-4870.
20. Yan, X.; Xu, D.; Chen, J.; Zhang, M.; Hu, B.; Yu, Y.; Huang, F., A self-healing supramolecular polymer gel with stimuli-responsiveness constructed by crown ether based molecular recognition. *Polymer Chemistry* **2013**, *4* (11), 3312-3322.
21. Krogsgaard, M.; Behrens, M. A.; Pedersen, J. S.; Birkedal, H., Self-Healing Mussel-Inspired Multi-pH-Responsive Hydrogels. *Biomacromolecules* **2013**, *14* (2), 297-301.
22. Wang, Z.; Urban, M. W., Facile UV-healable polyethylenimine-copper (C₂H₅N-Cu) supramolecular polymer networks. *Polymer Chemistry* **2013**, *4* (18), 4897-4901.
23. Basak, S.; Nanda, J.; Banerjee, A., Multi-stimuli responsive self-healing metallo-hydrogels: tuning of the gel recovery property. *Chemical Communication* **2014**, *50* (18), 2356-2359.
24. Potier, F.; Guinault, A.; Delalande, S.; Sanchez, C.; Ribot, F.; Rozes, L., Nano-building block based-hybrid organic-inorganic copolymers with self-healing properties. *Polymer Chemistry* **2014**, *5* (15), 4474-4479.
25. Wang, Z.; Fan, W.; Tong, R.; Lu, X.; Xia, H., Thermal-healable and shape memory metallosupramolecular poly(n-butyl acrylate-co-methyl methacrylate) materials. *RSC Advances* **2014**, *4* (49), 25486-25493.
26. Chen, Y.; Guan, Z., Multivalent hydrogen bonding block copolymers self-assemble into strong and tough self-healing materials. *Chemical Communications* **2014**, *50* (74), 10868-70.
27. Michael, P.; Döhler, D.; Binder, W. H., Improving autonomous self healing via combined chemical/physical principles. *Polymer* **2015**, *69*, 216-227.
28. Cabodi, M.; Choi, N. W.; Gleghorn, J. P.; Lee, C. S. D.; Bonassar, L. J.; Stroock, A. D., A Microfluidic Biomaterial. *Journal of the American Chemical Society* **2005**, *127* (40), 13788-13789.
29. Choi, N. W.; Cabodi, M.; Held, B.; Gleghorn, J. P.; Bonassar, L. J.; Stroock, A. D., Microfluidic scaffolds for tissue engineering. *Nature Materials* **2007**, *6* (11), 908-915.
30. Ooka, M.; Ozawa, H., Recent developments in crosslinking technology for coating resins. *Progress in Organic Coatings* **1994**, *23* (4), 325-38.
31. Oh, J. K.; Park, J. M., Iron oxide-based superparamagnetic polymeric nanomaterials: Design, preparation, and biomedical application. *Progress in Polymer Science* **2011**, *36* (1), 168-189.
32. Oh, J. K.; Drumright, R.; Siegwart, D. J.; Matyjaszewski, K., The development of microgels/nanogels for drug delivery applications. *Progress in Polymer Science* **2008**, *33* (4), 448-477.
33. Langer, R.; Vacanti, J. P., Tissue engineering. *Science* **1993**, *260* (5110), 920-926.
34. Hoffman, A. S., Applications of thermally reversible polymers and hydrogels in therapeutics and diagnostics. *Journal of Control Release* **1987**, *6*, 297-305.
35. Peppas, N. A.; Hilt, J. Z.; Khademhosseini, A.; Langer, R., Hydrogels in biology and medicine: from molecular principles to bionanotechnology. *Advanced Materials* **2006**, *18* (11), 1345-1360.
36. Slaughter, B. V.; Khurshid, S. S.; Fisher, O. Z.; Khademhosseini, A.; Peppas, N. A., Hydrogels in Regenerative Medicine. *Advanced Materials* **2009**, *21* (32-33), 3307-3329.
37. Blaiszik, B. J.; Kramer, S. L. B.; Olugebefola, S. C.; Moore, J. S.; Sottos, N. R.; White, S. R., Self-Healing Polymers and Composites. *Annual Review of Materials Research* **2010**, *40* (1), 179-211.
38. Burattini, S.; Greenland, B. W.; Chappell, D.; Colquhoun, H. M.; Hayes, W., Healable polymeric materials: a tutorial review. *Chemical Society Reviews* **2010**, *39* (6), 1973-1985.
39. Billiet, S.; Hillewaere, X. K.; Teixeira, R. F.; Du Prez, F. E., Chemistry of crosslinking processes for self-healing polymers. *Macromol Rapid Commun* **2013**, *34* (4), 290-309.
40. Syrett, J. A.; Mantovani, G.; Barton, W. R. S.; Price, D.; Haddleton, D. M., Self-healing polymers prepared via living radical polymerization. *Polymer Chemistry* **2010**, *1* (1), 102-106.
41. Shchukin, D. G., Container-based multifunctional self-healing polymer coatings. *Polymer Chemistry* **2013**, *4* (18), 4871-4877.
42. Zhao, Z.; Arruda, E. M., An internal cure for damaged polymers. *Science* **2014**, *344* (6184), 591-592.

43. Wei, Z.; Yang, J. H.; Zhou, J.; Xu, F.; Zrinyi, M.; Dussault, P. H.; Osada, Y.; Chen, Y. M., Self-healing gels based on constitutional dynamic chemistry and their potential applications. *Chemical Society Reviews* **2014**, 43 (23), 8114-31.
44. Garcia, S. J., Effect of polymer architecture on the intrinsic self-healing character of polymers. *European Polymer Journal* **2014**, 53, 118-125.
45. Zhang, M. Q.; Rong, M. Z., Intrinsic self-healing of covalent polymers through bond reconnection towards strength restoration. *Polymer Chemistry* **2013**, 4 (18), 4878-4884.
46. Chujo, Y.; Sada, K.; Nomura, R.; Naka, A.; Saegusa, T., Photogelation and redox properties of anthracene-disulfide-modified polyoxazolines. *Macromolecules* **1993**, 26 (21), 5611-14.
47. Tsarevsky, N. V.; Matyjaszewski, K., Reversible Redox Cleavage/Coupling of Polystyrene with Disulfide or Thiol Groups Prepared by Atom Transfer Radical Polymerization. *Macromolecules* **2002**, 35 (24), 9009-9014.
48. Rajan, V. V.; Dierkes, W. K.; Joseph, R.; Noordermeer, J. W. M., Science and technology of rubber reclamation with special attention to NR-based waste latex products. *Progress in Polymer Science* **2006**, 31 (9), 811-834.
49. Wiita, A. P.; Ainarapu, R. K.; Huang, H. H.; Fernandez, J. M., Force-dependent chemical kinetics of disulfide bond reduction observed with single-molecule techniques. *Proceedings of the National Academy of Sciences of the United States of America* **2006**, 103 (19), 7222-7227.
50. Fairbanks, B. D.; Singh, S. P.; Bowman, C. N.; Anseth, K. S., Photodegradable, Photoadaptable Hydrogels via Radical-Mediated Disulfide Fragmentation Reaction. *Macromolecules* **2011**, 44 (8), 2444-2450.
51. Caraballo, R.; Rahm, M.; Vongvilai, P.; Brinck, T.; Ramstroem, O., Phosphine-catalyzed disulfide metathesis. *Chemical Communications* **2008**, (48), 6603-6605.
52. Rekondo, A.; Martin, R.; Ruiz de Luzuriaga, A.; Cabanero, G.; Grande, H. J.; Odriozola, I., Catalyst-free room-temperature self-healing elastomers based on aromatic disulfide metathesis. *Materials Horizons* **2014**, 1 (2), 237-240.
53. Martin, R.; Rekondo, A.; Ruiz de Luzuriaga, A.; Cabanero, G.; Grande, H. J.; Odriozola, I., The processability of a poly(urea-urethane) elastomer reversibly crosslinked with aromatic disulfide bridges. *Journal of Materials Chemistry A: Materials for Energy and Sustainability* **2014**, 2 (16), 5710-5715.
54. Otsuka, H.; Nagano, S.; Kobashi, Y.; Maeda, T.; Takahara, A., A dynamic covalent polymer driven by disulfide metathesis under photoirradiation. *Chemical Communications* **2010**, 46 (7), 1150-1152.
55. Canadell, J.; Goossens, H.; Klumperman, B., Self-Healing Materials Based on Disulfide Links. *Macromolecules* **2011**, 44 (8), 2536-2541.
56. Lafont, U.; van Zeijl, H.; van der Zwaag, S., Influence of Cross-linkers on the Cohesive and Adhesive Self-Healing Ability of Polysulfide-Based Thermosets. *ACS Applied Materials & Interfaces* **2012**, 4 (11), 6280-6288.
57. Barcan, G. A.; Zhang, X.; Waymouth, R. M., Structurally Dynamic Hydrogels Derived from 1,2-Dithiolanes. *Journal of the American Chemical Society* **2015**, 137 (17), 5650-5653.
58. Abdollah Zadeh, M.; Esteves, A. C. C.; Zwaag, S.; Garcia, S. J., Healable dual organic-inorganic crosslinked sol-gel based polymers: Crosslinking density and tetrasulfide content effect. *Journal of Polymer Science, Part A: Polymer Chemistry* **2014**, 52 (14), 1953-1961.
59. An, S. Y.; Noh, S. M.; Nam, J. H.; Oh, J. K., Dual Sulfide-Disulfide Crosslinked Networks with Rapid and Room Temperature Self-Healability. *Macromolecular Rapid Communications* **2015**, Ahead of Print.
60. Chen, X.; Dam, M. A.; Ono, K.; Mal, A.; Shen, H.; Nutt, S. R.; Sheran, K.; Wudl, F., A thermally re-mendable cross-linked polymeric material. *Science* **2002**, 295 (5560), 1698-702.
61. Fleet, E. J.; Zhang, Y.; Hayes, S. A.; Smith, P. J., Inkjet printing of self-healing polymers for enhanced composite interlaminar properties. *Journal of Materials Chemistry A: Materials for Energy and Sustainability* **2015**, 3 (5), 2283-2293.

62. Murphy, E. B.; Bolanos, E.; Schaffner-Hamann, C.; Wudl, F.; Nutt, S. R.; Auad, M. L., Synthesis and Characterization of a Single-Component Thermally Remendable Polymer Network: Staudinger and Stille Revisited. *Macromolecules* **2008**, *41* (14), 5203-5209.
63. Postiglione, G.; Turri, S.; Levi, M., Effect of the plasticizer on the self-healing properties of a polymer coating based on the thermoreversible Diels-Alder reaction. *Progress in Organic Coatings* **2015**, *78*, 526-531.
64. Liu, Y.-L.; Chuo, T.-W., Self-healing polymers based on thermally reversible Diels-Alder chemistry. *Polymer Chemistry* **2013**, *4* (7), 2194-2205.
65. Kavitha, A. A.; Choudhury, A.; Singha, N. K., Controlled radical polymerization of furfuryl methacrylate. *Macromolecular Symposia* **2006**, *240* (Recent Trends in Ionic Polymerization), 232-237.
66. Kavitha, A. A.; Singha, N. K., A tailor-made polymethacrylate bearing a reactive diene in reversible Diels-Alder reaction. *Journal of Polymer Science, Part A: Polymer Chemistry* **2007**, *45* (19), 4441-4449.
67. Kavitha, A. A.; Singha, N. K., "Click Chemistry" in Tailor-Made Polymethacrylates Bearing Reactive Furfuryl Functionality: A New Class of Self-Healing Polymeric Material. *ACS Applied Materials & Interfaces* **2009**, *1* (7), 1427-1436.
68. Pramanik, N. B.; Nando, G. B.; Singha, N. K., Self-healing polymeric gel via RAFT polymerization and Diels-Alder click chemistry. *Polymer* **2015**, Ahead of Print.
69. Kavitha, A. A.; Singha, N. K., Smart "All Acrylate" ABA Triblock Copolymer Bearing Reactive Functionality via Atom Transfer Radical Polymerization (ATRP): Demonstration of a "Click Reaction" in Thermoreversible Property. *Macromolecules* **2010**, *43* (7), 3193-3205.
70. Bai, J.; Li, H.; Shi, Z.; Yin, J., An Eco-Friendly Scheme for the Cross-Linked Polybutadiene Elastomer via Thiol-Ene and Diels-Alder Click Chemistry. *Macromolecules* **2015**, *48* (11), 3539-3546.
71. Trovatti, E.; Lacerda, T. M.; Carvalho, A. J. F.; Gandini, A., Recycling Tires? Reversible Crosslinking of Poly(butadiene). *Advanced Materials* **2015**, *27* (13), 2242-2245.
72. Liu, Y.-L.; Chen, Y.-W., Thermally reversible cross-linked polyamides with high toughness and self-repairing ability from maleimide- and furan-functionalized aromatic polyamides. *Macromolecular Chemistry and Physics* **2007**, *208* (2), 224-232.
73. Wang, Y.; Xu, H.; Zhang, X., Tuning the Amphiphilicity of Building Blocks: Controlled Self-Assembly and Disassembly for Functional Supramolecular Materials. *Advanced Materials* **2009**, *21* (28), 2849-2864.
74. Pratama, P. A.; Peterson, A. M.; Palmese, G. R., The role of maleimide structure in the healing of furan-functionalized epoxy-amine thermosets. *Polymer Chemistry* **2013**, *4* (18), 5000-5006.
75. Pratama, P. A.; Sharifi, M.; Peterson, A. M.; Palmese, G. R., Room Temperature Self-Healing Thermoset Based on the Diels-Alder Reaction. *ACS Applied Materials & Interfaces* **2013**, *5* (23), 12425-12431.
76. Amamoto, Y.; Otsuka, H.; Takahara, A.; Matyjaszewski, K., Self-healing of covalently crosslinked polymers by reshuffling thiuram disulfide moieties in air under visible light. *Advanced Materials* **2012**, *24* (29), 3975-3980.
77. Nicolay, R.; Kamada, J.; Van Wassen, A.; Matyjaszewski, K., Responsive Gels Based on a Dynamic Covalent Trithiocarbonate Cross-Linker. *Macromolecules* **2010**, *43* (9), 4355-4361.
78. Deng, G.; Tang, C.; Li, F.; Jiang, H.; Chen, Y., Covalent Crosslinked Polymer Gels with Reversible Sol-Gel Transition and Self-Healing Properties. *Macromolecules* **2010**, *43* (3), 1191-1194.
79. Liu, F.; Li, F.; Deng, G.; Chen, Y.; Zhang, B.; Zhang, J.; Liu, C.-Y., Rheological Images of Dynamic Covalent Polymer Networks and Mechanisms behind Mechanical and Self-Healing Properties. *Macromolecules* **2012**, *45* (3), 1636-1645.
80. Deng, G.; Li, F.; Yu, H.; Liu, F.; Liu, C.; Sun, W.; Jiang, H.; Chen, Y., Dynamic Hydrogels with an Environmental Adaptive Self-Healing Ability and Dual Responsive Sol-Gel Transitions. *ACS Macro Letters* **2012**, *1* (2), 275-279.

81. Haldar, U.; Bauri, K.; Li, R.; Faust, R.; De, P., Polyisobutylene-Based pH-Responsive Self-Healing Polymeric Gels. *ACS Applied Materials & Interfaces* **2015**, 7 (16), 8779-8788.
82. Lu, Y. X.; Guan, Z., Olefin metathesis for effective polymer healing via dynamic exchange of strong carbon-carbon double bonds. *Journal of the American Chemical Society* **2012**, 134 (34), 14226-31.
83. Banerjee, S.; Tripathy, R.; Cozzens, D.; Nagy, T.; Keki, S.; Zsuga, M.; Faust, R., Photoinduced Smart, Self-Healing Polymer Sealant for Photovoltaics. *ACS Applied Materials & Interfaces* **2015**, 7 (3), 2064-2072.
84. van Gemert, G. M. L.; Peeters, J. W.; Söntjens, S. H. M.; Janssen, H. M.; Bosman, A. W., Self-Healing Supramolecular Polymers In Action. *Macromolecular Chemistry and Physics* **2012**, 213 (2), 234-242.
85. Herbst, F.; Schröter, K.; Gunkel, I.; Gröger, S.; Thurn-Albrecht, T.; Balbach, J.; Binder, W. H., Aggregation and Chain Dynamics in Supramolecular Polymers by Dynamic Rheology: Cluster Formation and Self-Aggregation. *Macromolecules* **2010**, 43 (23), 10006-10016.
86. Cordier, P.; Tournilhac, F.; Soulie-Ziakovic, C.; Leibler, L., Self-healing and thermoreversible rubber from supramolecular assembly. *Nature* **2008**, 451 (7181), 977-80.
87. Phadke, A.; Zhang, C.; Arman, B.; Hsu, C.-C.; Mashelkar, R. A.; Lele, A. K.; Tauber, M. J.; Arya, G.; Varghese, S., Rapid self-healing hydrogels. *Proceedings of the National Academy of Sciences of the United States of America* **2012**, 109 (12), 4383-4388.
88. Wilson, G. O.; Caruso, M. M.; Schelkopf, S. R.; Sottos, N. R.; White, S. R.; Moore, J. S., Adhesion Promotion via Noncovalent Interactions in Self-Healing Polymers. *ACS Applied Materials & Interfaces* **2011**, 3 (8), 3072-3077.
89. Kieltyka, R. E.; Pape, A. C.; Albertazzi, L.; Nakano, Y.; Bastings, M. M.; Voets, I. K.; Dankers, P. Y.; Meijer, E. W., Mesoscale modulation of supramolecular ureidopyrimidinone-based poly(ethylene glycol) transient networks in water. *Journal of the American Chemical Society* **2013**, 135 (30), 11159-64.
90. Chen, Y.; Kushner, A. M.; Williams, G. A.; Guan, Z., Multiphase design of autonomic self-healing thermoplastic elastomers. *Nature Chemistry* **2012**, 4, 467-472.
91. Hentschel, J.; Kushner, A. M.; Ziller, J.; Guan, Z., Self-healing supramolecular block copolymers. *Angewandte Chemie* **2012**, 51 (42), 10561-5.
92. Burattini, S.; Colquhoun, H. M.; Fox, J. D.; Friedmann, D.; Greenland, B. W.; Harris, P. J.; Hayes, W.; Mackay, M. E.; Rowan, S. J., A self-repairing, supramolecular polymer system: healability as a consequence of donor-acceptor pi-pi stacking interactions. *Chemical communications* **2009**, (44), 6717-9.
93. Burattini, S.; Greenland, B. W.; Merino, D. H.; Weng, W.; Seppala, J.; Colquhoun, H. M.; Hayes, W.; Mackay, M. E.; Hamley, I. W.; Rowan, S. J., A healable supramolecular polymer blend based on aromatic pi-pi stacking and hydrogen-bonding interactions. *Journal of the American Chemical Society* **2010**, 132, 12051-12058.
94. Hart, L. R.; Hunter, J. H.; Nguyen, N. A.; Harries, J. L.; Greenland, B. W.; Mackay, M. E.; Colquhoun, H. M.; Hayes, W., Multivalency in healable supramolecular polymers: the effect of supramolecular cross-link density on the mechanical properties and healing of non-covalent polymer networks. *Polymer Chemistry* **2014**, 5 (11), 3680-3688.
95. Fox, J.; Wie, J. J.; Greenland, B. W.; Burattini, S.; Hayes, W.; Colquhoun, H. M.; Mackay, M. E.; Rowan, S. J., High-strength, healable, supramolecular polymer nanocomposites. *Journal of the American Chemical Society* **2012**, 134 (11), 5362-8.
96. Vaiyapuri, R.; Greenland, B. W.; Colquhoun, H. M.; Elliott, J. M.; Hayes, W., Molecular recognition between functionalized gold nanoparticles and healable, supramolecular polymer blends – a route to property enhancement. *Polymer Chemistry* **2013**, 4 (18), 4902.
97. Weng, W.; Beck, J. B.; Jamieson, A. M.; Rowan, S. J., Understanding the Mechanism of Gelation and Stimuli-Responsive Nature of a Class of Metallo-Supramolecular Gels. *Journal of the American Chemical Society* **2006**, 128 (35), 11663-11672.

98. Burnworth, M.; Tang, L.; Kumpfer, J. R.; Duncan, A. J.; Beyer, F. L.; Fiore, G. L.; Rowan, S. J.; Weder, C., Optically healable supramolecular polymers. *Nature* **2011**, 472 (7343), 334-7.
99. Coulibaly, S.; Roulin, A.; Balog, S.; Biyani, M. V.; Foster, E. J.; Rowan, S. J.; Fiore, G. L.; Weder, C., Reinforcement of Optically Healable Supramolecular Polymers with Cellulose Nanocrystals. *Macromolecules* **2014**, 47 (1), 152-160.
100. Wang, Z.; Fan, W.; Tong, R.; Lu, X.; Xia, H., Thermal-healable and shape memory metallosupramolecular poly(n-butyl acrylate-co-methyl methacrylate) materials. *RSC Advances* **2014**, 4 (49), 25486.
101. Hong, G.; Zhang, H.; Lin, Y.; Chen, Y.; Xu, Y.; Weng, W.; Xia, H., Mechanoresponsive Healable Metallosupramolecular Polymers. *Macromolecules* **2013**, 46 (21), 8649-8656.
102. Yuan, J.; Fang, X.; Zhang, L.; Hong, G.; Lin, Y.; Zheng, Q.; Xu, Y.; Ruan, Y.; Weng, W.; Xia, H.; Chen, G., Multi-responsive self-healing metallo-supramolecular gels based on “click” ligand. *Journal of Materials Chemistry* **2012**, 22 (23), 11515.
103. Yuan, J.; Zhang, H.; Hong, G.; Chen, Y.; Chen, G.; Xu, Y.; Weng, W., Using metal-ligand interactions to access biomimetic supramolecular polymers with adaptive and superb mechanical properties. *Journal of Materials Chemistry B* **2013**, 1 (37), 4809-4818.
104. Mozhdehi, D.; Ayala, S.; Cromwell, O. R.; Guan, Z., Self-healing multiphase polymers via dynamic metal-ligand interactions. *Journal of the American Chemical Society* **2014**, 136 (46), 16128-31.
105. Basak, S.; Nanda, J.; Banerjee, A., Multi-stimuli responsive self-healing metallo-hydrogels: tuning of the gel recovery property. *Chemical communications* **2014**, 50 (18), 2356-9.
106. Wang, Z.; Urban, M. W., Facile UV-healable polyethylenimine-copper (C₂H₅N-Cu) supramolecular polymer networks. *Polymer Chemistry* **2013**, 4 (18), 4897-4901.
107. Jia, X.-Y.; Mei, J.-F.; Lai, J.-C.; Li, C.-H.; You, X.-Z., A self-healing PDMS polymer with solvatochromic properties. *Chemical Communications* **2015**, 51 (43), 8928-8930.
108. Gerth, M.; Bohdan, M.; Fokkink, R.; Voets, I.; van der Gucht, J.; Sprakel, J., Supramolecular Assembly of Self-Healing Nanocomposite Hydrogels. *Macromol. Rapid Commun.* **2014**, 35 (24), 2065-2070.
109. Bode, S.; Zedler, L.; Schacher, F. H.; Dietzek, B.; Schmitt, M.; Popp, J.; Hager, M. D.; Schubert, U. S., Self-Healing Polymer Coatings Based on Crosslinked Metallosupramolecular Copolymers. *Advanced Materials* **2013**, 25 (11), 1634-1638.
110. Wei, Z.; He, J.; Liang, T.; Oh, H.; Athas, J.; Tong, Z.; Wang, C.; Nie, Z., Autonomous self-healing of poly(acrylic acid) hydrogels induced by the migration of ferric ions. *Polymer Chemistry* **2013**, 4 (17), 4601-4605.
111. Zhong, M.; Liu, Y.-T.; Xie, X.-M., Self-healable, super tough graphene oxide-poly(acrylic acid) nanocomposite hydrogels facilitated by dual cross-linking effects through dynamic ionic interactions. *Journal of Materials Chemistry B* **2015**, 3 (19), 4001-4008.
112. Wang, Q.; Mynar, J. L.; Yoshida, M.; Lee, E.; Lee, M.; Okuro, K.; Kinbara, K.; Aida, T., High-water-content mouldable hydrogels by mixing clay and a dendritic molecular binder. *Nature* **2010**, 463 (7279), 339-43.
113. Luo, F.; Sun, T. L.; Nakajima, T.; Kurokawa, T.; Zhao, Y.; Sato, K.; Bin Ihsan, A.; Li, X.; Guo, H.; Gong, J. P., Oppositely Charged Polyelectrolytes Form Tough, Self-Healing, and Rebuildable Hydrogels. *Advanced Materials* **2015**, 27 (17), 2722-2727.
114. Huang, Y.; Lawrence, P. G.; Lapitsky, Y., Self-assembly of stiff, adhesive and self-healing gels from common polyelectrolytes. *Langmuir* **2014**, 30 (26), 7771-7.
115. Zhang, E.; Wang, T.; Zhao, L.; Sun, W.; Liu, X.; Tong, Z., Fast Self-Healing of Graphene Oxide-Hectorite Clay-Poly(N,N-dimethylacrylamide) Hybrid Hydrogels Realized by Near-Infrared Irradiation. *ACS Applied Materials & Interfaces* **2014**, 6 (24), 22855-22861.
116. Wang, X.; Liu, F.; Zheng, X.; Sun, J., Water-Enabled Self-Healing of Polyelectrolyte Multilayer Coatings. *Angewandte Chemie* **2011**, 50 (48), 11378-11381.
117. Gaulding, J. C.; Spears, M. W., Jr.; Lyon, L. A., Plastic deformation, wrinkling, and recovery in microgel multilayers. *Polymer Chemistry* **2013**, 4 (18), 4890-4896.

118. Dou, Y.; Zhou, A.; Pan, T.; Han, J.; Wei, M.; Evans, D. G.; Duan, X., Humidity-triggered self-healing films with excellent oxygen barrier performance. *Chemical Communications* **2014**, 50 (54), 7136-8.
119. Skorb, E. V.; Andreeva, D. V., Layer-by-Layer approaches for formation of smart self-healing materials. *Polymer Chemistry* **2013**, 4 (18), 4834.
120. South, A. B.; Lyon, L. A., Autonomic Self-Healing of Hydrogel Thin Films. *Angewandte Chemie* **2010**, 49 (4), 767-771.
121. Nakahata, M.; Takashima, Y.; Yamaguchi, H.; Harada, A., Redox-responsive self-healing materials formed from host-guest polymers. *Nature Communications* **2011**, 2, 511.
122. Peng, L.; Zhang, H.; Feng, A.; Huo, M.; Wang, Z.; Hu, J.; Gao, W.; Yuan, J., Electrochemical redox responsive supramolecular self-healing hydrogels based on host-guest interaction. *Polymer Chemistry* **2015**, 6 (19), 3652-3659.
123. Yan, Q.; Feng, A.; Zhang, H.; Yin, Y.; Yuan, J., Redox-switchable supramolecular polymers for responsive self-healing nanofibers in water. *Polymer Chemistry* **2013**, 4 (4), 1216-1220.
124. Zhang, M.; Xu, D.; Yan, X.; Chen, J.; Dong, S.; Zheng, B.; Huang, F., Self-healing supramolecular gels formed by crown ether based host-guest interactions. *Angewandte Chemie* **2012**, 51 (28), 7011-5.
125. Yan, X.; Xu, D.; Chen, J.; Zhang, M.; Hu, B.; Yu, Y.; Huang, F., A self-healing supramolecular polymer gel with stimuli-responsiveness constructed by crown ether based molecular recognition. *Polymer Chemistry* **2013**, 4 (11), 3312.
126. Syrett, J. A.; Becer, C. R.; Haddleton, D. M., Self-healing and self-mendable polymers. *Polymer Chemistry* **2010**, 1 (7), 978-987.
127. Hansen, C. J.; White, S. R.; Sottos, N. R.; Lewis, J. A., Accelerated Self-Healing Via Ternary Interpenetrating Microvascular Networks. *Advanced Functional Materials* **2011**, 21 (22), 4320-4326.
128. White, S. R.; Sottos, N. R.; Geubelle, P. H.; Moore, J. S.; Kessler, M. R.; Sriram, S. R.; Brown, E. N.; Viswanathan, S., Autonomic healing of polymer composites. *Nature* **2001**, 409 (6822), 794-797.
129. S. R. White, N. R. S., P. H. Geubelle, J. S. Moore, M. R. Kessler, S. R. Sriram, E. N. B. S. V. *Nature* **2001**, 409.
130. Wilson, G. O.; Caruso, M. M.; Reimer, N. T.; White, S. R.; Sottos, N. R.; Moore, J. S., Evaluation of Ruthenium Catalysts for Ring-Opening Metathesis Polymerization-Based Self-Healing Applications. *Chemistry of Materials* **2008**, 20 (10), 3288-3297.
131. Mauldin, T. C.; Rule, J. D.; Sottos, N. R.; White, S. R.; Moore, J. S., Self-healing kinetics and the stereoisomers of dicyclopentadiene. *Journal of the Royal Society, Interface* **2007**, 4 (13), 389-393.
132. Rule, J. D.; Brown, E. N.; Sottos, N. R.; White, S. R.; Moore, J. S., Wax-protected catalyst microspheres for efficient self-healing materials. *Advanced Materials* **2005**, 17 (2), 205-208.
133. Wilson, G. O.; Moore, J. S.; White, S. R.; Sottos, N. R.; Andersson, H. M., Autonomic healing of epoxy vinyl esters via ring opening metathesis polymerization. *Advanced Functional Materials* **2008**, 18 (1), 44-52.
134. Rule, J. D.; Sottos, N. R.; White, S. R., Effect of microcapsule size on the performance of self-healing polymers. *Polymer* **2007**, 48 (12), 3520-3529.
135. Jackson, A. C.; Bartelt, J. A.; Marczewski, K.; Sottos, N. R.; Braun, P. V., Silica-Protected Micron and Sub-Micron Capsules and Particles for Self-Healing at the Microscale. *Macromolecular Rapid Communications* **2011**, 32 (1), 82-87.
136. Zhao, Y.; Fickert, J.; Landfester, K.; Crespy, D., Encapsulation of self-healing agents in polymer nanocapsules. *Small* **2012**, 8 (19), 2954-8.
137. Kamigaito, M.; Ando, T.; Sawamoto, M., Metal-Catalyzed Living Radical Polymerization. *Chemical Reviews* **2001**, 101 (12), 3689-3745.
138. Matyjaszewski, K.; Xia, J., Atom Transfer Radical Polymerization. *Chemical Reviews* **2001**, 101 (9), 2921-2990.
139. Wang, H. P.; Yuan, Y. C.; Rong, M. Z.; Zhang, M. Q., Self-Healing of Thermoplastics via Living Polymerization. *Macromolecules* **2010**, 43 (2), 595-598.

140. Yao, L.; Yuan, Y. C.; Rong, M. Z.; Zhang, M. Q., Self-healing linear polymers based on RAFT polymerization. *Polymer* **2011**, *52* (14), 3137-3145.
141. Gragert, M.; Schunack, M.; Binder, W. H., Azide/alkyne-"click"-reactions of encapsulated reagents: toward self-healing materials. *Macromolecular Rapid Communications* **2011**, *32* (5), 419-25.
142. Blaiszik, B. J.; Caruso, M. M.; McIlroy, D. A.; Moore, J. S.; White, S. R.; Sottos, N. R., Microcapsules filled with reactive solutions for self-healing materials. *Polymer* **2009**, *50* (4), 990-997.
143. Yuan, Y. C.; Rong, M. Z.; Zhang, M. Q.; Chen, J.; Yang, G. C.; Li, X. M., Self-Healing Polymeric Materials Using Epoxy-Mercaptan as the Healant. *Macromolecules* **2008**, *41*, 5197-5202.
144. McIlroy, D. A.; Blaiszik, B. J.; Caruso, M. M.; White, S. R.; Moore, J. S.; Sottos, N. R., Microencapsulation of a Reactive Liquid-Phase Amine for Self-Healing Epoxy Composites. *Macromolecules* **2010**, *43* (4), 1855-1859.
145. Cho, S. H.; Andersson, H. M.; White, S. R.; Sottos, N. R.; Braun, P. V., Polydimethylsiloxane-Based Self-Healing Materials. *Advanced Materials* **2006**, *18* (8), 997-1000.
146. Keller, M. W.; White, S. R.; Sottos, N. R., A Self-Healing Poly(Dimethyl Siloxane) Elastomer. *Advanced Functional Materials* **2007**, *17* (14), 2399-2404.
147. Yang, J.; Keller, M. W.; Moore, J. S.; White, S. R.; Sottos, N. R., Microencapsulation of Isocyanates for Self-Healing Polymers. *Macromolecules* **2008**, *41* (24), 9650-9655.
148. Koh, E.; Kim, N.-K.; Shin, J.; Kim, Y.-W., Polyurethane microcapsules for self-healing paint coatings. *RSC Advances* **2014**, *4* (31), 16214.
149. Song, Y. K.; Jo, Y. H.; Lim, Y. J.; Cho, S. Y.; Yu, H. C.; Ryu, B. C.; Lee, S. I.; Chung, C. M., Sunlight-induced self-healing of a microcapsule-type protective coating. *ACS Applied Materials & Interfaces* **2013**, *5* (4), 1378-84.
150. Song, Y.-K.; Chung, C.-M., Repeatable self-healing of a microcapsule-type protective coating. *Polymer Chemistry* **2013**, *4* (18), 4940-4947.
151. Billiet, S.; Hillewaere, X. K. D.; Teixeira, R. F. A.; Du Prez, F. E., Chemistry of Crosslinking Processes for Self-Healing Polymers. *Macromolecular Rapid Communications* **2013**, *34* (4), 290-309.
152. Park, J.-H.; Braun, P. V., Coaxial Electrospinning of Self-Healing Coatings. *Advanced Materials* **2010**, *22* (4), 496-499.
153. White, S. R.; Moore, J. S.; Sottos, N. R.; Krull, B. P.; Santa Cruz, W. A.; Gergely, R. C. R., Restoration of Large Damage Volumes in Polymers. *Science* **2014**, *344* (6184), 620-623.
154. Chen, X.; Dam, M. A.; Ono, K.; Mal, A.; Shen, H.; Nut, S. R.; Sheran, K.; Wudl, F., A thermally remendable cross-linked polymeric material. *Science* **2002**, *295* (5560), 1698-1702.
155. Barthel, M. J.; Rudolph, T.; Teichler, A.; Paulus, R. M.; Vitz, J.; Hoepfner, S.; Hager, M. D.; Schacher, F. H.; Schubert, U. S., Self-Healing Materials via Reversible Crosslinking of Poly(ethylene oxide)-Block-Poly(furfuryl glycidyl ether) (PEO-b-PFGE) Block Copolymer Films. *Advanced Functional Materials* **2013**, *23* (39), 4921-4932.
156. Ying, H.; Cheng, J., Hydrolyzable Polyureas Bearing Hindered Urea Bonds. *Journal of the American Chemical Society* **2014**, *136* (49), 16974-16977.
157. Lu, Y.-X.; Guan, Z., Olefin Metathesis for Effective Polymer Healing via Dynamic Exchange of Strong Carbon-Carbon Double Bonds. *Journal of the American Chemical Society* **2012**, *134* (34), 14226-14231.
158. Gyarmati, B.; Nemethy, A.; Szilagyi, A., Reversible disulphide formation in polymer networks: A versatile functional group from synthesis to applications. *European Polymer Journal* **2013**, *49* (6), 1268-1286.
159. An, S. Y.; Lee, D. G.; Hwang, J. W.; Kim, K. N.; Nam, J. H.; Jung, H. W.; Noh, S. M.; Oh, J. K., Photo-induced thiol-ene polysulfide-crosslinked materials with tunable thermal and mechanical properties. *Journal of Polymer Science, Part A: Polymer Chemistry* **2014**, *52* (21), 3060-3068.
160. Hoyle, C. E.; Bowman, C. N., Thiol-Ene Click Chemistry. *Angewandte Chemie* **2010**, *49* (9), 1540-1573.

161. Hoyle, C. E.; Lowe, A. B.; Bowman, C. N., Thiol-click chemistry: a multifaceted toolbox for small molecule and polymer synthesis. *Chemical Society Reviews* **2010**, 39 (4), 1355-1387.
162. McNair, O. D.; Sparks, B. J.; Janisse, A. P.; Brent, D. P.; Patton, D. L.; Savin, D. A., Highly Tunable Thiol-Ene Networks via Dual Thiol Addition. *Macromolecules* **2013**, 46 (14), 5614-5621.
163. Silveira, C. C.; Mendes, S. R., Catalytic oxidation of thiols to disulfides using iodine and $\text{CeCl}_3 \cdot 7\text{H}_2\text{O}$ in graphite. *Tetrahedron Letters* **2007**, 48 (42), 7469-7471.
164. An, S. Y.; Arunbabu, D.; Noh, S. M.; Song, Y. K.; Oh, J. K., Recent strategies to develop self-healable crosslinked polymeric networks. *Chemical Communications* **2015**, 51 (66), 13058-13070.
165. Yoon, J. A.; Kamada, J.; Koynov, K.; Mohin, J.; Nicolay, R.; Zhang, Y.; Balazs, A. C.; Kowalewski, T.; Matyjaszewski, K., Self-Healing Polymer Films Based on Thiol-Disulfide Exchange Reactions and Self-Healing Kinetics Measured Using Atomic Force Microscopy. *Macromolecules* **2012**, 45 (1), 142-149.
166. Zheng, J.; Xiao, P.; Liu, W.; Zhang, J.; Huang, Y.; Chen, T., Mechanical Robust and Self-Healable Supramolecular Hydrogel. *Macromolecular Rapid Communications* **2016**, 37 (3), 265-270.
167. Basak, S.; Nanda, J.; Banerjee, A., Multi-stimuli responsive self-healing metallo-hydrogels: tuning of the gel recovery property. *Chemical Communications* **2014**, 50 (18), 2356-2359.
168. Li, C.-H.; Wang, C.; Keplinger, C.; Zuo, J.-L.; Jin, L.; Sun, Y.; Zheng, P.; Cao, Y.; Lissel, F.; Linder, C.; You, X.-Z.; Bao, Z., A highly stretchable autonomous self-healing elastomer. *Nature Chemistry* **2016**, 8 (6), 618-624.
169. Doehler, D.; Peterlik, H.; Binder, W. H., A dual crosslinked self-healing system: Supramolecular and covalent network formation of four-arm star polymers. *Polymer* **2015**, 69, 264-273.
170. Michael, P.; Doehler, D.; Binder, W. H., Improving autonomous self healing via combined chemical/physical principles. *Polymer* **2015**, 69, 216-227.
171. Zhu, D.; Ye, Q.; Lu, X.; Lu, Q., Self-healing polymers with PEG oligomer side chains based on multiple H-bonding and adhesion properties. *Polymer Chemistry* **2015**, 6 (28), 5086-5092.
172. Xu, C.; Cao, L.; Lin, B.; Liang, X.; Chen, Y., Design of Self-Healing Supramolecular Rubbers by Introducing Ionic Cross-Links into Natural Rubber via a Controlled Vulcanization. *ACS Applied Materials & Interfaces* **2016**, 8 (27), 17728-17737.
173. An, S. Y.; Noh, S. M.; Nam, J. H.; Oh, J. K., Dual Sulfide-Disulfide Crosslinked Networks with Rapid and Room Temperature Self-Healability. *Macromolecular Rapid Communications* **2015**, 36, 1255-1260.
174. Deng, G.; Li, F.; Yu, H.; Liu, F.; Liu, C.; Sun, W.; Jiang, H.; Chen, Y., Dynamic Hydrogels with an Environmental Adaptive Self-Healing Ability and Dual Responsive Sol-Gel Transitions. *ACS Macro Letters* **2012**, 1 (2), 275-279.
175. Zhang, Q.; Aleksanian, S.; Noh, S. M.; Oh, J. K., Thiol-responsive block copolymer nanocarriers exhibiting tunable release with morphology changes. *Polymer Chemistry* **2013**, 4 (2), 351-359.
176. Nevejans, S.; Ballard, N.; Miranda, J. I.; Reck, B.; Asua, J. M., The underlying mechanisms for self-healing of poly(disulfide)s. *Physical Chemistry Chemical Physics* **2016**, 18 (39), 27577-27583.
177. Nevejans, S.; Ballard, N.; Miranda, J. I.; Reck, B.; Asua, J. M., The underlying mechanisms for self-healing of poly(disulfide)s. *Physical Chemistry Chemical Physics* **2016**, 18 (39), 27577-27583.

Appendix A

Figure A.1 ^1H -NMR spectra of P1-3K (a), P1-6K (b) and P1-22K (c) in CDCl_3

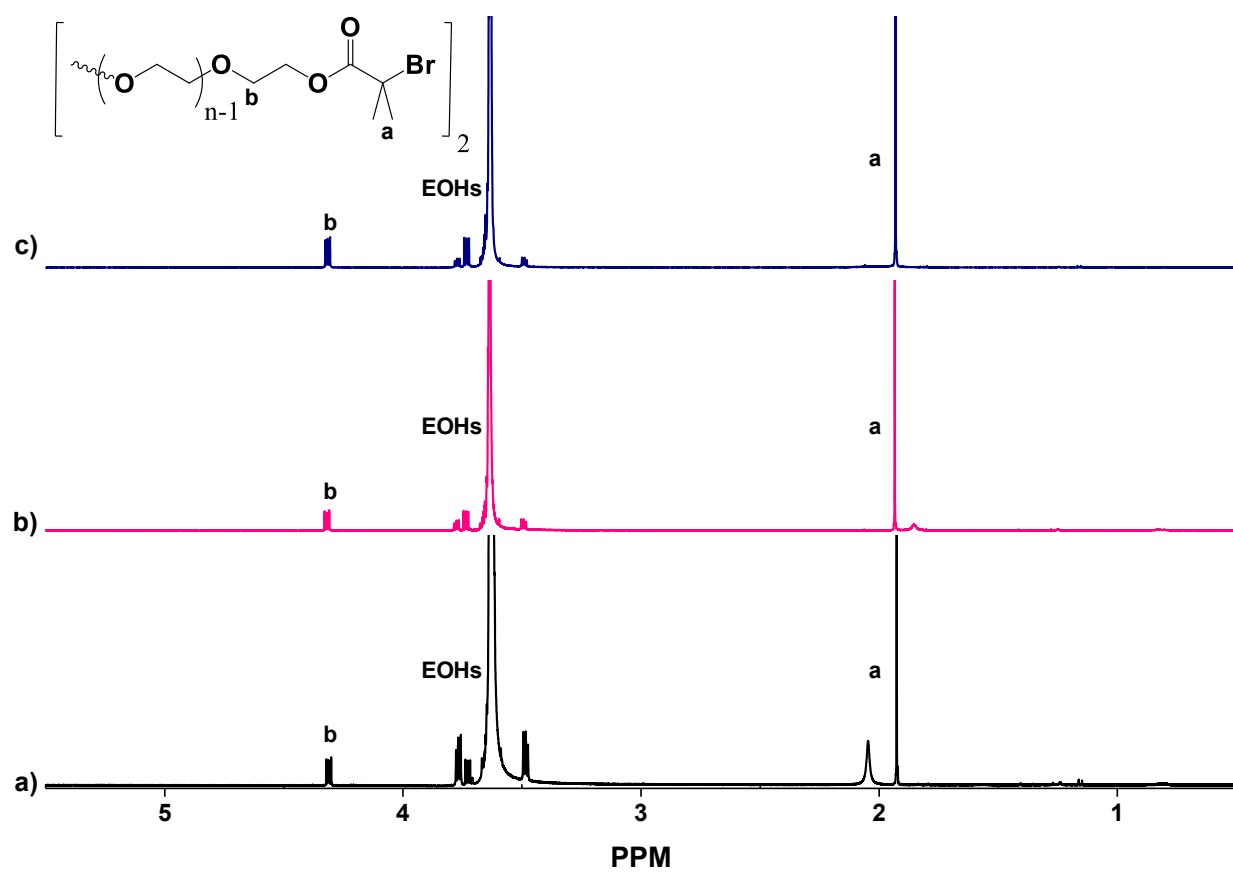


Figure A.2 ^1H -NMR spectra of P3-1 (a), P3-2 (b) and P3-4 (c) in CDCl_3

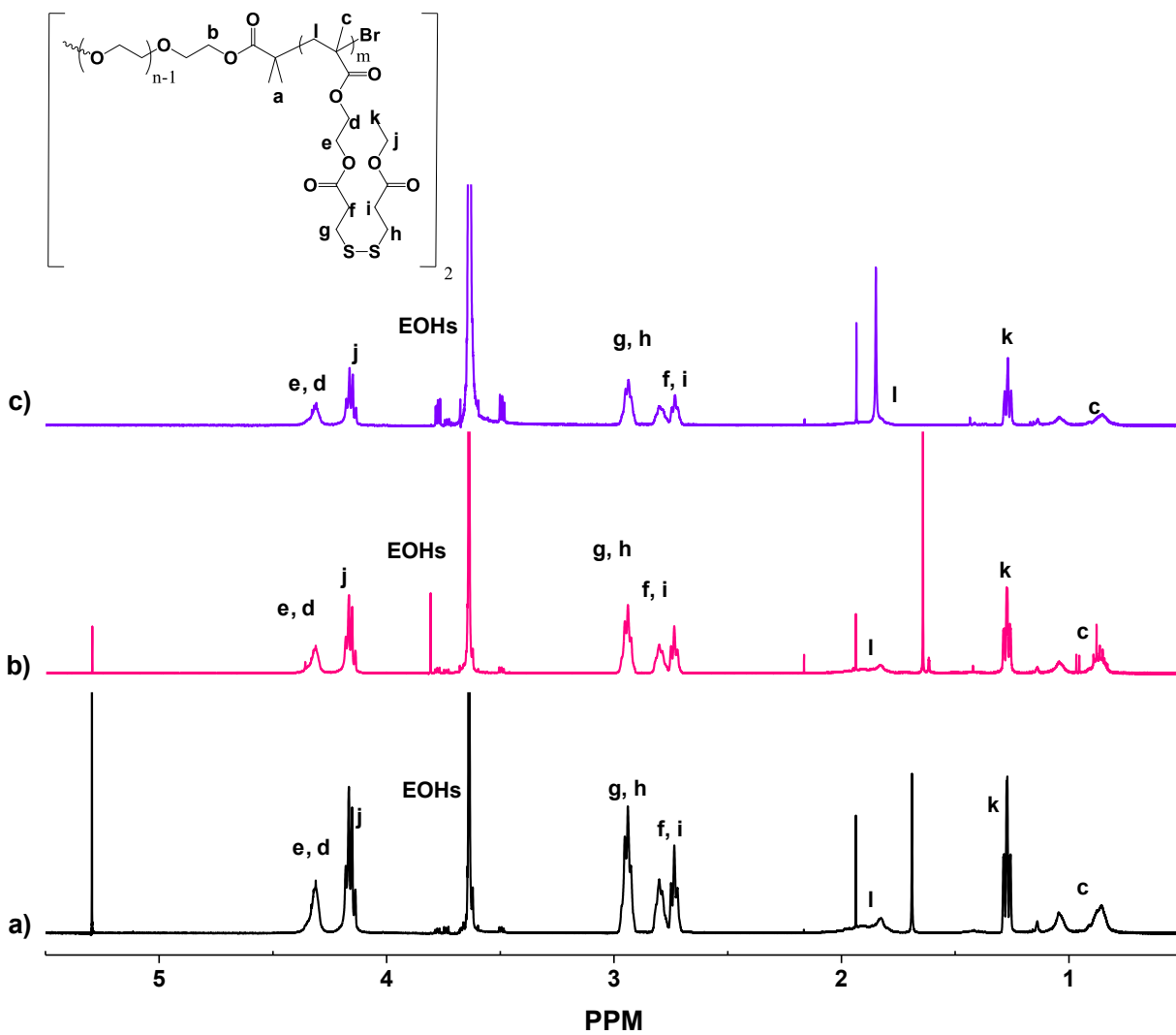


Figure A.3 GPC traces of P3 triblock copolymers

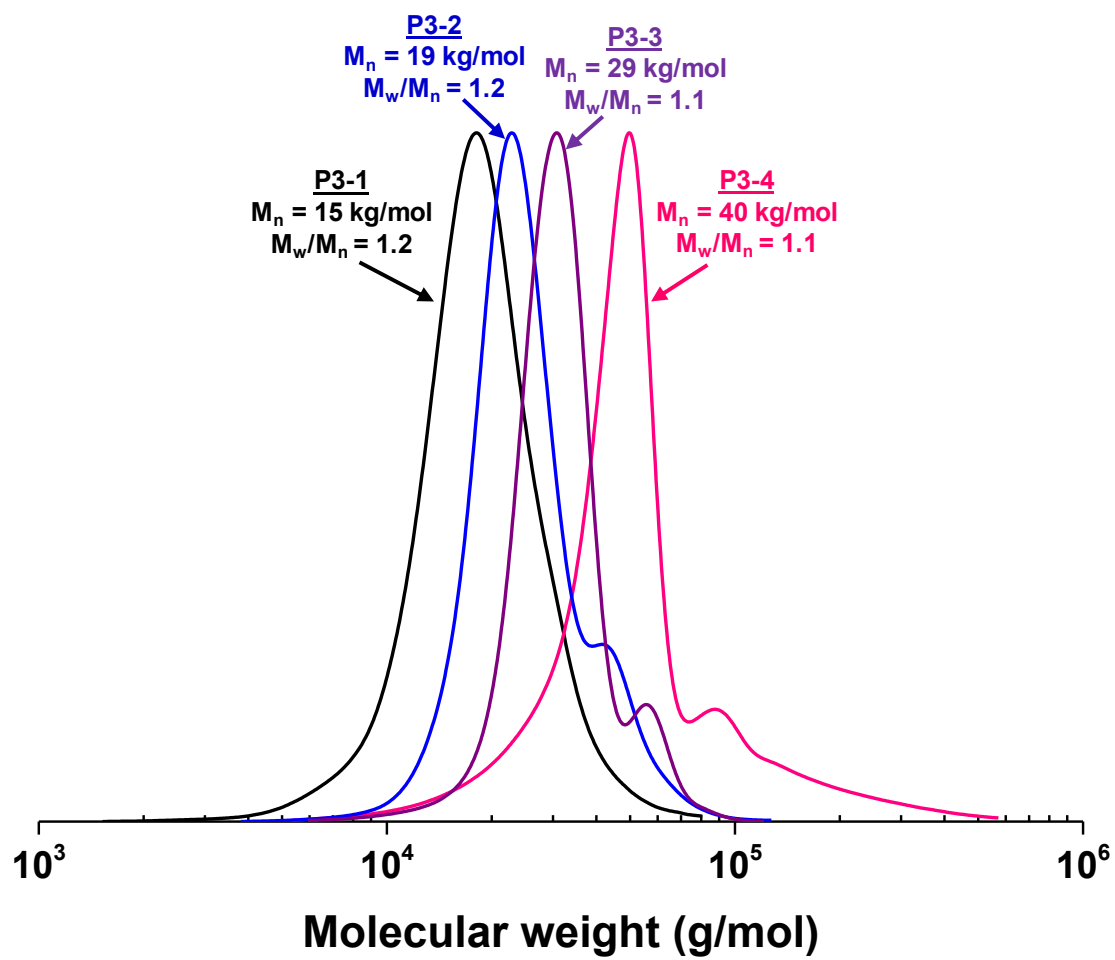


Figure A.4 GPC traces of P5 pentablock copolymer

